University of Nevada, Reno

A NOVEL ROLE FOR CYTOCHROME P450 G 35 (CYP4G35) IN ODOR PROCESSING IN *AEDES AEGYPTI* MOSQUITOES

A thesis submitted in partial fulfillment of the requirements for the degree of Master of Science in Biochemistry

by

Omar Garcia Cruz

Dr. Monika Gulia-Nuss/Thesis Advisor

May 2023

THE GRADUATE SCHOOL

We recommend that the thesis prepared
under our supervision by

Omar Garcia Cruz

entitled

A NOVEL ROLE FOR CYTOCHROME P450 G 35 (CYP4G35) IN ODOR PROCESSING IN *AEDES AEGYPTI* MOSQUITOES

be accepted in partial fulfillment of the
requirements for the degree of

MASTER OF SCIENCE

Monika Gulia-Nuss. Ph.D.
Advisor

Claudia Rueckert, Ph.D.
Committee Member

Andrew Nuss, Ph.D.
Committee Member

Dennis Mathew, Ph.D.
Graduate School Representative

Markus Kemmelmeier, Ph.D., Dean
Graduate School

May 2023

Abstract

Mosquitoes are vectors of various pathogens important to human health. The emergence of insecticide resistance has put pressure on identifying new avenues for mosquito control. These genetics tools require novel targets, which only come with a better understanding of mosquito biology.

Chemo sensation is essential for insects to interpret their environments. Three primary appendages mediate chemoreception, esp. olfaction in mosquitoes: antennae, maxillary palps, and proboscis. These appendages have sensilla hairs covering their exterior structure. The sensilla hair houses many chemoreceptors, including odorant, ionotropic, and gustatory receptors. The volatile odorants enter the sensilla lymph through pores to bind to the receptors. Maintaining odor receptor sensitivity through degrading these odorants is essential for odor perception. Many enzymes, such as esterases and cytochrome P450s (CYPs), have been hypothesized to function as odor-degrading enzymes; however, none is yet functionally characterized.

Most insects have 1 or 2 CYP4G genes, an insect-specific class of CYPs. The Dipteran insect genomes have two genes. Similar to other dipterans, the *Ae. aegypti* genome expresses two CYP4G genes: CYP4G36 (CYP4G1) and CYP4G35 (CYP4G15). Previous work in the Gulia-Nuss and Blomquist labs showed that *Ae. aegypti* CYP4G36 is an oxidative decarbonylase that catalyzes the last two steps in cuticular hydrocarbon synthesis, a function consistent with the findings in other insects (unpublished data). From the preliminary data in the Gulia-Nuss lab, we hypothesized that CYP4G35 is an odor-degrading enzyme (ODE). An important consideration for an ODEs is its localization. If CYP4G35 were to have an olfactory function, it would need to localize in the sensilla (Chapter 2). To understand the potential pathways in which CYP4G35 might be involved, we knockout CYP4G35 in mosquitoes. We separated both mutant and wild-

type samples' head and carcass/body tissue to identify head-specific differences in protein expression in CYP4G35 mutant mosquitoes (Chapter 3). To identify the direct target (substrate) for the CYP4G35 enzyme, we expressed CYP4G35 and used these microsomes with different chained-length alcohol and aldehyde substrates (Chapter 4). GC-MS was used to analyze the breakdown product of a particular substrate.

Our data support our hypothesis that CYP4G35 has a function in odor perception. However, it is unclear whether it directly breaks down odor molecules or is a general detoxification enzyme that helps clear the lymph to avoid odor molecule buildup.

This thesis is dedicated to my family.

Ruben Garcia

Leticia Cruz

Eliseo Garcia-Cruz

Joseph Garcia-Cruz

Selena Garcia-Cruz

Acknowledgments

I want to express my deepest gratitude to my advisor, Dr. Monika Gulia-Nuss, for her invaluable mentoring and assistance in developing the experiments, interpreting the data, and writing this dissertation. I want to thank all my committee members, who provided valuable advice to me to approach this thesis project from different approaches. I would also like to thank and acknowledge the work done by Manoj Mathew and Fiza Arshad, who were responsible for the initial work done on CYP4G35.

Many individuals devoted their time to making this thesis possible. Dr. Maclean shared her knowledge and expertise of CYP4Gs which was vital to this project. I thank Dr. Arvind Sharma for all his contributions to this project. Dr. Jeremiah Reyes helped me with the bioinformatic analysis. Dr. Reyes's guidance was vital throughout the bioinformatic analysis. Dr. Michael Pham has provided valuable advice and insight into troubleshooting many experiments.

The labs and facilities at the University of Nevada, Reno, made this work possible. Dr. Juli Petereit of the INBRE Nevada Bioinformatics Core provided her expertise in proteomics data analysis. The INBRE Proteomics Core and its members, Dr. Quilici and Rebekah Woolsey, carried out the proteomics work. I am equally indebted to the members of the Core Analytical Lab, especially Dr. Dunham-Cheatum, who helped me relentlessly to troubleshoot the GC-MS work. I would also like to thank the Kosma lab for generously allowing the use of their GC-MS and Brenda Trinh for taking the time to train me. I would also like to thank Dr. Kosma for his expertise in troubleshooting extraction methods for substrate assays. Finally, this work would not have been possible without the support of all of my lab mates, friends, and family.

TABLE OF CONTENTS

Section	Pages
Abstract	**i**
Acknowledgments	**iv**
List of Tables	**vi**
List of Figures	**vii**
List of Abbreviations	**ix**
Chapter 1 Introduction and Review of Literature	**1**
Chapter 2 Localization of Cytochrome P450s, CYP4G35, and CYP4G36, in mosquito olfactory tissues by *in situ* hybridization and immunohistochemistry	**25**
Chapter 3 Proteomics analysis of CYP4G35 knock-out mosquitoes to understand its mechanisms and potential functional pathways.	**50**
Chapter 4 Characterization of functional substrate groups for CYP4G35	**79**
Chapter 5 Conclusion and Prospects	**99**

LIST OF TABLES

Table 3.1 Guide RNAs designed used to target CYP4G35 in Ae. aegypti. 72

Table 3.2: Primers for PCR amplify and sequence the CYP4G35 for transgenic lines. 73

Table 3.3. Top five up or downregulated differentially expressed proteins in CYP4G35 mutants. 74

Table 3.4. Top five up or downregulated differentially expressed proteins in CYP4G35 mutants. 75

LIST OF FIGURES

Figure 1.1. The proposed mechanism for odorant degradation within the insect olfactory sensilla. 23

Figure 1.2. Phylogeny of the CYP4G genes. 24

Figure 2.1. Localization of CYP4G35 in Ae. aegypti female antennae using Whole-mount fluorescent immunohistochemistry. 37

Figure 2.2. Localization of the CY4G35 in Ae. aegypti female antennae using whole-mount fluorescent in-situ hybridization. 39

Figure 2.3. Localization of CYP4G35 in Ae. aegypti female proboscis using Whole-mount fluorescent in-situ hybridization & fluorescent immunohistochemistry. 41

Figure 3.1. CYP4G35 knockout using CRISPR-Cas9. 64

Figure 3.2. PCA plot illustrating variations among data sets. 65

Figure 3.3. Total differentially expressed proteins in head & body tissue in CYP4G35 KO vs. WT. 66

Figure 3.4. Volcano plot of DEPs in carcass tissue of the CYP4G35 mutant vs. wild type. 67

Figure 3.5. Venn diagram of up and down-regulated proteins found in both head and body of CYP4G35 KO mutant 68

Figure 3.6. Bubble plot of molecular function enrichment for CYP4G35 KO head tissue. 69

Figure 3.7. Bubble plot of molecular function enrichment for CYP4G35 KO body tissue. 70

Figure 3.8. KEGG analysis of the metabolic pathways within CYP4G35 KO and WT **71**

Figure 4.1. Validation of functional Cytochrome P450 using CO difference spectrum for CYP4G35 and CYP4G55. **86**

Figure 4.2. Cytochrome P450 partner reductase activity using NADPH reduction assay for CYP4G35-CPR and CYP4G55-CPR. **87**

Figure 4.3. Products from incubations of CYP4G55-CPR and CYP4G35-CPR with decanal. **89**

Figure 4.4. Products from incubations of CYP4G55-CPR and CYP4G35-CPR with octadecanol. **90**

LIST OF ABBREVIATIONS

Abbreviation	Full form
CCE	Carboxylesterases
CLB	Cell lysis buffer
CO	Carbon monoxide
CPR	Cytochrome p450 reductase
CYP	Cytochrome(s) P450
CYP4G	Cytochrome P450 from the G subfamily
DEP	Differential expressed protein
FAR	Fatty acyl-Co-A reductase
FC	Fold change
FDA	Food & drug administration
GC-MS	Gas chromatography-mass spectroscopy
GO	Gene ontology
HF-CPR	House Fly cytochrome P450 reductase
LVP	Liverpool *Aedes aegypti* mosquito strain
Mb-VLCFA	Methyl-branch very long chain Fatty acid
OBP	Odor binding protein
ODE	Odor degrading enzyme
OR	Odor receptor
ORCO	Odorant receptor co-receptor
ORN	Odor receptor neuron
OSN	Odor sensory Neuron

PDE	Pheromone degrading enzyme
qRT-PCR	Quantitative (Real-Time) reverse transcriptase-polymerase Chain Reaction.
SPME	Spatial pressure microextraction
WM-FIHC	Immunohistochemistry
WM-FISH	Whole-mount - Fluorescent *in situ* hybridization
WT	Wild-type

CHAPTER 1

INTRODUCTION AND REVIEW OF LITERATURE

I. Introduction

Adult mosquitoes use their sense of smell to find vertebrate hosts, nectar sources, and oviposition sites. Several mosquito species, such as *Aedes aegypti*, prefer to feed on humans (Brown et al., 2011; McBride et al., 2014), leading to public health issues. The anthropophilic mosquito species are vectors of many pathogens, such as *Plasmodium* parasites, filarial nematodes, and arboviruses, such as dengue, and Zika, chikungunya. A vital aspect of a female mosquito's life cycle is the uptake of multiple bloodmeals from different vertebrate hosts, facilitating pathogen transmission. Female mosquitoes rely on specific sensory cues: human-derived odors, exhaled CO_2, body moisture and heat, and visual cues (Konopka et al., 2021). Mosquitoes find their hosts using these cues and interpret them through olfactory, gustatory, thermal, and visual stimuli. In addition, female mosquitoes heavily rely on chemoreception for their host-seeking behavior. These chemoreceptors fall into three general categories odor receptors (ORs), gustatory receptors (GRs), and ionotropic receptors (IRs). These receptors are housed in diverse sensilla hairs covering mosquito olfactory appendages: antennae, maxillary palps, and proboscis. The sensilla sub-type contains different sets and combinations of IRs, GRs, and ORs. The primary appendage facilitating olfaction in mosquitoes is the antennae. The antennae are covered in sensilla hairs that house many chemosensory receptors, most abundantly ORs. These ORs form heterotetrameric complexes with an OR co-receptor (ORCO) (Butterwick et al., 2018). OR-ORCO complexes are expressed on olfactory receptor neurons (ORNs) alongside chemoreceptors, found primarily in the antennae and

maxillary palps (Riabinina et al., 2016). Odorants are proposed to enter through the cuticle pores of the sensilla surface and come into the sensilla lymph making their way to receptors on the dendrite of the ORN (Steinbrecht, 1997). The binding of odorants to these chemosensory receptors activates signal transduction generating an action potential.

The maintenance of sensitivity and selectivity of these ORN-based signaling in mosquitoes is poorly understood, leaving important molecular events unclear. Many factors are involved in insect odorant detection, including various proteins that could interfere with ligand-receptor interaction before or after ligand binding (Maıbeche, 2021). Among these "peri receptor events," the step of signal termination is crucial to sustaining the kinetics of the olfactory response (Leal, 2013; Maıbeche, 2021). Antennal enzymes called Odorant-Degrading Enzymes (ODEs) present in the vicinity of receptors may participate in signal termination by degrading odor molecules into inactive compounds (Maıbeche, 2021). In insects, many esterases, cytochrome P450s, and glutathione S-transferases have been either characterized or posited to be ODEs (Leal, 2013). Most potential ODEs are identified through transcript expression. ODEs could be specific to an odor or may take part in the general catabolism of odorant molecules within the sensilla, allowing chemicals to be removed from the olfactory hairs and protecting olfactory neurons from possible harmful molecules. Despite this wide range of potential roles, ODEs have not been well-studied.

In this thesis, I will present the identification of a putative ODE, CYP4G35, through 1) its localization in olfactory tissues, 2) its proposed mechanism of action based on proteome studies, and 3) discuss our work towards identification of its potential substrate.

II. Review of Literature

Mosquitoes as disease vectors

Over 3,500 species of mosquito have been described in the family *Culicidae*, inhabiting every continent except Antarctica (Knight and Stone, 1977). Although not all mosquito species require a blood meal or are disease vectors, blood-feeding mosquitoes are unquestionably the most medically relevant arthropod vectors of human pathogens (Weaver, 2018). Females in several genera, such as *Aedes*, *Anopheles*, and *Culex*, require a blood meal to develop eggs (Briegel & Horler, 1993; Harrington et al., 2001). This dependency on a blood meal makes them excellent vectors of various pathogens. The maintenance and transmission of the pathogens that cause malaria, lymphatic filariasis, and numerous arboviral infections depend on the availability of competent mosquito vectors. Human malaria, caused primarily by the protozoan species *Plasmodium falciparum* and *Plasmodium vivax*, affects nearly 500 million people annually and is responsible for an estimated 619, 000 deaths in 2021 (WHO Malaria Report, 2021; Carter & Mendis, 2002; Guerra et al., 2010). The nematodes *Wuchereria bancrofti* and *Brugia malayi* are the principal etiologic agents of lymphatic filariasis, affecting over 100 million individuals (World Health Organization Global Program to Eliminate Lymphatic Filariasis: Progress Report on Mass Drug Administration, 2012).

Similarly, hundreds of thousands of mosquito-borne virus infections occur annually around the globe (*Vector-borne diseases*, 2020). *Aedes aegypti* alone is responsible for 1 million dengue virus infections annually worldwide (Brady, 2020). Although the medical community has known for over a century the role mosquitoes play in the transmission of pathogens, mosquito-borne diseases continue to have a devastating influence due to their

global presence throughout the tropical, subtropical, and to some extent in the temperate regions of the world (Leta, 2018). Numerous environmental, economic, sociological, political, and demographic factors have played significant roles in the reemergence of malaria and other infectious and parasitic diseases. Companies are hesitant to invest the financial resources necessary to bring a new drug to trial for these maladies (Andrews et al., 2018), leading the US Food and Drug Administration (FDA) to offer tropical disease priority review vouchers (Berman & Radhakrishna, 2017). These vouchers have provided significant financial incentives for pharmaceutical companies to develop drugs for malaria (Berman & Radhakrishna, 2017; Ridley, 2017; Ridley et al., 2021). Drug resistance cases further exacerbate the difficulties and risks involved in drug development for mosquito-borne diseases (Hecht & Fogel, 2012; Pongtavornpinyo et al., 2008).

Another avenue to tackle these vector-borne diseases is through mosquito control programs. Through environmental perturbation and pesticide application, mosquito control was the primary strategy for controlling mosquito-borne diseases. However, environmental and human health concerns and the development of pesticide resistance limit the usefulness of these traditional approaches (Macedo et al., 2010; Peterson et al., 2006; Soderlund, 2012; Tang et al., 2018). Consequently, molecular biology and genomics tools are applied in vector biology to develop novel mosquito control strategies (Alphey, 2014; Alphey et al., 2020; Gantz et al., 2015; Hammond et al., 2016). The development of CRISPR/Cas9 technology has provided a powerful tool to target the mosquito genome. However, understanding basic mosquito biology is needed to develop such tools and identify relevant targets for mosquito control. An intriguing question in mosquito research has been how mosquitoes find their hosts.

Chemoreception in mosquitoes

To interpret chemosensory cues, mosquitoes rely on various receptors. These receptors are divided into olfactory receptors (ORs), ionotropic receptors (IRs), and gustatory receptors (GRs). Insect chemosensory systems detect a wide range of volatile and soluble chemicals and are important for finding and assessing the quality of food sources, identifying mates, and oviposition sites. In many insects, olfactory sensilla are present in the antennae and the maxillary palps. In females, gustatory sensilla are present on several body parts, including the external and internal mouthparts, the legs, the wing margins, and the ovipositor. Physiological and behavioral analysis has shown that GRs are tuned to four classes of compounds: sugars (attractants), bitter compounds (repellents), salts, and water (Rodrigues & Siddiqi, 1978).

Organization of the olfactory system

The nervous system detects myriad volatile chemicals in the environment (Ache and Young, 2005). Odor detection is mediated by large, divergent repertoires of olfactory receptors, which localize to the ciliated dendritic endings of olfactory sensory neurons (OSNs) (Touhara and Vosshall, 2009). In most animals, the vast majority of OSNs express a single odorant receptor (OR) gene, which defines the selectivity of OSN responses to odor stimuli (Fuss and Ray, 2009). The olfactory system is highly conserved across insects and shares similar organization across the animal kingdom between vertebrates and invertebrates (Steinbrecht, 1997). In all insects, including mosquitoes, olfaction occurs within sensory appendages: antennae, proboscis, and palps.

Like other insects, mosquitoes detect odor molecules by binding the ORs on the olfactory neurons within hair-like sensilla on their sensory appendages. These odorants

reach the ORs by entering through the sensilla into pores in the cuticle (Steinbrecht, 1997) and are either transported by odorant-binding proteins (OBPs) (Rihani, 2021; Li, 2008) or diffuse through the aqueous hemolymph to the ORs (Leal, 2013; Pelosi et al., 2018). The ORs of mosquitoes and other insects form heterodimers with an olfaction receptor co-receptor (ORCO). This OR-ORCO complex functions as a ligand-gated ion channel (Vosshall and Hansson, 2011) that can bind to one type of odor molecule or several classes of odorant molecules (Larsson et al., 2004; Carey et al., 2010). When odor molecules bind to ORs, the ion pore opens, allowing the olfactory receptor neuron (ORN) to depolarize and propagate an action potential (Carraher et al., 2015; Leal, 2013; Wicher, 2018; Wicher & Miazzi, 2021).

The number of olfactory receptors varies across mosquito species, ranging from 79 OR genes in *An. gambiae* to 110 in *Ae. aegypti*, and 177 in the southern house mosquito, *Culex quinquefasciatus* (Hill et al., 2002; Bohbot et al., 2007; Leal et al., 2013; Zhou et al., 2014). ORNs send their axons to the central brain, called the antennal lobe. There, ORNs expressing the same OR converge in a ball-shaped zone called the glomerulus, where they synapse onto projection neurons that then relay olfactory information to higher-order centers. Olfactory information from the antennal lobes is encoded into memory and used to elicit behavioral actions (Guidobaldi et al., 2014; Zhao & McBride, 2020).

Several molecular steps are involved in odorant detection within insect olfactory sensilla, including receptor and peri-receptor events. Among these peri-receptor events, signal termination is hypothesized to be crucial to sustaining the kinetics of the olfactory response (Guidobaldi et al., 2014; Schmidt & Benton, 2020).

Ionotropic Receptors

The second type of olfactory insect receptors is represented by ionotropic receptors (IRs) homologous to ionotropic glutamate receptors (iGluR). The ionotropic glutamate receptors are known to be involved in the formation of synaptic contacts in the nervous system of vertebrates and invertebrates (Benton et al., 2009). In contrast to other receptor repertoires, IRs represent a highly divergent subfamily of ionotropic glutamate receptors (iGluRs) present across the protostome branch of the animal kingdom (Croset et al., 2010). IRs are sensitive to acids, amines, and aldehydes. Receptors function as heterotetramers consisting of an odor-specific receptor protein IRx and a constant co-receptor protein IRcoY (Abuin et al., 2011). IRs were recently proposed to detect volatile chemicals in olfactory cilia. Analysis of IR expression in the antenna of the fruit fly *D. melanogaster* revealed complex combinatorial expression patterns, with individual OSNs expressing 2–5 distinct IR genes (Benton et al., 2009). IRs concentrate in olfactory cilia and not at synapses, and misexpression of IRs in other (IR-containing) neurons is sufficient to confer novel odor responsiveness, supporting the hypothesis that they function directly in odor detection (Benton et al., 2009).

Gustatory system

The third type of chemosensory receptors are gustatory receptors or taste receptors. GR genes are expressed in subsets of gustatory receptor neurons (GRNs) in one or more gustatory tissues, including the proboscis, legs, wing margins, and internal mouthparts (Dunipace et al., 2001; Scott et al., 2001). Expression of at least three GR genes has been detected in the antenna of *D. melanogaster*, suggesting that some might have an olfactory function (Scott et al., 2001). GR21a in *D. melanogaster* is expressed in

a neuron that is narrowly tuned to CO_2 (Suh et al., 2004), but its role in this response is unclear.

GRs are the primary taste receptors and are also involved in CO_2 detection. Three members of the insect GR family are expressed in olfactory neurons that detect airborne CO_2 and other odorants: GR1, GR2, and GR3 (MacWilliam et al., 2018; Tauxe et al., 2013; Turner et al., 2011). These receptors are conserved in holometabolous insect orders except Hymenoptera (MacWilliam et al., 2018; Robertson & Kent, 2009). In mosquitoes, they are expressed in specialized neurons called cpA, which detect CO_2 (Jones et al., 2007; Lu et al., 2007; Syed & Leal, 2007) and a number of additional compounds, including many found in human skin odor (Lu et al., 2007; Tauxe et al., 2013; Turner et al., 2011; Turner & Ray, 2009). These neurons play a critical role in the host-seeking behavior of mosquitoes (Gillies, 1980; McMeniman et al., 2014; Tauxe et al., 2013; Turner et al., 2011). GR3 in *Ae. aegypti* encodes the essential subunit for CO_2 detection (Jones et al., 2007; Kwon et al., 2007). The removal of GR3 causes mosquitoes to lose all sensitivity to CO_2 but can still detect a vertebrate host (McMeniman et al., 2014). Another complexity of the mosquito olfactory system is the lack of adherence to the "one-receptor-to-one-neuron-to-one-glomerulus" belief in olfactory systems. In *Ae. aegypti*, there is no direct relation of the number of chemosensory receptors to the number of glomeruli, with at least twice as many receptors as glomeruli (Ignell et al., 2005; Shankar and McMeniman, 2020; Zhao et al., 2022). The combination of ORs and IRs in their conserved co-receptors further complicates the understanding of mosquito olfaction. In *Ae. aegypti*, some neurons express only an individual co-receptor and

ligand-selective receptor pair, while others express different sets of frequently co-expressed receptor subunits (Herre et al., 2022).

Signal Termination/Odor Degradation

Detecting volatile chemical cues is essential for insects to interpret their environment and communicate. A proposed mechanism for ODEs (Fig. 1.1) involves odorants that enter through the sensilla pore to interact with OR/IR/GRs and the degradation of odorants through enzymatic degradation in the lymph. Pioneer studies in moths suggested that enzymatic degradation of odorants occurs in the sensilla lymph (Kasang, 1971; Vogt & Riddiford, 1981). Rapid catabolism of odorant molecules into inactive or poorly active forms by extracellular ODEs or Pheromone-Degrading Enzymes (PDEs) may regulate odorant/pheromone concentration, participating in signal termination.

Only a few insect ODE/PDE have been cloned and functionally characterized to date (Vogt, 2005; Jacquin-Joly & Maibeche-Coisne et al., 2009). A male-specific sensilla carboxylesterase, ApolPDE, has been proposed to break down pheromones in the silk moth *Antheraea polyphemus* (Vogt and Riddiford, 1981; Vogt et al., 1985, Klein, 1987). ApolPDE was later cloned and functionally characterized *in vitro*, confirming its possible involvement in rapid signal inactivation *in vivo* (Ishida & Leal, 2005). In Japanese beetles, *Popilia japonica*, there are male-specific antennal esterases. Some of these esterases have been associated with the rapid degradation of sex pheromone, PjapPDE, *in vitro* (Ishida & Leal, 2018). In the moth *Spodoptera littoralis*, antennal esterases hydrolyze plant volatile but not the sex pheromone components (Durand et al., 2010). Another esterase, EST6, is localized in the lymph and support cells surrounding ORN's

dendrite and functions as an ODE in *D. melanogaster* (Chertemps et al., 2015, Younus et al., 2017). Some other ODE/PDE candidates belonging to various enzyme families are present across different species but without molecular or functional characterization (Durand et al., 2011; Durand et al., 2010; Leal, 2013). Based on available studies, antennal enzymes such as cytochrome P450s (CYPs), dehydrogenases, oxidases, carboxylesterases (CCEs), and esterases (Calla et al., 2018; Wu et al., 2022; Younus et al., 2017; Zhang et al., 2022) have been shown to act as ODEs or PDEs. However, the molecular mechanism and mode of action for ODEs have yet to be fully characterized (Vogt & Riddiford, 1981; Vogt et al., 1985).

Cytochrome P450s (CYPs) in insects

The large and diverse CYP superfamily encodes enzymes with a broad spectrum of monooxygenase and related activities. In humans, about 56% of the CYP genes play a role in physiological processes, including detoxication, and the remainder are of unknown function (Guengerich and Cheng, 2011). However, much less is known about the roles of insect CYP genes (Feyereisen, 2015). The cytochrome P450 enzymes (mixed function oxidases, cytochrome P450 monooxygenases) are found in virtually all insect tissues and carry out various functions, from synthesizing and degrading ecdysteroid and juvenile hormones to the metabolism of foreign chemicals (Feyereisen, 1999). Microsomal and mitochondrial CYPs are present in insects and are well known to metabolize insecticides, resulting in detoxification (Marteniz-Paz et al., 2015). The significant expression of CYPs in olfactory tissues indicates a role in degrading odorants or pheromones apart from other metabolic processes.

CYPs expression in olfactory tissues

In the silk moth *Bombyx mori*, several CYP genes were highly expressed in the antennae of male moths (Laughlin et al., 2008). Males of this species use pheromones to locate females; thus, the CYPs might be associated with a function in pheromone degradation. In cotton leafworm, *Spodoptera littoralis*, antennal transcripts show higher expression of several CYPs (Pottier et al., 2012). In the mountain pine beetle, *Dendroctonus ponderosae*, 6 CYPs were identified in the antennae of both males and females. In the Asian citrus psyllid, *Diaphorina citri*, tissue expression analysis revealed six CYPs highly expressed in male and female antennae compared to other non-olfactory tissues (Kuang et al., 2022). DcCYP4d8 had the highest expression levels in the antennae and legs of both sexes (Kuang et al., 2022); however, the function of CYP4d8 is poorly understood. In *Picromerus lewisi*, a stink bug species, six CYPs genes were significantly enriched in antennae tissue compared to the head (He et al., 2022). In *D. melanogaster*, CYPs such as CYP6G1, CYP4E1, and CYP4G15 were highly expressed in the antennae of both males and females (Younus et al., 2014). CYP6G1 upregulation is associated with DDT resistance (Daborn et al., 2001; Daborn et al., 2002). CYP4E2 upregulation in the *Drosophila* larvae is associated with exposure to ethanol or methanol (Wang et al., 2012). CYP4G15 is highly expressed in the antennae of adults and localized in the brain of larvae of *D. melanogaster* (Maibeche-Coisne et al., 2000); however, it has not yet been functionally characterized. Overall, the high expression of certain CYPs in insect antennae suggests that these enzymes may play essential roles in the olfactory system and the adaptation of insects to their environment.

Cytochrome P450 G subfamily (CYP4Gs)

The CYP4G subfamily is insect-specific (Despres et al., 2007). A preliminary survey of CYP4G sequences in insects (Qiu et al., 2012) revealed 1-2 CYP4G genes in most insect orders. CYP4G genes have conserved +44-residue insertion between the G and H helices, which protrude from the globular structure of the enzyme distally from the membrane anchor (Feyereisen, 2020). A phylogenetic analysis of all sequenced CYP4G genes suggests two distinct clades: a *D. melanogaster* CYP4G1-like and *D. melanogaster* CYP4G15-like (Fig. 1.2) (Feyereisen, 2020). In the first global CYP transcriptome analysis of *D. melanogaster* (Daborn et al., 2002), the CYP4G1 gene was the most highly expressed P450 gene throughout the body. Similarly, CYP4G19 (CYP4G1-like) was among the twenty most abundant genes from the transcriptome of the cockroach *Blattella germanica* (Zhou et al., 2014).

CYP4G1 RNAi flies were deficient in cuticular hydrocarbon (CHC) production and were susceptible to death due to desiccation (Qiu et al., 2012). The impaired courtship behavior in these CYP4G1 knockdown flies suggested its function in pheromones regulation. Furthermore, a recombinant *Musca domestica* CYP4G2 was shown to catalyze the last two steps in CHC biosynthesis, resulting in the oxidative decarbonylation of long-chain fatty aldehydes (Qiu et al., 2012). Balabanidou et al. (2016) showed that both *An. gambiae* CYP4Gs: CYP4G16 and CYP4G17, were highly expressed in the oenocytes. CYP4G16 (CYP4G1-like) was shown to function as an oxidative decarbonylase for CHC biosynthesis but not CYP4G17 (CYP4G15-like), suggesting another function for CYP4G17 enzyme (Kefi et al., 2019). Only the CYP4G16 gene, alone or in combination with CYP4G17, could rescue the lethal phenotype of CYP4G1 knockdown in transgenic *D. melanogaster*. RNAi of CYP4G102

in *Locusta migratoria* (Yu et al., 2016) and CYP4G51 in the pea aphid *Myzus persicae* (Chen et al., 2016) led to increased mortality and decreased CHC content and desiccation tolerance. In the honeybee, *Apis mellifera*, CYP4G11 catalyzes the oxidative decarbonylation of fatty aldehydes to tridecane (C13) and heptadecane (C17) (Calla et al., 2018). The breakdown of different substrates with different length carbon chains suggests two different functions: one as a decarbonylase for producing long-chain cuticular hydrocarbons and another to break down shorter carbon chain molecules. In the mountain pine beetle, *D. ponderosae*, both CYP4G enzymes were active in the biosynthesis of CHC and (Z)-3-nonene (a short chain carbon molecule), an intermediate in pheromone exo-brevicomin production (MacLean et al., 2018). In another coleopteran, *Tenebrio molitor*, RNAi of the two CYP4G genes decreased CHC content and desiccation tolerance (Wang et al., 2019a). In brown planthopper, *Nilaparvata lugens*, the RNAi of the two CYP4Gs reduced overall CHC content (Wang et al., 2019b). Thus, direct and indirect evidence from phylogenetically distant species strongly suggests that CYP4G1-like enzymes share a common biochemical function as oxidative decarbonylases essential in hydrocarbon biosynthesis.

Constitutive overexpression of CYP4G genes in insecticide-resistant strains also provided indirect evidence for the role of CYP4G genes in insecticide resistance. Initial observations were only correlative, i.e., high CYP4G expression and resistance (Pittendrigh et al., 1997, Pridgeon et al., 2003, Müller et al., 2008, Jones et al., 2013). RNAi of CYP4G19 in *B. germanica* and of CYP4G14 in *Tribolium castaneum* increases the toxicity of pyrethroids (Guo et al., 2010, Chen et al., 2019, Kalsi and Palli, 2017). The control of CHC production by CYP4G enzymes appears to prevent insecticide

penetration, contributing to resistance (Balabanidou et al., 2016, Balabanidou et al., 2018, Balabanidou et al., 2019, Wang et al., 2019). In the DTT-resistant strain of *D. melanogaster*, 91-R, CYP4G1 was one of several constitutively overexpressed genes, leading to increased CHC content. CYP4G1 RNAi also suggested its role in representing penetration through the high production of CHCs in *D. melanogaster* (Kim et al., 2018).

While the function of CYP4Gs as an oxidative decarbonylase in CHC synthesis is now well documented, other functions are yet to be determined. In many insects where multiple CYP4Gs occur, only one with CHC synthesis function (CYP4G1 clade) is well characterized. For instance, *D. melanogaster* CYP4G1 is functionally characterized as an oxidative decarbonylase, whereas the function of CYP4G15 is unclear. CYP4G15 is localized in the brain of larvae and antennae of adults (Maibeche-Coisne et al., 2000; Chung et al., 2009). In *An. gambiae*, CYP4G16 is a CHC-producing enzyme, but CYP4G17 is poorly understood, and its function remains unknown. The honeybee, CYP4G11, is an ortholog of CYP4G15 and is highly expressed in antennae and mesothoracic legs (Mao et al., 2015). CYP4G11 expression in these olfactory appendages varies from lowest to highest from emerged workers to nurses to foragers (Nie et al., 2018). The maximal expression of CYP4G11 in the antennae and metathoracic leg in foragers suggests a function in chemosensory perception (Mao et al., 2015; Nie et al., 2018).

As discussed above, most insects have at least one representative of each CYP4G1 and CYP4G15 clade. While the functions of CYP4G1 clade members are consistent with desiccation resistance, the CYP4G15 clade is poorly understood and is the focus of this thesis.

III. References

Alphey, L. (2014). Genetic Control of Mosquitoes. In M. R. Berenbaum (Ed.), *Annual Review of Entomology, Vol 59, 2014* (Vol. 59, pp. 205-224). Annual Reviews. https://doi.org/10.1146/annurev-ento-011613-162002

Alphey, L. S., Crisanti, A., Randazzo, F., & Akbari, O. S. (2020). Standardizing the definition of gene drive [Editorial Material]. *Proceedings of the National Academy of Sciences of the United States of America*, *117* (49), 30864-30867. https://doi.org/10.1073/pnas.2020417117

Andrews, K. A., Wesche, D., McCarthy, J., Mohrle, J. J., Tarning, J., Phillips, L., . . . Grasela, T. (2018). Model-Informed Drug Development for Malaria Therapeutics. In P. A. Insel (Ed.), *Annual Review of Pharmacology and Toxicology*, *Vol 58* (Vol. 58, pp. 567-582). Annual Reviews. https://doi.org/10.1146/annurev-pharmtox-010715-103429

Berman, J., & Radhakrishna, T. (2017). The Tropical Disease Priority Review Voucher: A Game-Changer for Tropical Disease Products [Review]. *American Journal of Tropical Medicine and Hygiene*, *96*(1), 11-13. https://doi.org/10.4269/ajtmh.16-0099

Briegel, H., & Horler, E. (1993). Multiple blood meals as a reproductive strategy in anopheles (Diptera, culcidae). *Journal of Medical Entomology*, *30*(6), 975-985. https://doi.org/10.1093/jmedent/30.6.975

Calla, B., MacLean, M., Liao, L. H., Dhanjal, I., Tittiger, C., Blomquist, G., & Berenbaum, M. (2018). Functional characterization of CYP4G11a highly

conserved enzyme in the western honey bee Apis mellifera [Article]. *Insect Molecular Biology*, *27*(5), 661-674. https://doi.org/10.1111/imb.12516

Chiu, C. C., Keeling, C. I., & Bohlmann, J. (2019). Cytochromes P450 Preferentially Expressed in Antennae of the Mountain Pine Beetle. *Journal of Chemical Ecology*, *45*(2), 178-186. https://doi.org/10.1007/s10886-018-0999-0

Daborn, P., Boundy, S., Yen, J., Pittendrigh, B., & Ffrench-Constant, R. (2001). DDT resistance in Drosophila correlates with Cyp6g1 over-expression and confers cross-resistance to the neonicotinoid imidacloprid [Article]. *Molecular Genetics and Genomics*, *266*(4), 556-563. https://doi.org/10.1007/s004380100531

Daborn, P J et al. "A single p450 allele associated with insecticide resistance in Drosophila." Science (New York, N.Y.) vol. 297,5590 (2002): 2253-6. doi:10.1126/science.1074170

Despres, L., David, J. P., & Gallet, C. (2007). The evolutionary ecology of insect resistance to plant chemicals [Review]. *Trends in Ecology & Evolution*, *22*(6), 298-307. https://doi.org/10.1016/j.tree.2007.02.010

Durand, N., Carot-Sans, G., Bozzolan, F., Rosell, G., Siaussat, D., Debernard, S., . . . Maibeche-Coisne, M. (2011). Degradation of pheromone and plant volatile components by a same odorant-degrading enzyme in the cotton leafworm, *Spodoptera littoralis* [Article]. *Plos One*, *6*(12), 7, Article e29147. https://doi.org/10.1371/journal.pone.0029147

Durand, N., Carot-Sans, G., Chertemps, T., Montagne, N., Jacquin-Joly, E., Debernard, S., & Maibeche-Coisne, M. (2010). A diversity of putative carboxylesterases are expressed in the antennae of the noctuid moth Spodoptera littoralis [Article].

Insect Molecular Biology, *19*(1), 87-97. https://doi.org/10.1111/j.1365-2583.2009.00939.x

Feyereisen, R. (2020). Origin and evolution of the CYP4G subfamily in insects, cytochrome P450 enzymes involved in cuticular hydrocarbon synthesis [Article]. *Molecular Phylogenetics and Evolution*, *143*, 15, Article 106695. https://doi.org/10.1016/j.ympev.2019.106695

Gantz, V. M., Jasinskiene, N., Tatarenkova, O., Fazekas, A., Macias, V. M., Bier, E., & James, A. A. (2015). Highly efficient Cas9-mediated gene drive for population modification of the malaria vector mosquito Anopheles stephensi [Article]. *Proceedings of the National Academy of Sciences of the United States of America*, *112*(49), E6736-E6743. https://doi.org/10.1073/pnas.1521077112

Guidobaldi, F., May-Concha, I. J., & Guerenstein, P. G. (2014). Morphology and physiology of the olfactory system of blood-feeding insects. *Journal of Physiology-Paris*, *108*(2-3), 96-111. https://doi.org/10.1016/j.jphysparis.2014.04.006

Hammond, Andrew et al. “A CRISPR-Cas9 gene drive system targeting female reproduction in the malaria mosquito vector Anopheles gambiae.” Nature biotechnology vol. 34,1 (2016): 78-83. doi:10.1038/nbt.3439

Harrington, L. C., Edman, J. D., & Scott, T. W. (2001). Why do female Aedes aegypti (Diptera : Culicidae) feed preferentially and frequently on human blood? *Journal of Medical Entomology*, *38*(3), 411-422. https://doi.org/10.1603/0022-2585-38.3.411

Hecht, D., & Fogel, G. B. (2012). Modeling the evolution of drug resistance in malaria [Article]. *Journal of Computer-Aided Molecular Design*, *26*(12), 1343-1353. https://doi.org/10.1007/s10822-012-9618-2

Ignell, Rickard et al. "Neuronal architecture of the mosquito deutocerebrum." The Journal of comparative neurology vol. 493,2 (2005): 207-40. doi:10.1002/cne.20800

Keeling, C. I., Henderson, H., Li, M., Dullat, H. K., Ohnishi, T., & Bohlmann, J. (2013). CYP345E2, an antenna-specific cytochrome P450 from the mountain pine beetle, Dendroctonus ponderosae Hopkins, catalyses the oxidation of pine host monoterpene volatiles. *Insect Biochemistry and Molecular Biology*, *43*(12), 1142-1151. https://doi.org/10.1016/j.ibmb.2013.10.001

Laughlin, J. D., Ha, T. S., Jones, D. N. M., & Smith, D. P. (2008). Activation of pheromone-sensitive neurons is mediated by conformational activation of pheromone-binding protein [Article]. *Cell*, *133*(7), 1255-1265. https://doi.org/10.1016/j.cell.2008.04.046

Leal, W. S. (2013). Odorant Reception in Insects: Roles of Receptors, Binding Proteins, and Degrading Enzymes. In M. R. Berenbaum (Ed.), *Annual Review of Entomology, Vol 58* (Vol. 58, pp. 373-391). Annual Reviews. https://doi.org/10.1146/annurev-ento-120811-153635

Macedo, P. A., Schleier, J. J., Reed, M., Kelley, K., Goodman, G. W., Brown, D. A., & Peterson, R. K. D. (2010). Evaluation of efficacy and human health risk of aerial ultra-low volume applications of pyrethrins and piperonyl butoxide for adult mosquito management in response to west nile virus activity in sacramento

county, california [Article]. *Journal of the American Mosquito Control Association*, *26*(1), 57-66. https://doi.org/10.2987/09-5961.1

Maibeche-Coisne, M., Monti-Dedieu, L., Aragon, S., & Dauphin-Villemant, C. (2000). A new cytochrome P450 from Drosophila melanogaster, CYP4G15, expressed in the nervous system [Article]. *Biochemical and Biophysical Research Communications*, *273*(3), 1132-1137. https://doi.org/10.1006/bbrc.2000.3058

Peterson, R. K. D., Macedo, P. A., & Davis, R. S. (2006). A human-health risk assessment for West Nile virus and insecticides used in mosquito management [Article]. *Environmental Health Perspectives*, *114*(3), 366-372. https://doi.org/10.1289/ehp.8667

Pongtavornpinyo, W., Yeung, S., Hastings, I. M., Dondorp, A. M., Day, N. P. J., & White, N. J. (2008). Spread of anti-malarial drug resistance: Mathematical model with implications for ACT drug policies [Article]. *Malaria Journal*, *7*, 12, Article 229. https://doi.org/10.1186/1475-2875-7-229

Pottier, M. A., Bozzolan, F., Chertemps, T., Jacquin-Joly, E., Lalouette, L., Siaussat, D., & Maibeche-Coisne, M. (2012). Cytochrome P450s and cytochrome P450 reductase in the olfactory organ of the cotton leafworm Spodoptera littoralis [Article]. *Insect Molecular Biology*, *21*(6), 568-580. https://doi.org/10.1111/j.1365-2583.2012.01160.x

Ridley, D. B. (2017). Priorities for the Priority Review Voucher [Review]. *American Journal of Tropical Medicine and Hygiene*, *96*(1), 14-15. https://doi.org/10.4269/ajtmh.16-0600

Ridley, D. B., Ganapathy, P., & Kettler, H. E. (2021). US Tropical Disease Priority Review Vouchers: Lessons In Promoting Drug Development And Access [Review]. *Health Affairs*, *40*(8), 1243-1251. https://doi.org/10.1377/hlthaff.2020.02273

Schmidt, H. R., & Benton, R. (2020). Molecular mechanisms of olfactory detection in insects: beyond receptors [Review]. *Open Biology*, *10*(10), 11, Article 200252. https://doi.org/10.1098/rsob.200252

Shankar, Shruti, and Conor J McMeniman. "An updated antennal lobe atlas for the yellow fever mosquito *Aedes aegypti*." *PLoS neglected tropical diseases* vol. 14,10 e0008729. 20 Oct. 2020, doi:10.1371/journal.pntd.0008729

Soderlund, D. M. (2012). Molecular mechanisms of pyrethroid insecticide neurotoxicity: recent advances [Review]. *Archives of Toxicology*, *86*(2), 165-181. https://doi.org/10.1007/s00204-011-0726-x

Tang, W. X., Wang, D., Wang, J. Q., Wu, Z. W., Li, L. Y., Huang, M. L., . . . Yan, D. Y. (2018). Pyrethroid pesticide residues in the global environment: An overview [Review]. *Chemosphere*, *191*, 990-1007. https://doi.org/10.1016/j.chemosphere.2017.10.115

Vogt, R G, and L M Riddiford. "Pheromone binding and inactivation by moth antennae." *Nature* vol. 293,5828 (1981): 161-3. doi:10.1038/293161a0

R.G. Vogt, 3.15 - Molecular Basis of Pheromone Detection in Insects, Editor(s): Lawrence I. Gilbert, Comprehensive Molecular Insect Science, Elsevier, 2005,

Pages 753-803, ISBN 9780444519245, https://doi.org/10.1016/B0-44-451924-6/00047-8.
(https://www.sciencedirect.com/science/article/pii/B0444519246000478)

Wang, Shu-Ping et al. “The involvement of cytochrome P450 monooxygenases in methanol elimination in Drosophila melanogaster larvae.” *Archives of insect biochemistry and physiology* vol. 79,4-5 (2012): 264-75. doi:10.1002/arch.21021

Wu, H. H., Liu, J. Y., Liu, Y. M., Abbas, M., Zhang, Y. C., Kong, W. A., . . . Zhang, J. Z. (2022). CYP6FD5, an antenna-specific P450 gene, is potentially involved in host plant recognition in Locusta migratoria [Article]. *Pesticide Biochemistry and Physiology*, *188*, 9, Article 105255. https://doi.org/10.1016/j.pestbp.2022.105255

Younus, F., Chertemps, T., Pearce, S. L., Pandey, G., Bozzolan, F., Coppin, C. W., . . . Oakeshott, J. G. (2014). Identification of candidate odorant degrading gene/enzyme systems in the antennal transcriptome of Drosophila melanogaster [Article]. *Insect Biochemistry and Molecular Biology*, *53*, 30-43. https://doi.org/10.1016/j.ibmb.2014.07.003

Younus, F., Fraser, N. J., Coppin, C. W., Liu, J. W., Correy, G. J., Chertemps, T., . . . Oakeshott, J. G. (2017). Molecular basis for the behavioral effects of the odorant degrading enzyme Esterase 6 in Drosophila [Article]. *Scientific Reports*, *7*, 12, Article 46188. https://doi.org/10.1038/srep46188

Zhang, L. Y., Shen, Y. D., Jiang, X. C., & Liu, S. (2022). Transcriptomic identification and expression profile analysis of odorant-degrading enzymes from the asian corn borer moth, Ostrinia furnacalis [Article]. *Insects*, *13*(11), 18, Article 1027. https://doi.org/10.3390/insects13111027

Zhao, Z. L., & McBride, C. S. (2020). Evolution of olfactory circuits in insects. *Journal of Comparative Physiology a-Neuroethology Sensory Neural and Behavioral Physiology*, *206*(3), 353-367. https://doi.org/10.1007/s00359-020-01399-6

IV. Figures

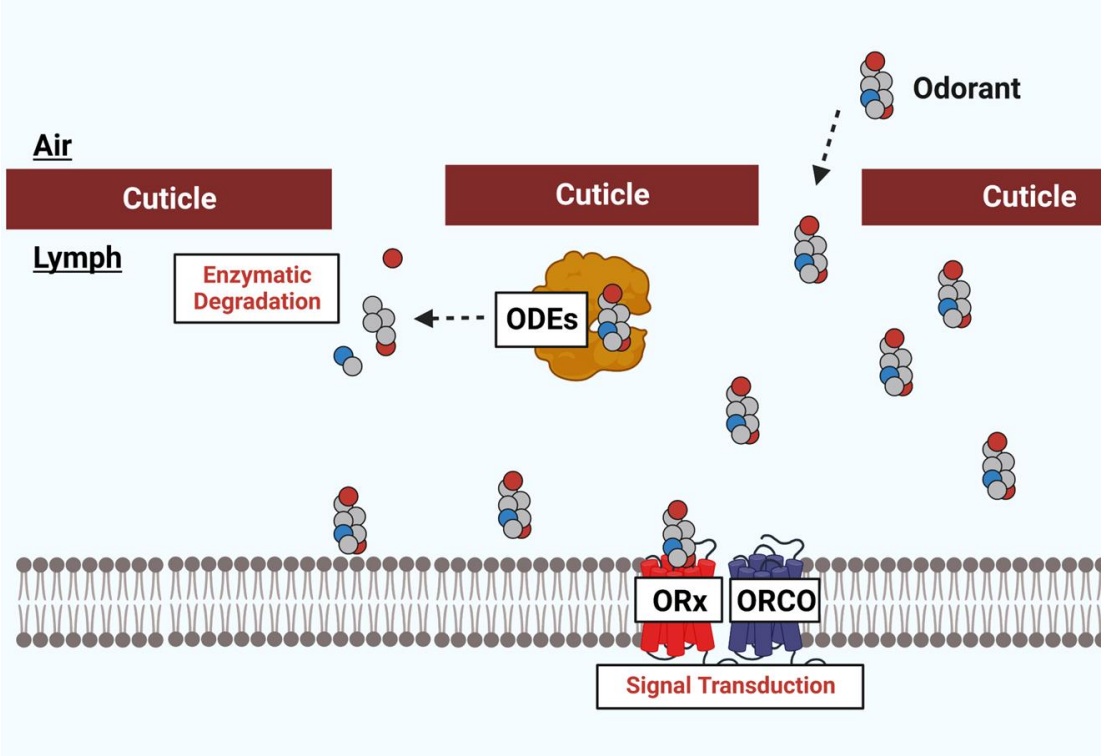

Figure 1.1. The proposed mechanism for odorant degradation within the insect olfactory sensilla. Odorant travels through pores into the sensilla lymph to reach the odorant receptor-co receptor (OR-ORCO) complex (or other chemoreceptors such as gustatory or ionotropic). Once the signal is transduced, odor molecule is released from the OR-ORCO complex and are likely degraded by ODEs. ODE: odorant-degrading enzyme; ORCO: olfactory receptor co-receptor; ORx: olfactory receptor.

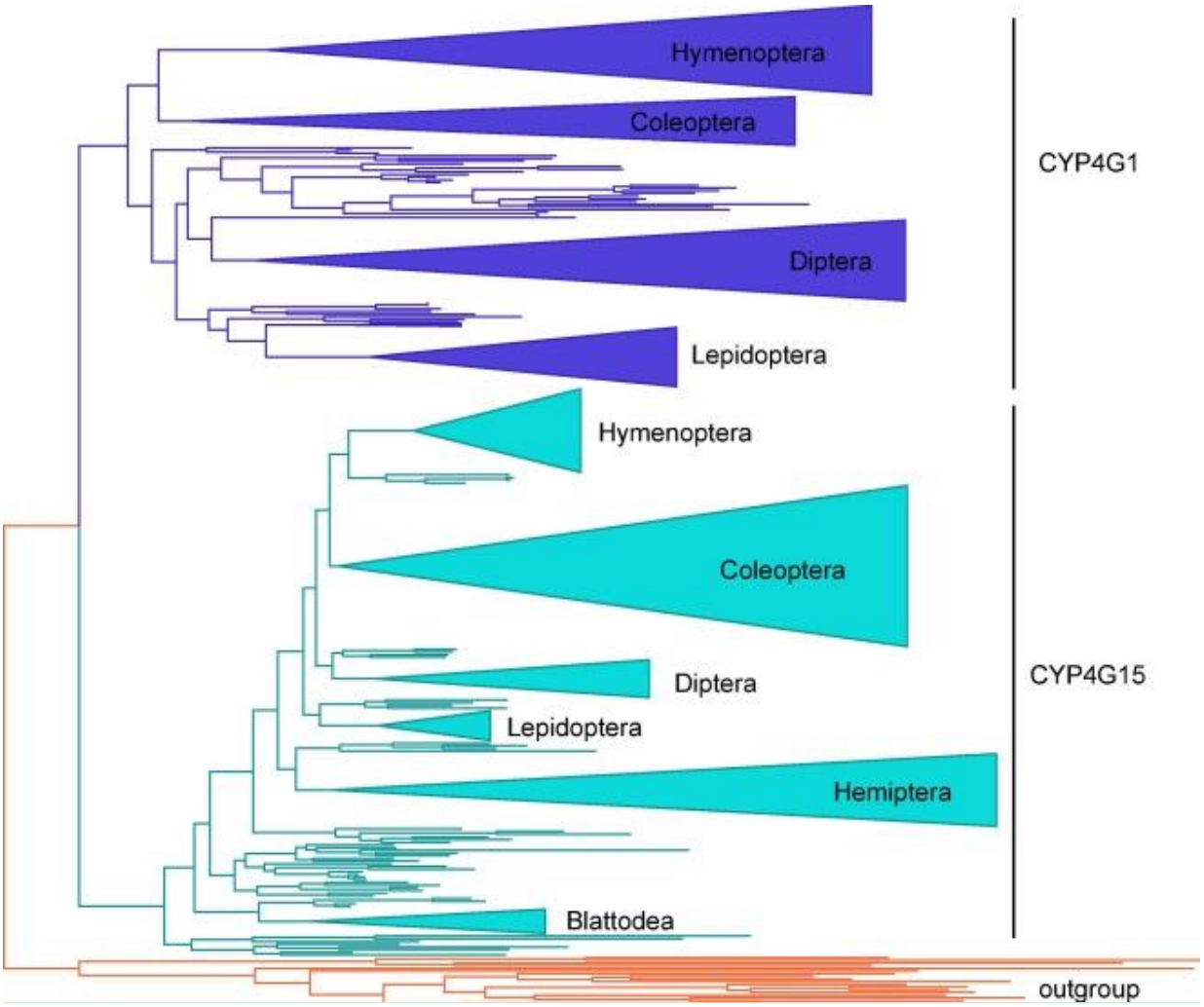

Figure 1.2. Phylogeny of the CYP4G genes. Sequences for CYP4G and closely related CYP4 clan P450s (outgroup) aligned by MAFFT and RAxML built the tree shown. Sequences in major insect orders collapsed for clarity. Adapted from (Feyereisen, 2020)

Chapter 2

Localization of Cytochrome P450s, CYP4G35, and CYP4G36, in mosquito olfactory tissues by in situ hybridization and immunohistochemistry

I. Abstract:

Mosquitoes rely on odor sensing for host-seeking behavior. The olfactory appendages of mosquitoes are covered in the sensilla hairs that house the olfactory receptors. Therefore, we hypothesized that an odor-degrading enzyme should localize in these sensilla hairs. To test this hypothesis, I used whole-mount immunohistochemistry and *in-situ* hybridization to locate the CYP4G35 protein and mRNA within *Aedes aegypti* olfactory tissues. CYP4G35 protein and mRNA transcript were present in the sensilla hairs of the antenna and proboscis, whereas results in another chemosensory tissue, maxillary palps, were inconclusive. This localization of CYP4G35 within the sensilla hair supports a putative role in olfaction, likely as an odor-degrading enzyme.

II. Introduction

Aedes aegypti is an anautogenous mosquito and an important disease vector transmitting numerous pathogens such as arboviruses: dengue, chikungunya, and Zika virus and nematodes (Souza-Neto et al., 2019; Weaver et al., 2018). Mosquitoes use olfaction, gustation, and vision to find sugar sources or, for a female mosquito, a vertebrate host (Melo et al., 2004; Sparks et al., 2018). Mosquitoes rely on olfactory senses to seek vertebrate hosts using chemical cues (Takken and Knols, 1999). The olfactory systems process signals through the rapid inactivation of the odor molecules once they have activated their receptors (Maıbeche, 2021). Odorant molecules can vary in

the chemical structure; therefore, diverse metabolic enzymes such as cytochrome P450, dehydrogenases, oxidases, reductases, and esterases can potentially serve as odor-degrading enzymes (ODEs) (Baldwin et al., 2021; Krieger et al., 2005; Leal, 2013).

Cytochrome P450s (CYPs) constitute one of the most prominent gene families among all living organisms. *Aedes aegypti* has 160 putatively catalytically active CYPs (Strode et al., 2008). In insects, CYP fall into four clans: CYP2, CYP3, CYP4, and mitochondrial CYPs (Dermauw et al., 2022). Two other clans were identified recently, CYP16 and CYP20, but these are not found in Neoptera (Dermauw et al. 2020). Both mitochondrial and CYP2 clans participate in core functions related to insect development and physiology, whereas CYP3 and CYP4 clans are associated with interactions with environmental volatiles (Scott & Wen, 2001). The CYP4 clan is a diverse clan within the insect genomes (Feyereisen, 2020), with some members involved in insecticide resistance and others with different roles, including biosynthesis of endogenous compounds and odor processing (Feyereisen, 2012, 2020; Leal, 2013; Zhang et al., 2022).

With the exception of some Hemipterans, insect genomes encode one or two CYP4G genes. The model organism *D. melanogaster* genome has two CYP4Gs: CYP4G1 and CYP4G15. Similarly, *Ae. aegypti* genome also has two CYP4G genes, CYP4G35 (CYP4G-15 like) and CYP4G36 (CYP4G-1 like). CYP4G1 from *D. melanogaster* has been well characterized. CYP4G1 has been localized in oenocytes and catalyzes the last two steps of the cuticular hydrocarbon (CHC) biosynthesis (Qiu et al., 2012). Similarly, CYP4G1 orthologs in other insects are known oxidative decarbonylase catalyzing CHC biosynthesis (Balabanidou et al., 2016; Calla et al., 2018; Jing et al., 2022; Kefi et al., 2019; MacLean et al., 2018; Qiu et al., 2012; Wang et al., 2019; Wu et al., 2020)

suggesting that *Ae. aegypti* CYP4G36 may have a similar role. However, the potential function of orthologs that belong to the CYP4G15 clade remains unknown. In *D. melanogaster* CYP4G15 (ortholog of *Ae. aegypti* CYP4G35) was localized in the central nervous system and brain of larvae (Chung et al., 2009; Maibeche-Coisne et al., 2000) and was expressed in adult antennae (Younus et al., 2014). In bark beetles and honeybees, CYP4G35 orthologs were localized in the antennae (Cano-Ramirez et al., 2013; Mao et al., 2015). In *Anopheles gambiae,* CYP4G17 (*Ae. aegypti* CYP4G35 ortholog) appears to have a role in xenobiotic metabolism (Kefi et al., 2019; (Balabanidou et al., 2016).

Our preliminary data showed that CYP4G35 transcripts were significantly higher in adult olfactory appendages: antennae, proboscis, and palps compared to other tissues tested, such as the legs, midgut, and reproductive tissues. Knockdown of CYP4G35 using RNAi resulted in altered host-seeking behavior suggesting its function in odor perception. Other CYPs in insect olfactory tissues have been characterized to function as pheromone-degrading enzymes (PDEs) (Ahmad & Ray, 1987; Nie et al., 2018; Wojtasek & Leal, 1999) and as odor-degrading enzymes (ODEs) for plant-volatiles (Dickens et al., 1992). These CYPs are expressed in the antennae, presumably involved in signal termination by limiting odorants from the olfactory sensilla (Cano-Ramirez et al., 2013). I hypothesized that for CYP4G35 to function as an ODE, it should localize in the olfactory tissue. I used immunohistochemistry and in situ hybridization to test this hypothesis for localizing CYP4G35 in antennae, proboscis, and maxillary palps.

III. Materials and Methods

Mosquito Rearing

Aedes aegypti (LVP strain) colonies were maintained at 27 °C and 60-70% relative humidity (RH) with a photoperiod of 16 h light and 8 h dark in a dedicated insectary. Eggs were hatched overnight in small plastic cups in deionized water. First instar larvae were counted (100 per 1.5-gallon pan) and reared in 500 mL of deionized water on a powdered fish food diet (Tetramin®, Melle, Germany), as described in detail in (Pooraiiouby et al. 2018). Pupae were collected from the rearing container and transferred to adult emergence cages. Adults were fed a 10% sucrose solution containing food color for regular colony maintenance. Adult females were blood-fed 4 days after emergence, and egg cups lined with a paper towel were placed in the cage 48 h after blood feeding. The egg cups were removed from the cages 3 days later; egg sheets were washed and dried overnight at room temperature and stored in a plastic bag.

Antibody generation

Antibodies for both CYP4G35 (XP_001658068.2: KLPSPSLSEIIAKEESESKESLP-Cys (24aa) and CYP4G36 (XP_001648376.1: KTAEFEKPKSNINTNSVEGLS-Cys (22aa) were generated by Pacific Immunology (Pacific Immunology National Institutes of Health animal welfare assurance No. A41820-01). These synthetic peptides were used with complete Freund's adjuvant (CFA) and incomplete Freund's adjuvant (IFA) to immunize two rabbits per peptide. Pre-immune sera (5 ml.) were collected from all four rabbits. The first immunization with CFA was carried out on the same day as pre-immune sera collection. After that, two booster doses of IFA were given at three weeks intervals each. Sera were collected for ELISA one week after the second booster and again a week and two weeks later (Production bleed). A third and final booster was injected four weeks after the last

booster, and rabbits were bled every week for four weeks. Rabbits were euthanized according to IACUC protocol.

Dot blot assay for detection of CYP4Gs antibodies

We used dot blots to determine the specificity of antisera to mosquito CYP4Gs. For protein extraction, mosquitoes were collected in phosphate buffer saline and protease inhibitor (1X PBS-PI) solution and homogenized with a pestle. Samples were centrifuged at 12,000 x g for 5 mins at 4°C, and the supernatant was collected and stored at 4°C. 2ul of protein was spotted onto the nitrocellulose membrane and allowed to dry at room temperature (RT). The membrane was rewetted in Tris buffer saline- Triton (TBS-T) and blocked with blocking buffer (5% dry milk-TBS-T– 0.03% Triton X-100). Membranes were then incubated in primary antiserum diluted in BSA-TBS-T (1/500, 1/1000, 1/5000, 1/25000) for 1 hr. at RT. The membrane was rinsed in TBS-T three times, 5 mins. each at RT and incubated with the anti-rabbit conjugated secondary antibody Alexa flour 647 (1:10,000 dilution) (Jackson Immuno) for 1 hour at RT, followed by three washes in TBS-T for 5 mins each. The membrane was scanned on an Odyssey Scanner at 700 – 800 nm wavelength for visualization.

Whole-mount – fluorescent immunohistochemistry (WM - FIHC)

Heads of 6-7 day-old female mosquitoes' (8 heads; containing a pair of antennae) were removed from cold anesthetized mosquitoes using fine forceps and transferred directly to zinc formaldehyde (0.25% ZnCl2, 1% formaldehyde, 135 mM NaCl, 1.2 % sucrose, 0.03% Triton X-100) for 24 h (Schultze et al., 2013). Following fixation for 24 h at room temperature (RT), antennae were washed with Hepes Buffer Saline (HBS) for 15 mins (150 mM NaCl, 5 mM KCl, 25 mM sucrose, 10 mM Hepes, 5 mM CaCl2, 0.03%

Trition X-100). The mosquito heads were transferred into a concave glass slide that contained HBS buffer under a microscope using ultra-fine forceps. The antennae were removed from the head of the mosquito and were carefully squeezed about ten times with ultra-fine forceps and transferred to PCR tubes. The antennae were incubated in an HBS buffer for 15 min and in 80% Methanol / 20% DMSO (Schultze et al., 2013). Subsequently, the antennae were incubated in a 5% BSA blocking solution (PBS, 5% BSA, 1% DMSO, 0.03% Triton X-100) overnight. The solution was replaced by a 5% BSA blocking solution containing CYP4G35 primary antibody (dilution 1:100), and the PCR tube was placed for 30 sec in a water bath sonifier (FS30 Ultrasonic Cleaner, Fischer Scientific) at 40 Hz. Antennae were incubated for four days at 6°C, repeating the sonication on the second day. This was followed by washing thrice for 15 min each at RT in PBS, 1% DMSO, and 0.03% Triton X-100. The secondary antibody (anti-Rabbit Alexa Fluor 555) was diluted (1:1000) in a blocking solution and added to the samples. To increase the permeabilization of the antibody, samples were sonicated for 30 sec in a water bath sonifier and then incubated for three days at 6°C. After incubation, the samples were washed three times for 15 min each in PBS with 1% DMSO, 0.03% Triton X-100 and a short rinse in PBS antennae. Once placed on charged slides, the antennae were mounted in Mowiol (Sigma-Aldrich) mounting media. The coverslip then covered the sample for 24-48 hours before sealing it with nail polish the sample or stored at -4°C.

Whole-mount fluorescent *in-situ* hybridization (WM-FISH)

Female *Ae. aegypti* heads were dissected from cold anesthetized mosquitoes and transferred directly to zinc formaldehyde (as explained in WM-IHC protocol) for 24 hrs. (Schultze et al., 2013). After fixation for 24 hr. at RT, antennae were washed with HBS

buffer and transferred onto a concave glass slide that contained HBS buffer. Under a microscope using ultra-fine forceps, the samples were squeezed, with each forceps holding one end of the antennae. These were then carefully washed in HBS buffer for 15 min and incubated in 80% Methanol / 20% DMSO (as explained in WM-IHC protocol) (Schultze et al., 2013). The antennae were transferred to a PCR tube and then incubated in prehybridization solution (50% formamide, 5xSSC, 1x Denhardt's reagent, 50 μg/ml yeast RNA, 1% Tween 20, 0.1% Chaps, 5 mM EDTA pH 8.0) at 45°C for 5–6 hrs and followed by incubation for three days at 55°C in the same solution containing a DIG-labeled antisense RNA at (1:10-1:100). In control experiments, DIG-labeled sense RNA probes instead of antisense RNA probes were used. Once prehybridization was completed, the antennae were washed in 0.1 x SSC, 0.03% Triton X-100 four times for 15 min each, and the antennae were treated with a blocking solution (Schultze et al., 2013). Then blocking solution containing the anti-DIG Alexa Flour 647 (1:1000) (Jackson Immuno) was added. Subsequently, the tubes were placed for 30 sec in a water bath sonifier (FS30 Ultrasonic Cleaner, Fischer Scientific) and then incubated for three days at 6°C. Once secondary antibody incubation of the antennae was completed, they were washed three times for 15 min each in PBS with 1% DMSO, 0.03% Triton X-100 and a short rinse in PBS antennae. Once placed on charged slides, the antennae were mounted in Mowiol mounting media. The coverslip then covered the sample for 24-48 hours before sealing it with nail polish the sample or stored at -4°C.

Microscopy

Analysis of samples by microscopy: Antennae, proboscis, and palps samples from WM-IHC and WM-FISH experiments were analyzed for fluorescence using a BZ-X800

Keyence microscope (Keyence, United States). Images of the red (protein) and green (mRNA probe) fluorescence channels were recorded. Image stacks were used to generate pictures representing projections of selected optical planes, with the red and green fluorescence channels overlaid with the transmitted-light channel or shown separately. All images were captured at 10X magnification. Those artifacts were removed for images containing bleached edges due to bubbles forming in the mounting media.

Settings for Confocal SP8: The samples used in Keyence BZ-X microscopy were used for imaging at higher magnifications using a confocal microscope (Leica SP8 confocal microscope). Antennae joint autofluorescence was removed by selecting specific excitation (smart) wavelength of 555 nm specific to the secondary antibody AF 555 for evident fluorescence. All images were taken at 100 or 125x magnification.

DIG-labeled RNA probes construction

Primers were designed to amplify the transcript of interest. A 584-nucleotide sequence was amplified for the CY4P35 mRNA probe, a region unique to CYP4G35. The PCR product for the CYP4G35 RNA probes was cloned into the pMiniT 2.0 vector using NEB® PCR Cloning Kit. The pMiniT2.0 cloning vector contains T7 and Sp6 polymerase priming sites that enable the production of sense and antisense run-off transcription products from a single clone. The cloned amplicon was sequenced to verify the sequence fidelity and orientation within the vector plasmid. Restriction digestion was performed with the BamHI and NotI enzymes to produce antisense and a sense-strand RNA probe. Gel electrophoresis was used to verify that the pMiniT2.0 clone was linearized entirely. The linearized plasmid DNA was purified (Zymo PCR purification kit). The digoxigenin (DIG)- labeled single-stranded RNA probe was prepared by

performing an *in vitro* transcription reaction using 1µg of the linearized plasmid DNA as a template. The reaction was prepared with SP6/T7 RNA polymerase, transcription buffer, and DIG RNA labeling mix as described by the manufacturer's instruction (Roche, DIG RNA labeling Kit (SP6/T7) (Juhn & James, 2012). A total of 75 ng/ml of DIG-labelled mRNA was made for both the antisense and sense probe. The DIG-labeled control is used alongside the CYP4G35 DIG-labeled probe (serial dilutions) on the nylon membrane to check the probe yield.

IV. Results

Localization of CYP4G35:

WM-FIHC and WM-FISH were used to determine the localization of CYP4G35 protein and mRNA in olfactory tissues.

Antennae: Antennae from female mosquitoes were fixed and incubated with either an antibody against CYP4G35 or CYP4G36 (control) for protein localization (WM-IHC). Similarly, fixed antennae were also incubated with DIG-labeled RNA probes for mRNA localization (WM-ISH/FISH). CYP4G35 stained antenna samples with specific fluorescence in the sensilla hair (Fig. 2.1A-C). This fluorescence was unique to the CYP4G35 antibody because neither the anti-CYP4G36 (Fig. 2.1 D-F) nor the control (no primary antibody/secondary antibody alone) (Fig. 2.1G-I) had similar staining in the sensilla hair of the antennae. The higher magnification images further show localized expression of CYP4G35 in the antennal sensilla base and shaft (Fig. 2.1 J-K). Antennal joints were fluoresced in all samples, suggesting either autofluorescence or non-specific secondary antibody binding.

In the WM-FISH experiment, CYP4G35 mRNA transcripts localization used a CYP4G35 antisense DIG-labelled RNA probe and a secondary anti-DIG antibody. The sense-DIG-labeled probes were used as a negative control. The fluorescent labeling of WM-FISH indicated the presence of CYP4G35 transcript at the root of the sensilla and throughout the sensilla hair (Fig. 2.2A-C). This fluorescence signal was absent in both sense probes (Fig. 2.2 D-F) and the no probe control (Fig. 2.2 G-I). Both protein and mRNA are localized in the sensilla space, suggesting that this protein is not secreted into the sensilla hair.

Proboscis: IHC and ISH were carried out in the same (dual IHC-ISH) samples for the proboscis staining. Fluorescent labeling of CYP4G35 protein was concentrated at the tip of the proboscis, which is covered in sensilla hair (Fig. 2.3A-B). The FISH results also showed a similar pattern of expression (Fig. 2.3 C). No specific fluorescence was noted in the negative control samples (no primary antibody and sense mRNA probe) (Fig 2.3E-H). This difference in staining with CYP4G35 and the primary antibodies was evident in higher magnification images where CYP4G35 is expressed in the proboscis (Fig. 2.3I) versus the negative control (Fig. 2.3J).

Maxillary Palps: IHC staining of the maxillary palps were used to evaluate whether the tissue expressed CYP4G35. The WM-IHC with CYP4G35 antibody showed no specific binding in palps (Fig 2.4A-C). The fluorescence was similar to that of the CYP4G36 antibody (Fig. 2D-F), suggesting non-specific binding. An extended z-stack analysis showing the fluorescence around the sensilla root resembling a ring both in the control and experiment is not shown.

V. Discussion

In this chapter, CYP4G35 mRNA and protein were localized in the mosquito olfactory tissues. In addition, CYP4G36 was used as a control to demonstrate the specificity of CYP4G35 expression. This data suggest that CYP4G35 mRNA and protein are expressed in the sensilla hair of the antenna and proboscis, but maxillary palp data was inconclusive. The primary olfactory appendages are the antennae, and the presence of an ODE would be reasonable as it contains many ORs. CYP4G35 at the proboscis tip suggests that CYP4G35 might also be involved in gustation. The chemosensory receptors housed in the sensilla of the proboscis are more diverse than the antenna, containing multiple IRs, ORs, and GRs. The staining of conserved ionotropic co-receptor IR25a revealed its presence at the tip of the proboscis (Herre et al., 2022). The sensilla at the proboscis tip house a combination of ORs and IRs (Herre et al., 2023); however, both receptors are involved in olfaction.

The inconclusive results of CYP4G35 staining in the maxillary palps may be due to difficulty permeating the antibody through the tissue; other studies have used a chitin/chymotrypsin mixture to treat the palps to increase antibody permeability prior to staining (Herre et al., 2023). In future experiments, we will pretreat palps to make them more permeable.

One central question about CYP4G35 is its location, whether it is present in the sensillary lymph or bound to the membrane. The topology analysis (TOPCONS) of CYP4G35 is inconsistent; the majority consensus from the analysis is that the CYP4G35 active site is inside the membrane. There was no signal peptide suggesting that it is unlikely to be secreted. CYPs are heme-thiolate proteins; their most conserved structural features are related to heme binding. Vertebrate CYPs have been shown in many different

subcellular membrane compartments, including the plasma membrane, endoplasmic reticulum, Golgi apparatus, peroxisomes, lysosomes, and mitochondria (Seliskar & Rozman, 2007). In prokaryotes, CYPs are membrane-bound and soluble proteins (Werck-Reichhart et al., 2000). CYP2E1 in humans is present in the cytosol and is induced by chronic alcohol consumption (Zakhari, 2006). In *An. gambiae*, the CYP4G17 (CYP4G35 ortholog) showed the protein dispersed throughout the cytoplasm and did not have a specific membrane-bound localization like CYP4G16 (Kefi et al., 2019). Therefore, it is possible that CYP4G35 also has this unique localization, and it might be cytosolic.

VI. Figures

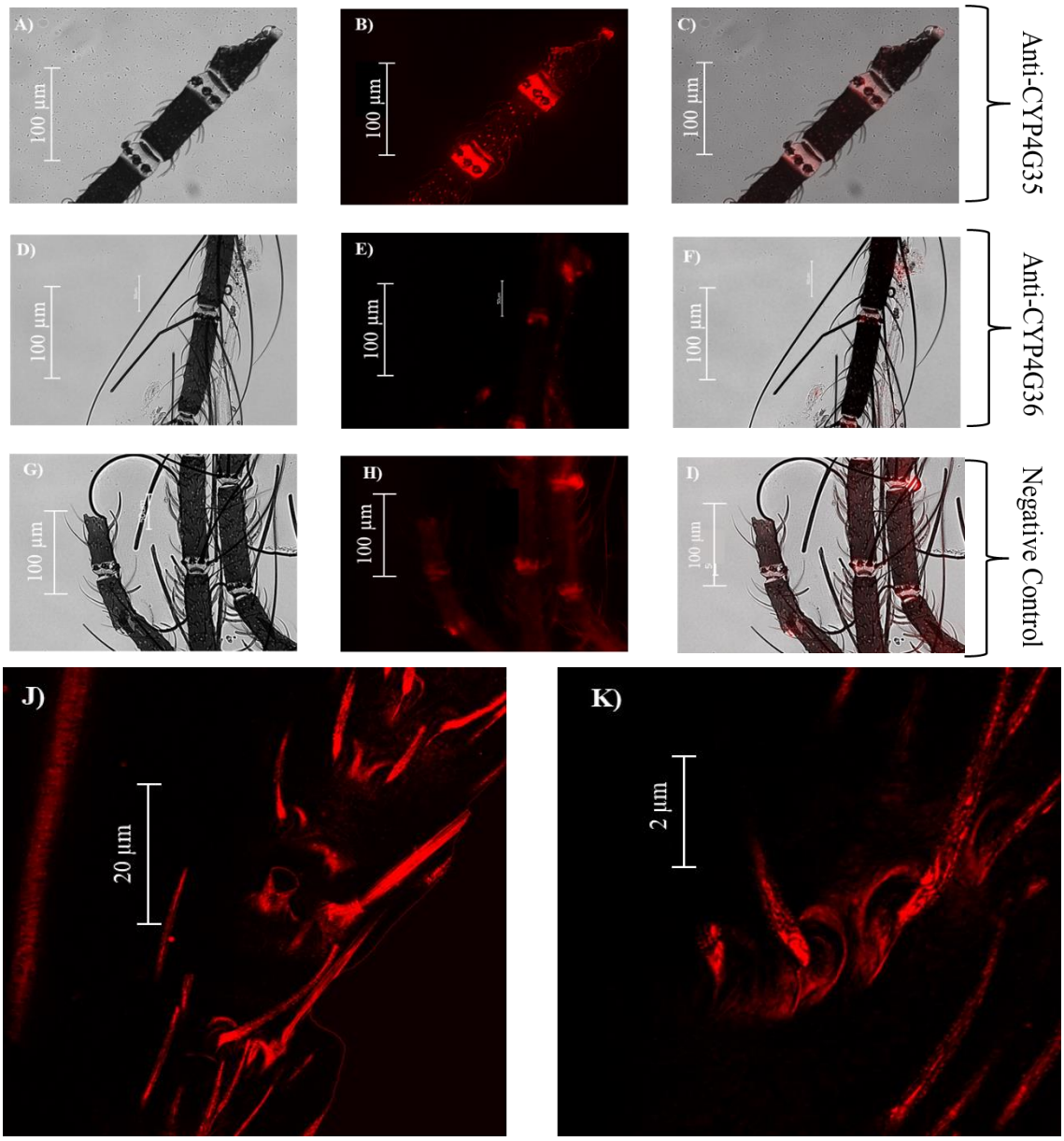

Figure 2.1. Localization of CYP4G35 in *Ae. aegypti* female antennae using Whole-mount fluorescent immunohistochemistry. Whole-mount fluorescent immunohistochemistry (WM-FIHC) antennae staining with CYP4G35 antibody alongside secondary antibody, AF 555. (A-C). A) Bright field image of the tissue. B)

CYP4G35 antibody fluorescent staining (BZ-X Filter TRITC). C) Overlay of images A and B. In the first set of control experiments for antennae staining, CYP4G36 antibody alongside a secondary antibody (AF 555) was used (D-F). D) Bright field image of the antenna tissue. E) CYP4G36 antibody body fluorescent staining (BZ-X Filter TRITC). F) Overlay of images D and E. In the second set of control experiments, only the secondary antibody AF 555 was used for staining (G-I). G) Bright-field image of the antennae tissue. H) Secondary antibody AF 555 fluorescent staining (BZ-X Filter TRITC). I) Overlay of images G and H. Images were taken on a Keyence BZ-X at 40 x magnification. Magnified images of the sample in B were taken at SP8 confocal (Lighting setting, Max resolution to speed setting) at 100x (K) and 125x (J).

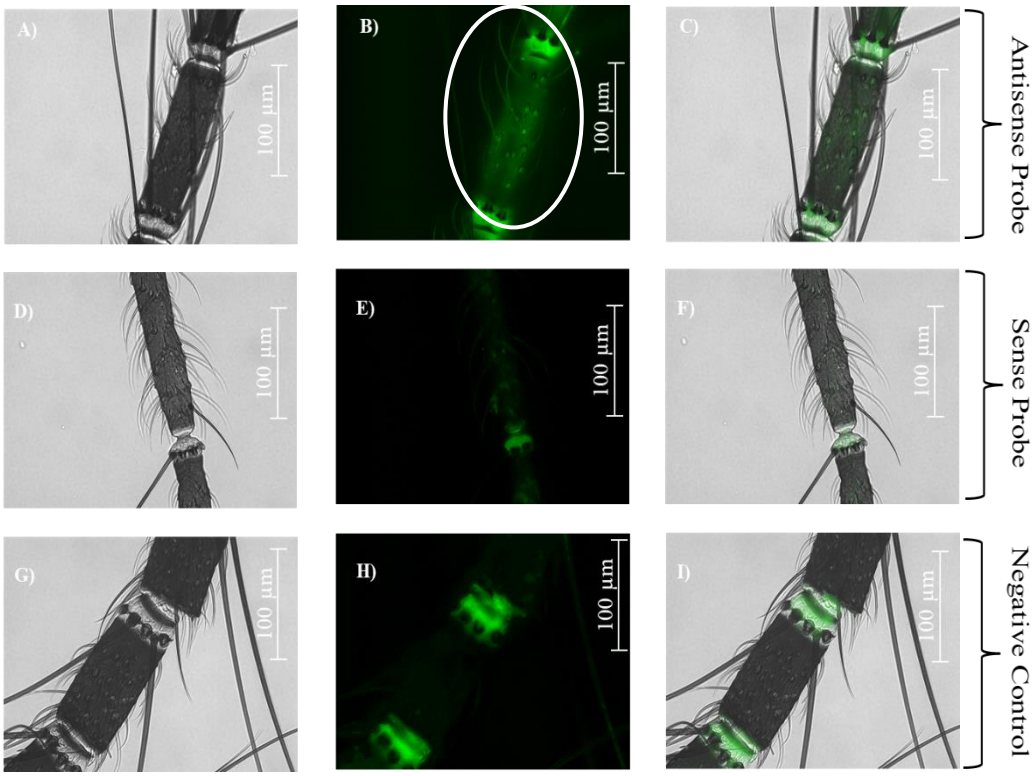

Figure 2.2. Localization of the CY4G35 in *Ae. aegypti* female antennae using whole-mount fluorescent *in-situ* hybridization. Whole-mount fluorescent *in-situ* hybridization in (WM-FISH) antennae staining with CYP4G35 antisense DIG-labeled probe and secondary anti-DIG AF 647 (A-C). A) Bright field image of the antenna tissue. B) CYP4G35 antisense DIG-labeled probe fluorescent staining (BZ-X Filter CY5). C) Overlay of images A and B. A control experiment using a CYP4G35 sense DIG-labeled probe and secondary anti-DIG AF 647 was used for WM-FISH (D-F). A control experiment using only secondary anti-DIG AF 647 for WM-FISH staining (G-I). D) Bright field image of the antenna tissue. E) CYP4G35 sense DIG-labeled probe and secondary anti-DIG AF 647 fluorescent staining (BZ-X Filter CY5). F) Overlay of images D and E. G) Bright field image of the antenna tissue. H) Only secondary anti-DIG

AF 647 fluorescent staining (BZ-X Filter CY5). I) Is an overlay of figures G and H, captured on a Keyence BZ-X at 40 x magnification.

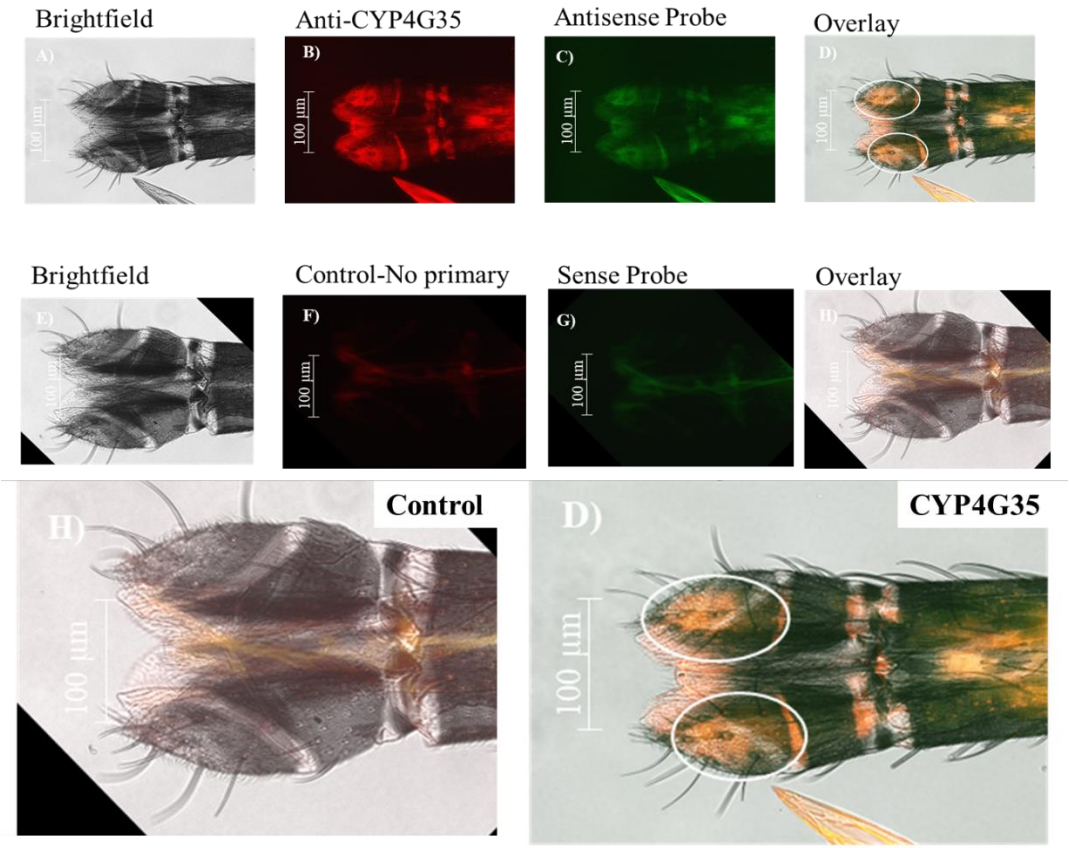

Figure 2.3. Localization of CYP4G35 in *Ae. aegypti* female proboscis using Whole-mount fluorescent *in-situ* hybridization & fluorescent immunohistochemistry. Whole-mount fluorescent *in-situ* hybridization & fluorescent immunohistochemistry (WM-FISH/FIHC) staining used a combination of CYP4G35 primary antibody (FIHC) and CYP4G35 antisense DIG-labeled probe (FISH), imaged at 40x magnification (A-D). A) Brightfield image of the probosci's tissue. B) CYP4G35 antibody body fluorescent staining (BZ-X Filter TRITC). C) CYP4G35 antisense DIG-labeled probe fluorescent staining (BZ-X CY5 filter). D) Overlay image of images A-C. In the control experiment for proboscis, WM-FIHC/FISH samples were stained with; CYP4G36 primary antibody (FIHC) and CYP4G35 sense DIG-labeled probe (FISH), imaged at 40x magnification (E-H). E) Brightfield image of the probosci's tissue. F) CYP4G36 antibody body fluorescent

staining (BZ-X Filter TRITC). G) CYP4G35 antisense DIG-labeled probe fluorescent staining (BZ-X CY5 filter). H) Overlay image of images E-G. I) Magnified image of image D at 60x, the sensilla, and its roots at the proboscis tip. J) Magnified image of image H at 60x, the sensilla, and its roots at the proboscis tip. The BZ-X Keyence microscope captured images. Post-capture analysis of the images was done through BZ-X analysis software.

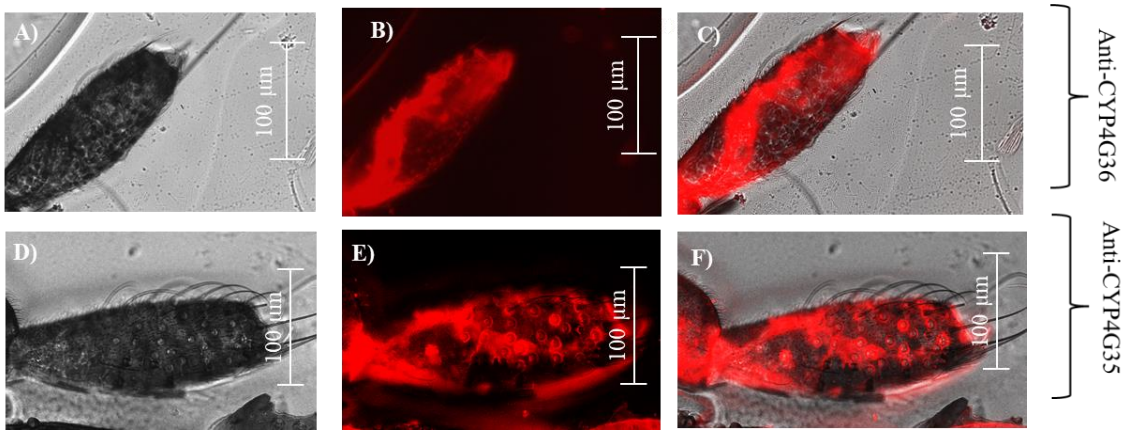

Figure 2.4. Localization of CYP4G36 and CYP4G35 in maxillary palps of *Ae. aegypti* female. Whole-mount fluorescent immunohistochemistry (WM-FIHC) maxillary palp was used to localize CYP4G36 (A-C) and CYP4G35 (D-F). A) Bright field image of the maxillary palp tissue. B) CYP4G36 antibody fluorescent staining (BZ-X Filter TRITC). C) Overlay of images A and B. D) Bright field image of the maxillary palp tissue. E) CYP4G35 antibody fluorescent staining (BZ-X Filter TRITC). F) Overlay of images D and E.

VII. References

Ahmad, I., & Ray, P. K. (1987). Factors conferring resistance to endosulfan in developmental biology of *Musca-domestica*. *Journal of Cellular Biochemistry*, 24-24.

Balabanidou, Vasileia, et al. "Cytochrome P450 associated with insecticide resistance catalyzes cuticular hydrocarbon production in Anopheles gambiae." Proceedings of the National Academy of Sciences of the United States of America vol. 113,33 (2016): 9268-73. doi:10.1073/pnas.1608295113

Baldwin, S. R., Mohapatra, P., Nagalla, M., Sindvani, R., Amaya, D., Dickson, H. A., & Menuz, K. (2021). Identification and characterization of CYPs induced in the Drosophila antenna by exposure to a plant odorant [Article]. *Scientific Reports*, *11*(1), 14, Article 20530. https://doi.org/10.1038/s41598-021-99910-9

Bansal, R., & Michel, A. (2018). Expansion of cytochrome P450 and cathepsin genes in the generalist herbivore brown marmorated stink bug. *Bmc Genomics*, *19*, Article 60. https://doi.org/10.1186/s12864-017-4281-6

Calla, B., MacLean, M., Liao, L. H., Dhanjal, I., Tittiger, C., Blomquist, G., & Berenbaum, M. (2018). Functional characterization of CYP4G11a highly conserved enzyme in the western honey bee Apis mellifera [Article]. *Insect Molecular Biology*, *27*(5), 661-674. https://doi.org/10.1111/imb.12516

Cano-Ramirez, C., Lopez, M. F., Cesar-Ayala, A. K., Pineda-Martinez, V., Sullivan, B. T., & Zuniga, G. (2013). Isolation and expression of cytochrome P450 genes in the antennae and gut of pine beetle Dendroctonus rhizophagus (Curculionidae:

Scolytinae) following exposure to host monoterpenes. *Gene*, *520*(1), 47-63. https://doi.org/10.1016/j.gene.2012.11.059

Chung, H., Sztal, T., Pasricha, S., Sridhar, M., Batterham, P., & Daborn, P. J. (2009). Characterization of Drosophila melanogaster cytochrome P450 genes. *Proceedings of the National Academy of Sciences of the United States of America*, *106*(14), 5731-5736. https://doi.org/10.1073/pnas.0812141106

Dickens, J. C., Billings, R. F., & Payne, T. L. (1992). Green leaf volatiles interrupts aggregation pheromone response in bark beetles infesting southern pines [Article]. *Experientia*, *48*(5), 523-524. https://doi.org/10.1007/bf01928180

Feyereisen, R. (2012). *Insect CYP Genes and P450 Enzymes*. Elsevier Academic Press Inc. https://doi.org/10.1016/b978-0-12-384747-8.10008-x

Feyereisen, R. (2020). Origin and evolution of the CYP4G subfamily in insects, cytochrome P450 enzymes involved in cuticular hydrocarbon synthesis [Article]. *Molecular Phylogenetics and Evolution*, *143*, 15, Article 106695. https://doi.org/10.1016/j.ympev.2019.106695

Jing, T. X., Yuan, C. Y., Meng, L. W., Hou, Q. L., Liu, X. Q., Dou, W., . . . Wang, J. J. (2022). CYP4G100 contributes to desiccation resistance by mediating cuticular hydrocarbon synthesis in Bactrocera dorsalis. *Insect Molecular Biology*, *31*(6), 772-781. https://doi.org/10.1111/imb.12803

Juhn, J., & James, A. A. (2012). Hybridization in situ of Salivary Glands, Ovaries, and Embryos of Vector Mosquitoes [Article]. *Jove-Journal of Visualized Experiments*(64), 18, Article e3709. https://doi.org/10.3791/3709

Kefi, M., Balabanidou, V., Douris, V., Lycett, G., Feyereisen, R., & Vontas, J. (2019). Two functionally distinct CYP4G genes of Anopheles gambiae contribute to cuticular hydrocarbon biosynthesis [Article]. *Insect Biochemistry and Molecular Biology*, *110*, 52-59. https://doi.org/10.1016/j.ibmb.2019.04.018

Krieger, J., Grosse-Wilde, E., Gohl, T., & Breer, H. (2005). Candidate pheromone receptors of the silkmoth Bombyx mori [Article]. *European Journal of Neuroscience*, *21*(8), 2167-2176. https://doi.org/10.1111/j.1460-9568.2005.04058.x

Leal, W. S. (2013). Odorant Reception in Insects: Roles of Receptors, Binding Proteins, and Degrading Enzymes. In M. R. Berenbaum (Ed.), *Annual Review of Entomology, Vol 58* (Vol. 58, pp. 373-391). Annual Reviews. https://doi.org/10.1146/annurev-ento-120811-153635

MacLean, M., Nadeau, J., Gurnea, T., Tittiger, C., & Blomquist, G. J. (2018). Mountain pine beetle (Dendroctonus ponderosae) CYP4Gs convert long and short chain alcohols and aldehydes to hydrocarbons. *Insect Biochemistry and Molecular Biology*, *102*, 11-20. https://doi.org/10.1016/j.ibmb.2018.09.005

Maıbeche, T. C. a. M. (2021). Odor degrading enzymes and signal termination. In *Insect pheromone biochemistry and molecular biology* (2nd ed., pp. 619 - 644). Academic Press is an imprint of Elsevier.

Maibeche-Coisne, M., Monti-Dedieu, L., Aragon, S., & Dauphin-Villemant, C. (2000). A new cytochrome P450 from Drosophila melanogaster, CYP4G15, expressed in the nervous system [Article]. *Biochemical and Biophysical Research Communications*, *273*(3), 1132-1137. https://doi.org/10.1006/bbrc.2000.3058

Mao, W., Schuler, M. A., & Berenbaum, M. R. (2015). Task-related differential expression of four cytochrome P450 genes in honeybee appendages [Article]. *Insect Molecular Biology*, *24*(5), 582-588. https://doi.org/10.1111/imb.12183

Melo, A. C. A., Rutzler, M., Pitts, R. J., & Zwiebel, L. J. (2004). Identification of a chemosensory receptor from the yellow fever mosquito, Aedes aegypti, that is highly conserved and expressed in olfactory and gustatory organs [Article]. *Chemical Senses*, *29*(5), 403-410. https://doi.org/10.1093/chemse/bjh041

Nie, H. Y., Xu, S. P., Xie, C. Q., Geng, H. Y., Zhao, Y. Z., Li, J. H., . . . Su, S. K. (2018). Comparative transcriptome analysis of Apis mellifera antennae of workers performing different tasks [Article]. *Molecular Genetics and Genomics*, *293*(1), 237-248. https://doi.org/10.1007/s00438-017-1382-5

Qiu, Y., Tittiger, C., Wicker-Thomas, C., Le Goff, G., Young, S., Wajnberg, E., . . . Feyereisen, R. (2012). An insect-specific P450 oxidative decarbonylase for cuticular hydrocarbon biosynthesis [Article]. *Proceedings of the National Academy of Sciences of the United States of America*, *109*(37), 14858-14863. https://doi.org/10.1073/pnas.1208650109

Scott, J. G., & Wen, Z. M. (2001). Cytochromes P450 of insects: the tip of the iceberg [Article; Proceedings Paper]. *Pest Management Science*, *57*(10), 958-967. https://doi.org/10.1002/ps.354

Souza-Neto, J. A., Powell, J. R., & Bonizzoni, M. (2019). Aedes aegypti vector competence studies: A review [Review]. *Infection Genetics and Evolution*, *67*, 191-209. https://doi.org/10.1016/j.meegid.2018.11.009

Sparks, J. T., Botsko, G., Swale, D. R., Boland, L. M., Patel, S. S., & Dickens, J. C. (2018). Membrane Proteins Mediating Reception and Transduction in Chemosensory Neurons in Mosquitoes [Review]. *Frontiers in Physiology*, *9*, 14, Article 1309. https://doi.org/10.3389/fphys.2018.01309

Strode, C., Wondji, C. S., David, J. P., Hawkes, N. J., Lumjuan, N., Nelson, D. R., . . . Ranson, H. (2008). Genomic analysis of detoxification genes in the mosquito Aedes aegypti [Article]. *Insect Biochemistry and Molecular Biology*, *38*(1), 113-123. https://doi.org/10.1016/j.ibmb.2007.09.007

Wang, S. Y., Price, J. H., & Zhang, D. (2019). Hydrocarbons catalysed by TmCYP4G122 and TmCYP4G123 in Tenebrio molitor modulate the olfactory response of the parasitoid Scleroderma guani. *Insect Molecular Biology*, *28*(5), 637-648. https://doi.org/10.1111/imb.12581

Weaver, S. C., Charlier, C., Vasilakis, N., & Lecuit, M. (2018). Zika, Chikungunya, and Other Emerging Vector-Borne Viral Diseases. In C. T. Caskey (Ed.), *Annual Review of Medicine, Vol 69* (Vol. 69, pp. 395-408). Annual Reviews. https://doi.org/10.1146/annurev-med-050715-105122

Wojtasek, H., & Leal, W. S. (1999). Degradation of an alkaloid pheromone from the pale-brown chafer, Phyllopertha diversa (Coleoptera : Scarabaeidae), by an insect olfactory cytochrome P450 [Article]. *Febs Letters*, *458*(3), 333-336. https://doi.org/10.1016/s0014-5793(99)01178-3

Wu, L. X., Zhang, Z. F., Yua, Z. T., Yu, R. R., Ma, E. B., Fan, Y. L., . . . Zhang, J. Z. (2020). Both LmCYP4G genes function in decreasing cuticular penetration of

insecticides in Locusta migratoria. *Pest Management Science*, *76*(11), 3541-3550. https://doi.org/10.1002/ps.5914

Younus, F., Chertemps, T., Pearce, S. L., Pandey, G., Bozzolan, F., Coppin, C. W., . . . Oakeshott, J. G. (2014). Identification of candidate odorant degrading gene/enzyme systems in the antennal transcriptome of Drosophila melanogaster [Article]. *Insect Biochemistry and Molecular Biology*, *53*, 30-43. https://doi.org/10.1016/j.ibmb.2014.07.003

Zhang, L. Y., Shen, Y. D., Jiang, X. C., & Liu, S. (2022). Transcriptomic Identification and Expression Profile Analysis of Odorant-Degrading Enzymes from the Asian Corn Borer Moth, Ostrinia furnacalis [Article]. *Insects*, *13*(11), 18, Article 1027. https://doi.org/10.3390/insects13111027

Chapter 3

Proteomics analysis of CYP4G35 knock-out mosquitoes to understand its mechanisms and potential functional pathways.

I. Abstract

Odorant-degrading enzymes (ODEs) are proposed to have a role in olfactory signal termination in the chemosensory system through the rapid degradation of odorants. The clearance of odorants from sensilla may facilitate the detection of new odorants for a rapid behavioral response. Conversely, losing ODE activity may lead to altered behavior, such as defective odor perception. Previous experiments in our lab using CYP4G35 knockout (KO) mosquitoes showed altered responses of female mosquitoes to odors and negatively impacted host-seeking behavior. To understand the effect of CYP4G35 KO on mosquito physiology, we analyzed the global proteome of mosquito heads and carcasses. We identified 7,552 proteins from both the mutant and wild-type samples. One hundred one proteins were significantly differentially expressed in the head of the mutant females. The most upregulated proteins were involved in olfaction or detoxification. Additionally, odor-binding proteins and transport proteins were upregulated, suggesting a compensatory mechanism for CYP4G35 loss.

II. Introduction

Aedes aegypti females are primary vectors for the pathogens and cause significant human suffering (Powell, 2018). Because of the urban distribution of this mosquito, *Ae. aegypti* has evolved to prefer human hosts and responds well to the human odorant profile (Brown, 2013). Many aspects of the insect olfactory system are well studied, but others, such as Odorant-Degrading Enzymes (ODEs), are still poorly understood (Leal,

2013). The ODEs are assumed to play an essential role in maintaining the sensitivity of the olfactory system through the rapid inactivation of odors or pheromones once they have activated their receptors (Vogt, 2005). The candidate ODEs identified in various transcriptomes to date belong to various detoxification enzyme families, including cytochrome P450s (CYPs), esterases, carboxylesterases, and glutathione S-transferases (He et al., 2017; Heydel et al., 2010; W. Li et al., 2022; W. H. Li et al., 2022; Liu et al., 2015; Nie et al., 2018; Younus et al., 2014). The antennal transcriptomes of several lepidopteran, coleopteran, and dipteran species have revealed a large number of detoxification enzymes belonging to these families, many of which are potential ODEs (Gu et al., 2015; Leitch et al., 2015; Pitts et al., 2011; Younus et al., 2014; Zhang et al., 2022).

A cytochrome P450 family member, CYP4G35, was previously detected in the sensilla of the olfactory appendages (proboscis and antennae) in female *Ae. aegypti* (Chapter 2), suggesting a potential role in olfaction. We used proteomics analysis to build upon the previous chapter and provide support for CYP4G35 as ODE. Proteomics allowed us to analyze the effect of CYP4G35 loss on other pathways. We dissected the head (with sensory appendages) and carcass (body devoid of head) of CYP4G35 knockout (KO) and wild-type (WT) females. Proteins were extracted and used for 11-plex Tandem Mass Tag (TMT) analysis. Data were analyzed using scaffold Data - independent acquisition mass spectrometry (DIA-MS). Out of thousands of proteins identified, cytochrome P450s, hemocyanins, dehydrogenases/ reductases, ribonucleoproteins, polyketide synthetases, and pheromone/ odor binding proteins were

upregulated by more than 2 fold in the heads of CYP4G35 KO mosquitoes suggesting their role in olfaction.

III. Methods

Mosquito Rearing

Aedes aegypti (LVP strain) colonies were maintained at 27 °C and 60-70% relative humidity (RH) with a photoperiod of 16 h light and 8 h dark in a dedicated insectary. Eggs were hatched overnight in small plastic cups in deionized water. First instar larvae were counted (100 per 1.5-gallon pan) and reared in 500 mL of deionized water on a powdered fish food diet (Tetramin®, Melle, Germany), as described in detail in (Pooraiiouby et al. 2018). Pupae were collected from the rearing container and transferred to adult emergence cages. Adults were fed a 10% sucrose solution containing food color for regular colony maintenance. Adult females were blood-fed 4 days after emergence, and egg cups lined with a paper towel were placed in the cage 48 h after blood feeding. The egg cups were removed from the cages 3 days later; egg sheets were washed and dried overnight at room temperature and stored in a plastic bag.

Single guide RNA (sgRNA) design and construction

The sgRNAs were designed by manually searching genomic regions for protospacer-adjacent motifs (PAMs) with the sequence NGG, where N is any nucleotide. Sequences of sgRNA were required to be 18–20 bp in length, excluding the PAM, and contain one or two 5′ terminal guanines to facilitate transcription by T7 RNA polymerase. sgRNA sequences were tested for potential off-target binding using the following two web tools: CRISPR (http://crispor.tefor.net/) (Haeussler et al., 2016) and ChopChop (https://chopchop.rc.fas.harvard.edu/) (Labun et al., 2019). Three sgRNA sequences were

selected for optimal efficacy. sgRNAs were prepared using a PCR template amplified by CRISPR_F primers designed for each target gene and CRISPR_R primers and synthesized using short primer design and *in vitro* transcription (IVT) in the laboratory using the PCR template and GeneArt™ Precision gRNA Synthesis Kit (Thermo Fisher) per the manufacturer's instructions. The Cas9 protein (Manufacturer) and multiplexed sgRNA were injected into mosquito embryos as described by Kistler et al., 2015. The G_0 adults were backcrossed with WT and laid eggs that generated the G_1 offspring.

Generation of CYP4G35 transgenic mosquitoes

The synthesized sgRNAs (a pool of three) were mixed (120 ng/µl) with injection-ready Cas9 protein (300 ng/µl: PNA Bio) in an injection buffer. SgRNA and Cas9 mix were sent to the Insect Transformation facility at the University of Maryland and were injected into ~250 pre-blastoderm-stage embryos. Injected embryos were allowed to recover for three days and then hatched under a vacuum. The resulting G_0 females were backcrossed to wild-type (WT) males and were set up individually to collect eggs for the next generation, and the next generation was screened again. Genomic DNA (gDNA) was extracted from half of a mosquito leg. Mosquitoes were anesthetized in a 4℃ fridge before leg removal. The tissue sample was placed in a PCR tube that contained 200 µl of 10% Chelex 100 resin: Water (V/V) (Sigma-Aldrich, CAS #:11139-85-8). Ensuring the sample was embedded in the Chelex portion of the solution. The PCR tubes with the sample were then heated to 95℃. The samples were vortexed for 5 secs and centrifuged for 15 secs. The supernatant was then used for nested PCR to amplify regions surrounding the putative CRISPR-Cas9 cut site from the gDNA of a given generation using primers in Table 2. For nested PCR, a housekeeping gene actin was used as a

control with the external CYP4G35 specific primers: CYP4G35 FWD 5', AATGAGATCATGGAGCGGGC 3', and CYP4G35 REV 5' ATGACCGGAAGCGGTTCTTT 3'. All reactions were performed with an initial 2 min at 95°C, followed by 39 cycles of 30 s at 95°C, 30s at 52°C, and 30 s at 72°C and a final extension at 72ºC for 10 min. PCR reactions were run on 1.2% agarose gel to confirm a positive PCR amplification. PCR products were sent for PCR clean-up and Sanger sequencing using a set of internal primers to screen the progeny for mutants. The sequences from injected individuals were aligned to the WT reference sequence and examined for insertions, deletions, or other polymorphisms. Synthego Inference of CRISPR Edits (ICE) analysis was used to determine gene editing and sgRNA contribution (Hsiau et al. 2019).

Proteomics sample collection and data analysis

For proteome samples, WT and CYP4G35-KO adult females were collected a week after adult eclosion. Head and body were separated from 20 WT (WT-Head, WT-Body) and CYP4G35KO (KO-Head, KO-Body) mosquitoes each (N=3). Tissues were washed in cold 1X PBS (Santa Cruz Biotechnology, Dallas, TX, USA) containing one PierceTM Protease Inhibitor tablet (Thermo Fisher, Rockford, IL, USA) (PBS+PI). Tissue samples were transferred to 1.7 mL microtubes containing 200 µl PBS+PI and homogenized using microtube pestles. After homogenization, 400 µL of PBS+PI was added to samples, followed by centrifugation for 10 min at 12,000 x g. The supernatant was then transferred to a new microtube and centrifuged at 12000 x g. Finally, the supernatant was collected and sent to the UNR Proteomics Core (University of Nevada, Reno).

Protein digestion

Protein content from prepared samples was estimated using the fluorescence-based protein assay EZQ (Invitrogen #R33200). During the enzymatic sample processing, 50 ug protein extracts were reduced, alkylated with iodoacetamide, and digested following the provided protocol in the Thermo Scientific EasyPep Mini MS Sample prep kit (Cat #A40006). The trypsin/Lys-C was added 1:10 (enzyme: protein) for digestion. At this point, the supernatant consisted of peptides and contaminants. The supernatant was placed in Peptide Clean-up column provided to remove contaminants through various washes by the Mini MS Sample prep kit (Cat #A40006). Following the instructions provided by the kit, the various flowthroughs would remove hydrophilic contaminants and hydrophobic contaminants. The sample was eluted from the column supplied with the kit. The peptides were dried in a vacuum centrifuge and resuspended in 100 µl of 0.1% formic acid for LC-MS analysis.

Liquid Chromatography

Samples were analyzed using an UltiMate 3000 RSLCnano system (Thermo Scientific, San Jose, CA). The peptides were trapped prior to separation on a 300 µm i.d. x 5 mm C18 PepMap 100 trap (Thermo Scientific, San Jose, CA) for 5 mins at 10 µl /min. Next, separation was performed on a 50cm uPAC C18 nano-LC column (PharmaFluidics, Ghent, Belgium) on an EasySpray source (Thermo Scientific, San Jose, CA) fitted with a 30-um ID stainless steel emitter (PepSep, Marslev, Denmark). Separation was performed at 350 nl/min using a gradient from 1% - 45% for 60 mins (Solvent A 0.1% Formic Acid, Solvent B Acetonitrile, 0.1% Formic Acid).

Mass spectrometry

Data Independent Acquisition (DIA) (Doerr, 2015; Gillet et al., 2012) was performed with a chromatographic library as described by (Gessulat et al., 2019; Searle et al., 2020). Briefly, six gas phase fractions (GPF) of the biological sample pool were used to generate a reference library. The GPF acquisition used 4 m/z precursor isolation windows in a staggered pattern (GPF1 398.4-502.5 m/z, GPF2 498.5-602.5 m/z, GPF3 598.5-702.6 m/z, GPF4 698.6-802.6 m/z, GPF5 798.6-902.7 m/z, GPF6 898.7-1002.7 m/z) at a resolution of 60,000, AGC target 4e5, maximum injection time 55 ms, and an NCE of 33 using higher-energy collision dissociation (HCD). Biological samples were run on an identical gradient as the GPFs using a staggered window scheme of 24 m/z over a mass range of 385-1015 m/z. Precursor isolation was performed at 60,000 resolution, maximum injection time of 55 ms, AGC target 4e6, and an NCE of 33 using HCD. An empirically corrected library that combines the GPF and the deep neural network Prosit (Gessulat et al., 2019) was used to generate predicted fragments and retention times.

ScaffoldDIA v 3.0.0 (Adusumilli & Mallick, 2017) was used to process the experimental samples allowing only peptides that were exclusively assigned to a given protein to be used for quantitative analysis and requiring a minimum of two peptides with a protein-level FDR of less than 1%. DIA-MS data files were converted to mzML format using ProteoWizard (3.0.19254). Deconvolution of staggered windows was performed. The intermediate chromatogram library was created by Encyclopedia (1.2.2). Reference samples were individually searched against (VectorBase62_Aaegypti LVP_AGWG_

AnnotatedProteins) containing 28,391 sequences with a peptide mass tolerance of 10.0 ppm and a fragment mass tolerance of 10.0 ppm. Fixed modifications considered were: Carbamidomethylation C. The digestion enzyme was assumed to be Trypsin, with a maximum of 1 missed cleavage site(s) allowed. Only peptides with charges in the range [2...3] and lengths in the range [6...30] were considered. Peptides identified in each search were filtered by Percolator (3.01. nightly-13-655e4c7-dirty) to achieve a maximum FDR of 0.01. Individual search results were combined, and peptides were again filtered to an FDR threshold of 0.01 for inclusion in the reference library. Individual search results were combined, and peptide identifications were assigned posterior error probabilities and filtered to an FDR threshold of 0.01 by Percolator. Peptide quantification was performed by EncyclopeDIAia, according to (Searle et al., 2018), which is a library search engine that can search for peptides using DIA-based chromatogram libraries. For each peptide, the 5 highest-quality fragment ions were selected for quantitation. Proteins that contained similar peptides and could not be differentiated based on MS/MS analysis were grouped to satisfy the principles of parsimony. Protein groups were a threshold to achieve a protein FDR of less than 1.0%.

Gene Ontology (GO) and pathway enrichment analysis of differentially expressed proteins (DEPs)

GO annotations were performed using the DAVID database (https://david.ncifcrf.gov/). GO terms were analyzed, and the primary process of GO analysis included blast, GO mapping, GO annotation, and interproScan for annotation augmentation. The differences in proteins were calculated using Fisher's exact test. GO enrichment of differential proteins was studied for biological processes, cellular

components, and molecular function using Blast2Go (Software Tool, https://www.blast2go.com),

KEGG pathway enrichment analysis was performed using the online analysis database on VectorBase. Up- and down-regulated DEPs were subjected to GO and pathway enrichment analysis separately. P value <0.05 was used as the threshold value. DEPs were clustered by the hierarchical cluster method, and data were presented as heat maps.

Protein-protein interaction (PPI) network analysis

The STRING database (http://string-db.org/) was used to identify the interactions between proteins encoded by DEPs based on experimental data. A combined score of >0.4 was set as the threshold value. PPI networks were constructed with Cytoscape software.

IV. Results

CRISPR-Cas9-based genome editing was used to generate mutant CYP4G35 mosquitoes. Out of a pool of three sgRNA, sgRNA2 was the most efficient and led to a 4 bp deletion resulting in a codon frameshift in the CYP4G35 gene (Fig. 3.1). These mosquitoes were reared in our lab for eight generations to achieve homozygous lines that were used in proteomic analysis.

Overview of DEPs in proteomic analysis:

The Principal Component Analysis (PCA) separated samples into four different groups (Fig. 3.2), suggesting that each sample set (mutant head, mutant body, WT head, and WT body) was distinct from each other. Globally, we identified 7,552 proteins from both the mutant and WT samples. 101 proteins were significantly differentially expressed

in the mutant females' head samples (Fig. 3.3A, 3.4A) and 97 in the body samples (Fig. 3.3B, 3.4B). 15 upregulated proteins (Fig. 3.5A) and 9 downregulated proteins (Fig. 3.5B) were common in both head and body samples.

Common differentially expressed proteins in head and body samples:

Of the 198 DEPs, 15 proteins were upregulated in both head and body of the CYP4G35 mutant mosquitoes (Fig 3.5). Several hexamerins (2-beta): AAEL008045, AAEL008817, AAEL011169, and AAEL013757, were upregulated in both head and body. Other upregulated proteins were AMP-dependent synthetase (AAEL002669), serine protease (AAEL011624), and serine/threonine protease (AAEL026028). KEGG pathway analysis revealed that these proteins were involved in methane metabolism (Fig. 3.8).

Nine proteins in total were downregulated in both head and body samples (Fig 3.5). These proteins consisted of dehydrogenases (AAEL026142, AAEL007669), hydrolases (AAEL010592, AAEL000642), and serine proteases (AAEL009554, AAEL024669, AAEL000252). KEGG pathway analysis revealed that these proteins were involved in ascorbate and aldarate metabolism (Fig. 3.8).

Differentially expressed proteins only in the head of CYP4G35 KO females:

One hundred and one proteins were differentially regulated in the CYP4G35 KO head, of which 40 were downregulated and 61 upregulated (Fig 3.2). Out of the 101 proteins, there only 77 were differentially expressed exclusively in the head of the CYP4G35 mutant mosquito. Gene ontology (GO) analysis was used to evaluate the protein functions of DEPs. Of those upregulated in the head their functions, a majority of the proteins have functions in oxidoreductase activity, heme and iron binding, and

microtubule binding (Fig. 3.6A). Those with oxidoreductase activity and heme/iron binding consisted of CYPs. Three CYPs: CYP6P12, CYP9J16, and CYP6A8, were upregulated in the head of the mutant females. While the upregulation of CYPs overall was not exclusive to the head of the mosquitoes. These three CYPs' differential expressions are exclusive to the head. The highest upregulated protein was a kinesin, AAEL004235 (kinesin motor domain) (Table 3.4), along with other microtubule-related proteins (KATNA1, AAEL013390). When investigating enzymes with olfactory-related functions: two odor/pheromone binding proteins were identified: OBP18 (AAEL004342) and OBP 99c (AAEL011730), which were significantly upregulated (Fig. 3.6). KEGG analysis of upregulated proteins in the head showed proteins were associated with retinol metabolism, bisphenol degradation, bile acid biosynthesis, methane metabolism, linoleic acid metabolism, biotin metabolism, cysteine, methionine, phenylalanine, tyrosine, and tryptophan biosynthesis (Fig 3.7).

Downregulated proteins in the head of the mutant mosquito were mainly proteases that belonged to hydrolase, endopeptidase, and peptidase activity (Fig. 3.6B). The downregulated pathways included insect hormone biosynthesis, chitin biosynthesis, a steroid hormone, and the inositol pathway (Fig. 3.6).

Differentially expressed proteins only in the carcass/body samples:

In the CYP4G35 KO head group, there are 97 DEPs, 74 of these proteins were differentially regulated exclusively in the CYP4G35 KO mutant body versus WT when analyzing proteins that upregulated for their function using GO analysis. In general, heme binding, carbohydrate binding, small molecule binding, and transferase activity (Fig. 3.7 B). The KEGG pathway analysis of the proteins that are upregulated indicates a role in

methane metabolism, arginine biosynthesis, and aminoacyl-tRNA biosynthesis. The top upregulated proteins were AAEL026231 (pyridoxal phosphate-dependent aminotransferase), AAEL017010 (DNA-directed RNA polymerase subunit beta), AAEL026253 (ectopic P granules protein 5 homolog (EPG5)), AAEL024216 (carboxylesterase type B), and AAEL000832 (cleavage and polyadenylation specificity factor, CPSF) (Table 3.3).

Downregulated proteins in the body of the mutant mosquito were identified as mainly related to metabolic processes or homeostasis functions. KEGG analysis revealed that these proteins were involved in phenylpropanoid, retinol metabolism, alkaloid biosynthesis, lipopolysaccharide biosynthesis, glycerophospholipid metabolism, fructose/mannose, terpenoid biosynthesis, and inositol metabolism (Fig. 3.7B, Fig. 3.8).

V. Discussion

In the presented work, we conducted proteomic analysis between CYP4G35 KO and wild-type *Ae. aegypti* to understand how the KO of CYP4G35 alters the expression of other proteins. The majority of differentially expressed proteins were involved in olfaction, detoxification, metabolism, protein translation, protein transport, signaling, and autophagy. Two OBPs, OBP18 (AAEL004342) and OBP 99c (AAEL011730), were upregulated. In *A. mellifera*, the Western Honey bee, OBP18 was highly expressed in the antennae and binds to fatty acids (oleic acid) (McAfee et al., 2018).

A HAD-super family member, AAEL024977 (HAD-superfamily hydrolase), was upregulated in the head. Several HAD-like enzymes function in the detoxification of phosphorylated substrates as well as pseudouridine (modified uracil that can stabilize structural RNAs such as tRNA or ribosomal) (Kuzetsova et al. 2015). CYP4G35 KO

resulted in significant downregulation of metabolic proteins AAEL007653 (Allantoinase) in the body and AAEL013410 (TMEM70 family) in the head. Allantoinase enzymes are involved in purine metabolism, while TMEM70 is a transmembrane protein in mitochondria. TMEM 70 is engaged in the assembly of the F1 and F0 subunits of ATP synthase and Complex I of the oxidative phosphorylation system (Sanchez-Caballero et al. 2020).

CYP4G35 KO mutant mosquitoes have upregulated kinesin (AAEL004235) expression in the head. Kinesins are known to be involved in the intracellular transport of proteins, vesicles, or organelles. Kinesins partly mediate the transport of cargo in neurons; for example, kinesin-2 binds and transports ORCO into the olfactory cilium of *D. melanogaster* (Jana et al. 2021). This upregulation of kinesin in CYP4G35 KO mosquitoes may be an attempt to increase the transport of cargo in neurons. The increase in protein levels of several transcription-associated proteins in the body (AAEL017010- DNA-directed RNA polymerase, AAEL000832- cleavage/polyadenylation specificity factor (CPSF) and in the head (AEEL006166- C-5 cytosine methyltransferase) suggests the CYPG35 KO leads to broad gene transcriptional changes. CPSF is involved in mRNA processing and maturation after transcription in humans (Murthy et al. 1995).

Signaling proteins were downregulated in both head and body of CYP4G35 KO mosquitoes compared to wild-type. In the head, AAEL024394 (MAM domain; Serine-threonine/tyrosine-protein kinase receptor), and in the body, AAEL001952 (28kDA phosphoprotein (PDGF-associated)) also predicted to be a Casein kinase substrate) were downregulated. There are no close orthologs of AAEL024394 or AAEL001952 that have been characterized functionally, so it is unclear how these proteins could be related to

CYP4G35 function. CYP4G35 KO mosquitoes had elevated AAEL026253 (Ectopic P granules protein 5 (EPG5)) compared to wild-type. EPG5 was initially identified in *C. elegans* as a regulator of autophagy (Tian et al. 2010).

Among the most upregulated and downregulated protein, CYP4G35 KO mosquitoes show potentially decreased mitochondrial metabolism in the head, increased detoxification enzymes in both the body and the head and decreased levels of an uncharacterized receptor kinase. These significant differences may indicate compensatory changes for the loss of CYP4G35 function.

In this chapter, we provide evidence that the lack of CYP4G35 causes changes in the *Ae. aegypti* physiology, specifically in the head of the mosquito. In future experiments will use these data to improve localization experiments and understand how the sensilla are potentially being remodeled. In this exploration, we focused on the changes in protein expression in the mutant head, which indicate changes in detoxification enzymes, OBPs, and kinesin, further suggesting a compensatory mechanism by either binding more odor molecules to the binding proteins or bringing more receptors to the surface of sensory cilia due to increased levels of odor molecules (decreased odor degradation). These data provide insight into the possible function of CYP4G35 as an ODE in *Ae. aegypti*.

V. Figures

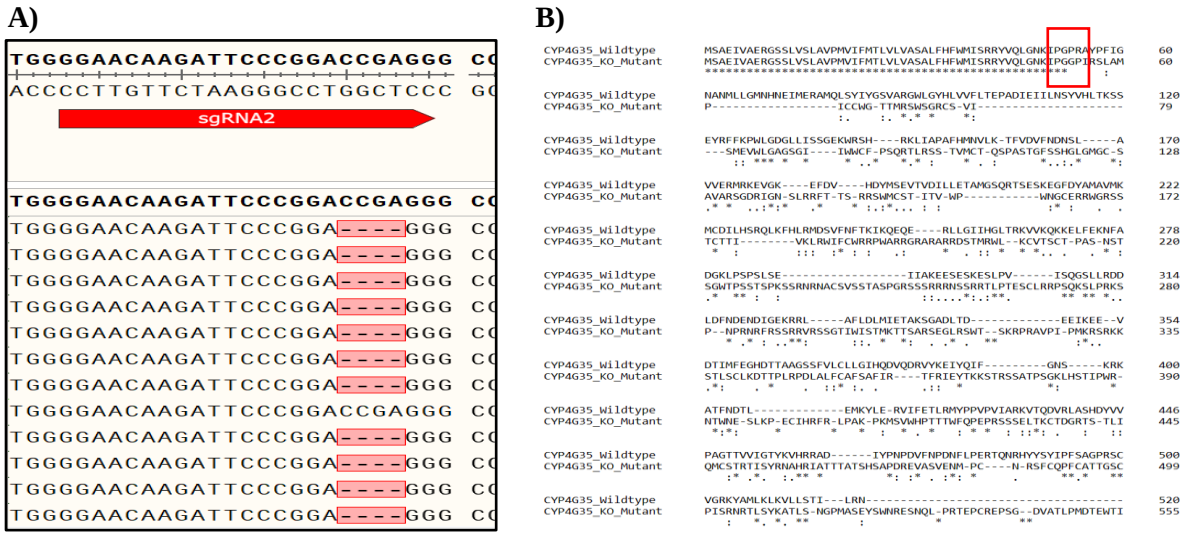

Figure 3.1. CYP4G35 knockout using CRISPR-Cas9. A) The sanger sequencing analysis of 12 individual mosquitoes shows 4 bp deletion corresponding to sgRNA2 in 11 of 12 individuals. B) Multiple alignments of the protein sequences of the CYYP4G35 mutant versus the wild type illustrate the generation of truncated protein caused a premature stop in translation in the CYP4G35 KO mutant compared to the wild type. A premature stop in translation (location indicated in red box) occurred due to a double-stranded break that led to CYP4G35 knockout.

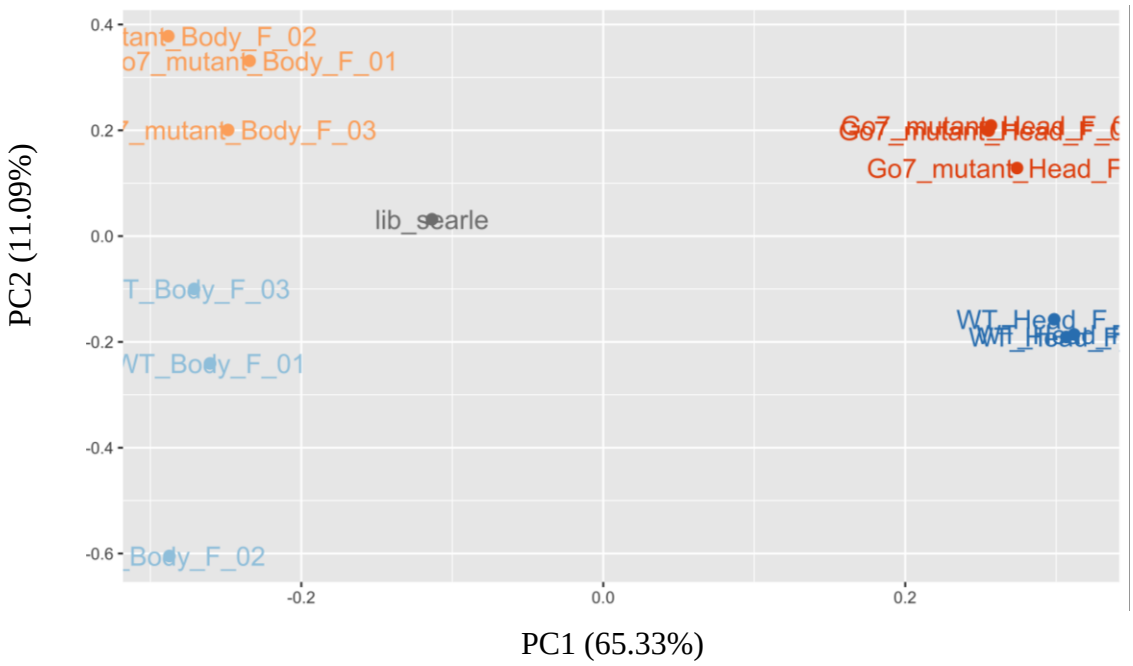

Figure 3.2. PCA plot illustrates variance stabilization normalization between data sets. The principal component analysis (PCA) shows the variance between the data set of head and body samples from both CYP4G mutant knock-out (CYP4G35 KO) and wild-type (WT). The red dots represent variance for head samples from CYP4G35 KO female *Ae. aegypti*. The orange dots represent variance for body samples from CYP4G35 KO female *Ae. aegypti*. The light blue dots represent sample variance for body samples from wild-type female *Ae. aegypti*. The dark blue dots represent sample variance for head samples from wild-type female *Ae. aegypti*.

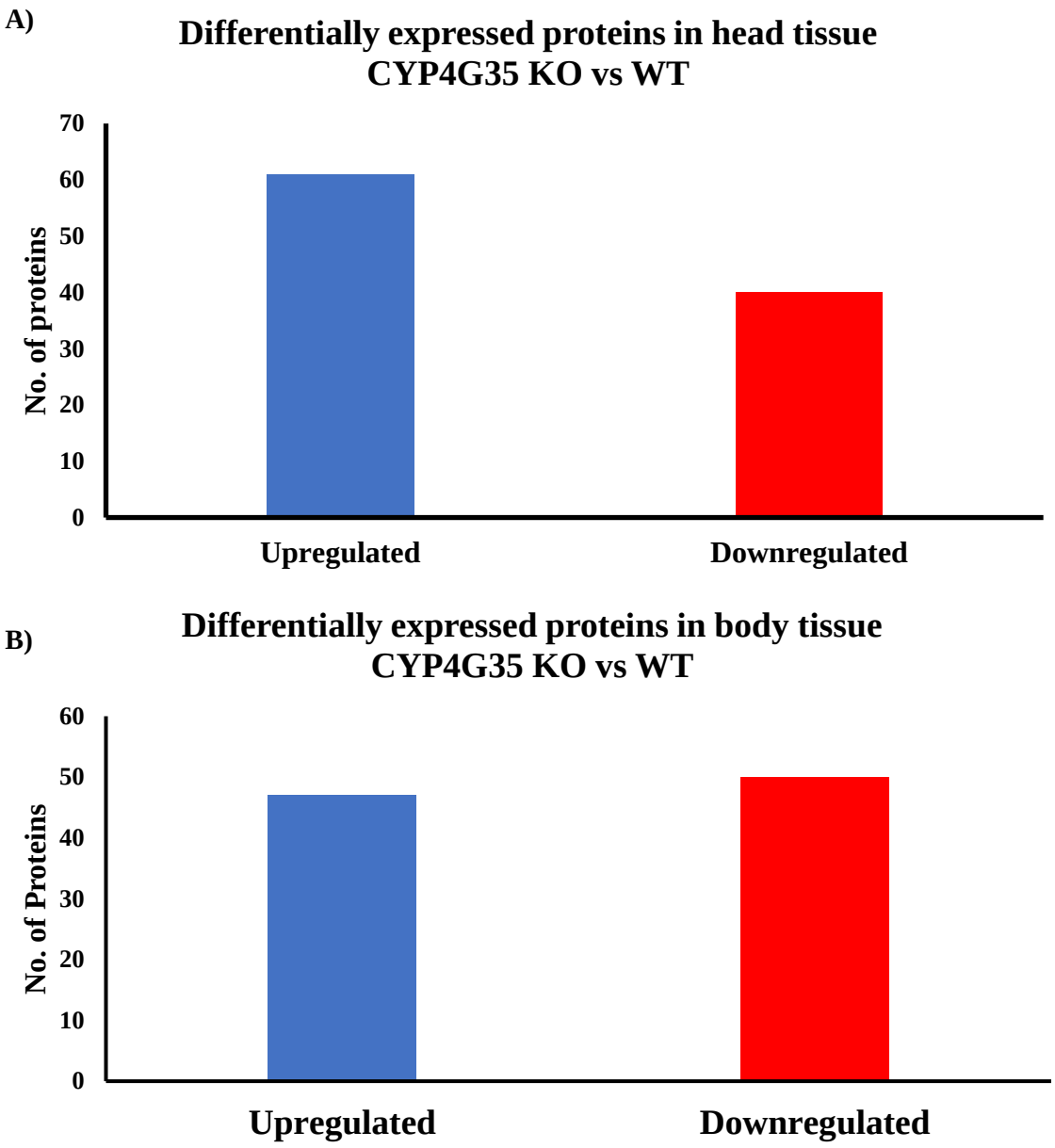

Figure 3.3. Total differentially expressed proteins in head & body tissue in CYP4G35 KO vs. WT. The number of DEPs up and down-regulated in head and body tissue in CYP4G35 KO. A) Total differentially expressed proteins in the head in CYP4G35 KO vs. WT. B) Total differentially expressed proteins in body tissue in CYP4G35 KO vs. WT.

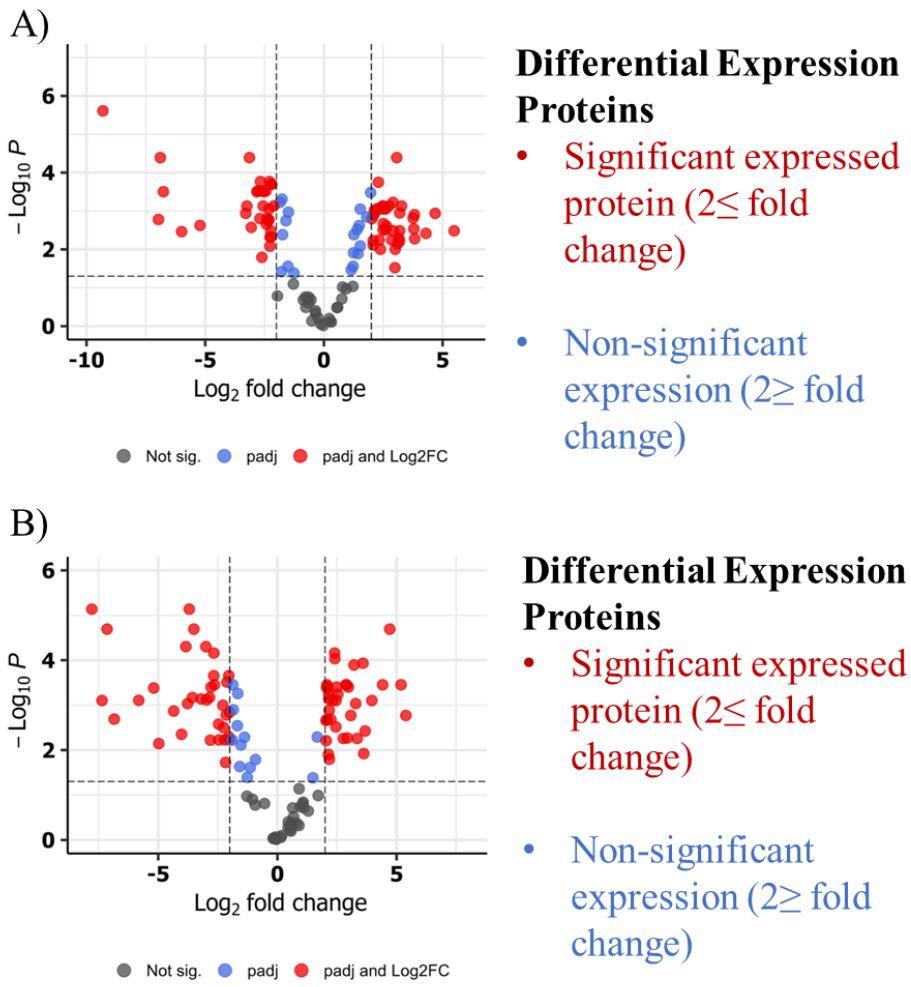

Figure 3.4. Volcano plot of DEPs in carcass tissue of the CYP4G35 mutant vs. wild type. Volcano plot showing the differential expressed proteins in the body of *Ae. aegypti* between the CYP4G35 mutant versus wild type for 97 proteins included on all platforms. The red dots represent proteins that were differentially expressed in the CYP4G35 knock-out mutant (Log fold-change >2 in either direction, adjusted P<0.05). The left-hand side red dots represent significantly downregulated proteins, whereas on the right-hand side are the upregulated proteins. The blue dots represent proteins that were not differentially expressed in the CYP4G35 knock-out mutant.

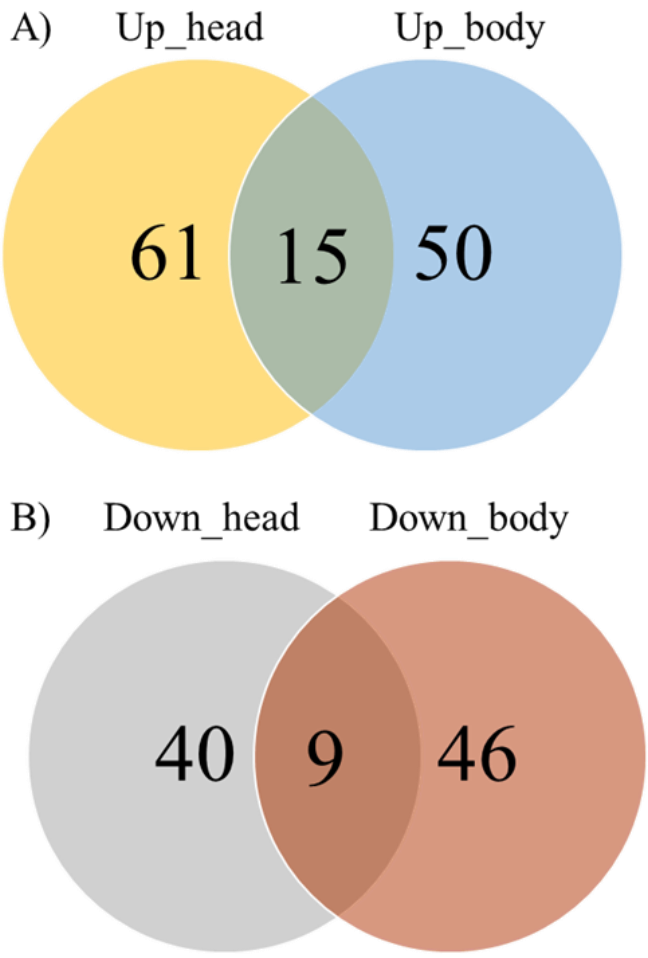

Figure 3.5. **Venn diagram of up and down-regulated proteins identified in head and body tissues of CYP4G35 KO mutant**. A) upregulated proteins in the head (yellow) and body (blue). The intersection represents common proteins in both samples. B) Downregulated proteins in the head (gray) and body (brown). The intersection of two circles represents proteins downregulated in both samples.

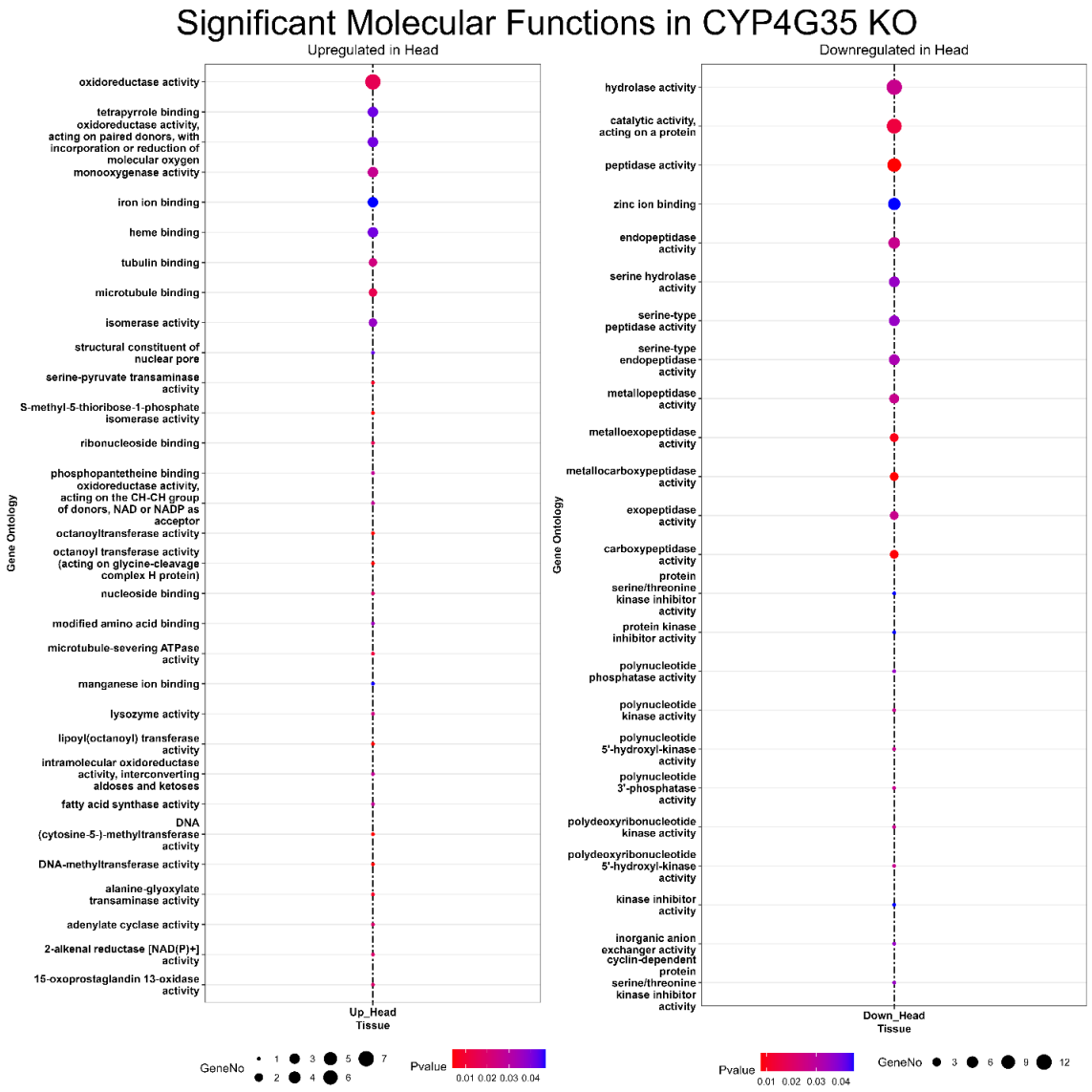

Figure 3.6. Bubble plot of molecular function enrichment for CYP4G35 KO head tissue. GO classification of biological process and molecular function for proteins upregulated in head CYP4G35 KO versus WT.

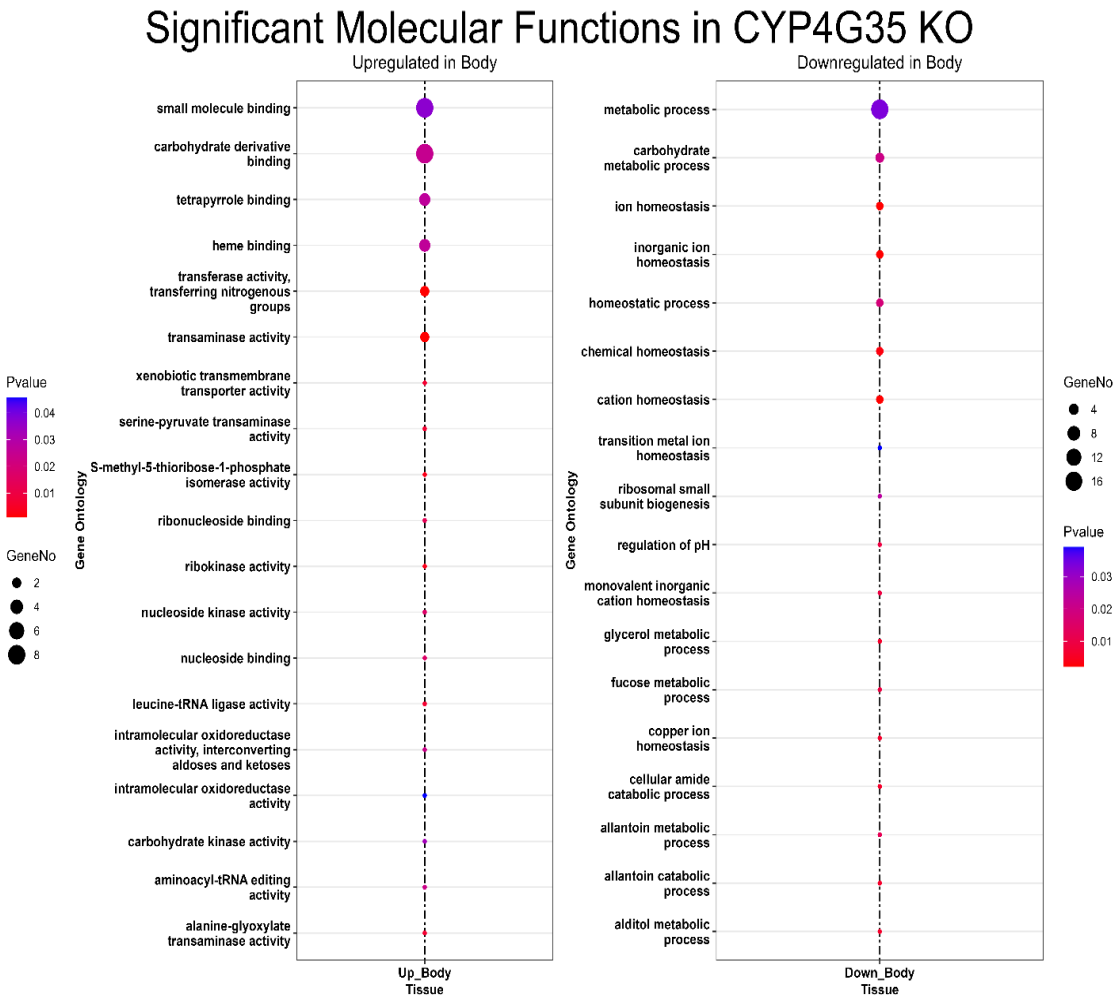

Figure 3.7. Bubble plot of molecular function enrichment for CYP4G35 KO body tissue. GO classification of biological process and molecular function for proteins upregulated in body CYP4G35 KO versus WT (left).

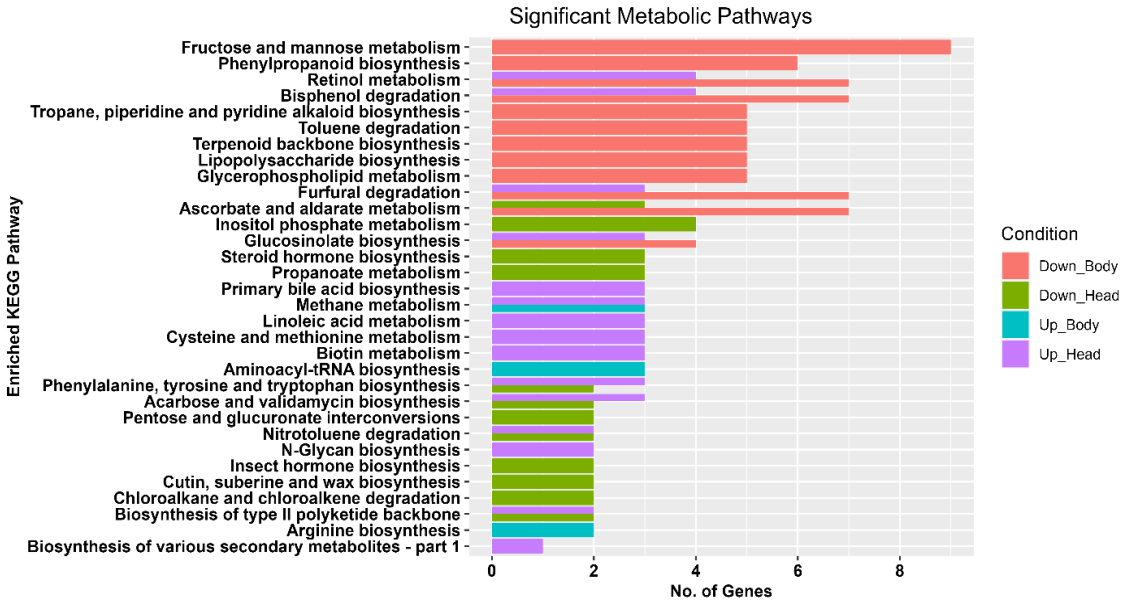

Figure 3.8. KEGG analysis of the metabolic pathways within CYP4G35 KO and WT. The metabolic pathway was identified to be upregulated and downregulated in the body proteome for CYP4G35 KO and WT. The metabolic pathway for identified to be upregulated and downregulated in the head proteome for CYP4G35 KO and WT.

Table 3.1 Guide RNAs designed used to target CYP4G35 in *Ae. aegypti*. Single-guide RNAs for CYP4G35 are shown with sgRNA name, length in base pairs (bp), target sequence, and PAM sequences. "*" indicates the successful sgRNA that made the edits in each CYP4G35 knock-out.

sgRNA name	Length (bp)	Target sequence	PAM
CYP4G35 (AAEL006824)			
sgRNA 1	20	GCGGAAATTGTGGCCGAGCG	GGG
sgRNA 2*	20	GGAACAAGATTCCCGGACCG	AGG
sgRNA 3	20	AGTGTGGCTCGGGGCTGGCT	CGG

Table 3.2: Primers for PCR amplify and sequence the CYP4G35 for transgenic lines. The internal primers set were primers: *Ae. aegypti* F2 and *Ae. aegypti* R2. The external primer set was primers: *Ae. aegypti* F1 and *Ae. aegypti* R1.

Primer Name	Sequence (5'-3')
CYP4G35 (AAEL006824)	
Ae. aegypti F1	CGATTTCGCCGCTTATAAATAC
Ae. aegypti R1	ATATTCACACAAAGAATCCCCG
Ae. aegypti F2 (Sequencing)	ATACACCATCCCGGGTCGTA
Ae. aegypti R2 (Sequencing)	GTTCATGTGAAACGCCGGAG

Table 3.3. Top five up or downregulated differentially expressed proteins in CYP4G35 KO body vs. WT body. DEPs from Gene Name, Gene ID, Fold change (Log2FC), and protein family the transcript belongs to.

Top 5 up or down-regulated DEPs			
Gene Name	**Gene ID**	**Log2FC**	**PFam Description**
Upregulated in CYP4G35 KO Body vs. WT Body			
Pyridoxal phosphate-dependent transferase	AAEL026231	6.97	Aminotransferase class-III;
DNA-directed RNA polymerase	AAEL017010	4.64	DNA-directed RNA polymerase
unspecified product	AAEL026253	4.64	Ectopic P granules protein 5
Carboxylesterase	AAEL024216	4.6	Carboxylesterase type B
cleavage and polyadenylation specificity factor CPSF	AAEL000832	4.24	Cleavage/polyadenylation specificity factor
Downregulated in CYP4G35 KO Body vs. WT Body			
allantoinase	AAEL007653	-4.56	Dihydroorotase
unspecified product	AAEL000950	-5.09	Low-temperature viability protein Ltv1
Nucleolar complex protein 2	AAEL004818	-6.15	Nucleolar complex protein 2, Armadillo-type fold
28 kDa heat- and acid-stable phosphoprotein (PDGF-associated protein), putative	AAEL001952	-7.04	Casein kinase substrate, phosphoprotein PP28
Serine proteases, trypsin domain; Peptidase S1A	AAEL009554	-8.05	chymotrypsin family; Peptidase S1, PA clan

Table 3.4. Top five up or downregulated differentially expressed proteins in CYP4G35 KO Head vs. WT Head. DEPs from Gene Name, Gene ID, Fold change (Log2FC), and protein family the transcript belongs to.

Top 5 up or down-regulated DEPs			
Gene Name	**Gene ID**	**Log2FC**	**PFam Description**
Upregulated CYP4G35 KO Head vs. WT Head			
kinesin-like protein Klp10A	AAEL004235	5.36	Kinesin motor domain
DNA (cytosine-5)-methyltransferase	AAEL006166	4.97	C-5 cytosine methyltransferase
phosphoglycolate phosphatase 1B	AAEL024977	4.91	HAD-superfamily hydrolase
EPGP 5 homolog isoform X2	AAEL026253	4.21	Ectopic P granules protein 5
Predicted Glycoprotein	AAEL019870	3.96	glycoprotein precursor (DUF1397)
Downregulated CYP4G35 KO Head vs. WT Head			
ALK tyrosine kinase receptor	AAEL024394	-4.91	MAM domain; Serine-threonine/tyrosine-protein kinase
transmembrane protein 70 homolog	AAEL013410	-4.94	TMEM70 family
polynucleotide phosphatase/kinase	AAEL025882	-5.14	Polynucleotide kinase 3 phosphatase; PNK, FHA domain
28 kDa phosphoprotein (PDGF-associated protein)	AAEL001952	-7.13	Casein kinase substrate, phosphoprotein PP28
serine protease 53	AAEL009554	-7.83	Serine proteases, trypsin domain

VI. References

Adusumilli, R., & Mallick, P. (2017). Data Conversion with ProteoWizard msConvert. *Proteomics: Methods and Protocols*, *1550*, 339-368. https://doi.org/10.1007/978-1-4939-6747-6_23

Doerr, A. (2015). DIA mass spectrometry. *Nature Methods*, *12*(1), 35-35. https://doi.org/10.1038/nmeth.3234

Gessulat, Siegfried, et al. "Prosit: proteome-wide prediction of peptide tandem mass spectra by deep learning." *Nature methods* vol. 16,6 (2019): 509-518. doi:10.1038/s41592-019-0426-7

Gillet, Ludovic C et al. "Targeted data extraction of the MS/MS spectra generated by data-independent acquisition: a new concept for consistent and accurate proteome analysis." *Molecular & cellular proteomics : MCP* vol. 11,6 (2012): O111.016717. doi:10.1074/mcp.O111.016717

He, Peng et al. "A reference gene set for sex pheromone biosynthesis and degradation genes from the diamondback moth, Plutella xylostella, based on genome and transcriptome digital gene expression analyses." *BMC genomics* vol. 18,1 219. 1 Mar. 2017, doi:10.1186/s12864-017-3592-y Heydel, J. M., Holsztynska, E. J., Legendre, A., Thiebaud, N., Artur, Y., & Le Bon, A. M. (2010). UDP-glucuronosyltransferases (UGTs) in neuro-olfactory tissues: expression, regulation, and function [Review]. *Drug Metabolism Reviews*, *42*(1), 74-97. https://doi.org/10.3109/03602530903208363

Juhn, Jennifer et al. “Spatial mapping of gene expression in the salivary glands of the dengue vector mosquito, Aedes aegypti.” Parasites & vectors vol. 4 1. 4 Jan. 2011, doi:10.1186/1756-3305-4-1Kanost, M. R., & Jiang, H. B. (2015). Clip-domain serine proteases as immune factors in insect hemolymph. *Current Opinion in Insect Science*, *11*, 47-55. https://doi.org/10.1016/j.cois.2015.09.003

Larter, N. K., Sun, J. S., & Carlson, J. R. (2016). Organization and function of Drosophila odorant binding proteins [Article]. *Elife*, *5*, 22, Article e20242. https://doi.org/10.7554/eLife.20242

Li, W.; Yang, B.; Liu, N.; Zhu, J.; Li, Z.; Ze, S.; Yu, J.; Zhao, N. Identification and Characterization of the Detoxification Genes Based on the Transcriptome of Tomicus yunnanensis. Diversity 2022, 14, 23. https://doi.org/10.3390/d14010023

Li, W. H., Wang, X. Y., Jiang, P., Yang, M. W., Li, Z. M., Huang, C. Y., & He, Y. P. (2022). A full-length transcriptome and gene expression analysis of three detoxification gene families in a predatory stink bug, Picromerus lewisi. *Frontiers in Physiology*, *13*, Article 1016582. https://doi.org/10.3389/fphys.2022.1016582

Liu, S., Rao, X. J., Li, M. Y., Feng, M. F., He, M. Z., & Li, S. G. (2015). Glutathione s-transferase genes in the rice leaffolder, cnaphalocrocis medinalis (lepidoptera: pyralidae): identification and expression profiles [Article]. *Archives of Insect Biochemistry and Physiology*, *90*(1), 1-13.

McAfee, Alison et al. “A death pheromone, oleic acid, triggers hygienic behavior in honey bees (Apis mellifera L.).” Scientific reports vol. 8,1 5719. 9 Apr. 2018, doi:10.1038/s41598-018-24054-2

Nie, H. Y., Xu, S. P., Xie, C. Q., Geng, H. Y., Zhao, Y. Z., Li, J. H., . . . Su, S. K. (2018). Comparative transcriptome analysis of Apis mellifera antennae of workers performing different tasks [Article]. *Molecular Genetics and Genomics*, *293*(1), 237-248. https://doi.org/10.1007/s00438-017-1382-5

Searle, Brian C et al. "Chromatogram libraries improve peptide detection and quantification by data independent acquisition mass spectrometry." Nature communications vol. 9,1 5128. 3 Dec. 2018, doi:10.1038/s41467-018-07454-w

Searle, B. C., Swearingen, K. E., Barnes, C. A., Schmidt, T., Gessulat, S., Kuster, B., & Wilhelm, M. (2020). Generating high quality libraries for DIA MS with empirically corrected peptide predictions. *Nature Communications*, *11*(1), Article 1548. https://doi.org/10.1038/s41467-020-15346-1

Xiao, S. K., Sun, J. S., & Carlson, J. R. (2019). Robust olfactory responses in the absence of odorant binding proteins [Article]. *Elife*, *8*, 17, Article e51040. https://doi.org/10.7554/eLife.51040

Younus, Faisal et al. "Identification of candidate odorant degrading gene/enzyme systems in the antennal transcriptome of Drosophila melanogaster.". *Insect Biochemistry and Molecular Biology*, *53*, 30-43. https://doi.org/10.1016/j.ibmb.2014.07.003

Chapter 4

Proteomics analysis of CYP4G35 knock-out mosquitoes to understand its mechanisms and potential functional pathways.

I. Abstract

CYP4Gs are insect-specific cytochrome P450s. Insect genomes typically encode one or two CYP4Gs and are divided into two clades: CYP4G1-like and CYP4G15-like. The CYP4G1 clade members have been shown to function as oxidative decarbonylases for long-chain hydrocarbon biosynthesis and express highly in oenocytes. However, the orthologs of CYP4G35 have been shown to oxidize short-chain carbon compounds. However, there is no general consensus on the substrate of this clade. All CYPs require cytochrome reductase partner (CPR) for their function as a monooxygenase. CYP4G35 fusion protein with a house-fly CPR was expressed and tested with short-chain aldehydes and long-chain alcohols as substrates. While the oxidation of the cofactor NADPH to NADP+ was observed, shorter-chain carbon products were not detected. The data is inconclusive as the positive control sample did not work in our assay.

II. Introduction

Enzymes are the catalysts in most biological reactions. The functions of enzymes vary, and several enzymes catalyze oxidations and reductions (Walsh et al., 1979). Cytochrome P450 (P450, CYP) enzymes are responsible for over 90% of catalytic reactions, especially in the metabolism of xenobiotics and natural chemicals. Most of the P450 reactions are oxidations and involve molecular oxygen, i.e., O_2. CYP450s almost always act as monooxygenases or mixed-function oxidases and require a Cytochrome

P450 reductase (CPR) partner that utilizes the pyridine nucleotide NADH or NADPH as a cofactor, and this cofactor is used to deliver electrons via a flavoprotein such as heme.

The CYP4G subfamily, an insect-specific CYP family, is distinguished from the more prominent P450 families by a 44 residue insertion between the G and H helixes. Most insects have two CYP4Gs, one in each CYP4G1-like and CYP4G15-like clades (Feyereisen, 2020). The CYP4G1-like enzymes have been shown to function as oxidative decarbonylases (Feyereisen et al., 2020; Calla et al., 2018; MacLean et al., 2018; Qiu et al., 2012; Wu et al., 2022). and convert aldehydes and alcohols to hydrocarbons (Holze et al. 2021). The CYP4G15 clade is hypothesized to have other functions and is most likely oxidizes shorter carbon chain compounds in the range of 9-13 carbon (Feyereisen, 2020; Calla et al., 2018; Martinez-Paz et al., 2012; Vogt et al., 1985; Wojtasek & Leal, 1999; Wu et al., 2022; Wu et al., 2020). For instance, CYP4G11 (CYPG15-like) in *A. mellifera* is highly expressed in the antennae and legs of the forager bees (Claudianos et al., 2006; Kamikouchi et al., 2004; Mao et al., 2015) and can accept short-chain aldehydes as substrates (Calla et al., 2018). These foragers bees collect pollen and rely on plant volatiles to interpret their environment.

Based on our previous data (chapters 3 and 4) on CYP4G35 localization, we hypothesize that this enzyme might also use short-chain carbon compounds (alcohols, aldehydes, and ketones) as a substrate. The odor profiles for humans and other vertebrate species relevant to mosquitoes comprise aldehydes, ketones, esters, and alcohol (Zhao et al., 2022), and these compounds make optimal candidates for CYP4G35 substrate.

To test these substrates, we used recombinant CYP4G enzymes as fusion proteins with the catalytic domain of the house fly CPR as described in (Qiu et al., 2012).

CYP4G55-CPR fusion proteins convert C10 alcohols and aldehydes to hydrocarbons, including the conversion of (Z)-7-decanal, a putative intermediate in the exo-brevicomin pheromone biosynthetic pathway, to (Z)-3-nonene. (MacLean et al., 2018). In our previous work, wildtype *Ae. aegypti* females were exposed to several odors, and they were attracted to short-chain carbon compounds (shorter than 12 carbon chains), including decanal. Our CYP4G35 knockout mosquitoes lack this attraction in olfactometer assays. Therefore, we considered testing this and other short-chain carbon compounds as substrates for CYP4G35.

III. Methods

Sf9 Cell Cultures

Sf9 cultures were maintained in a complete medium with 10% Fetal Bovine Serum (FBS) (GenClone; Fetal Bovine Serum USDA Approved Origin, Cat #: 25-550) and 1x Penicillin-Streptomycin (GIBCO™, Penicillin-Streptomycin (10,000 U/mL), Cat. #: 15140122) at 28°C in a suitable incubator without CO_2 following instructions described in (MacLean et al., 2018).

Baculovirus Infection and Microsome Extraction

Serum-adapted cells were infected for 72 h in adherent cultures in Sf900 II serum-free media (Gibco, Grand Island, NY) supplemented with 10% (vol/vol) FBS (Atlas Biologicals, Fort Collins, CO), 0.3 mM δ-aminolevulinic acid, and 0.2 mM ferric citrate. Cells expressing CYP4G35-CPR and CYP4G55-CPR were then harvested by transferring each expression culture to 50 mL and centrifuged at 3,000 x g for 10 min at 4ºC. The pellet was resuspended in 6 ml cell lysis buffer (100 mM sodium phosphate, pH 7.6, 20% (vol/vol) glycerol, and 1.1 mM EDTA) supplemented with 100 μM DTT, 200 μM

PMSF (Sigma-Aldrich, CAS #: 329-98-6), and Protease Inhibitor Cocktail (RPI, Cas #: 30827-99-7) The cells were centrifuged at 3,000 x g for 10 min at 4ºC. The cells were resuspended in 3 ml of cell lysis buffer and were lysed by sonication (Fisher Scientific, Fisher Model 100 Sonic Dismembrator Cell Disruptor) with a 4-watt output for 1 second on and rest for 1 second off, 60 x times, and cell debris and more prominent organelles were pelleted at 3,000 x g for 1 hour at 4ºC. The supernatant was removed and centrifuged at 175,000 x g (58,000 rpm) for 20 mins using a Beckman Optima MaxE Ultracentrifuge fitted with a TLA 110 rotor. The supernatant was discarded, and the pellet was resuspended in 1.5 ml cell lysis buffer. The resuspended pellet was centrifuged at 145,000 x g (53,000 rpm) for 1 hour and 30 mins using Beckman Optima MaxE Ultracentrifuge using the TLA 110 rotor. The supernatant was discarded, and the pellet was resuspended in 1.5 ml cell lysis buffer.

Carbon monoxide (CO) difference spectrum

CYP4G-CPR-containing microsomes were assessed for functional activity as a measure of proper folding and peak at 450 nm by CO-difference spectrum analysis (Choi et al., 2003; Omura, Tsuneo; Sato, 1964; Song et al., 2013). A spectrophotometer (VWR, SpectraMax® M5/M5e Multimode Plate Reader) measuring 400 to 500 nm was used to observe a Soret band absorption from the heme group after incubation with CO gas. Denatured CYP4G has only one Soret peak at 420 nm when saturated with CO gas (Fig. 4.1). Fully reduced CYP4G has an additional Soret peak at 450 nm in its absorption spectra (Fig. 4.1). In duplicate, microsomes were added to a 96-well plate (UV half-star plate). One of the two microsome samples was sealed to prevent CO gas from entering the well. The plate was then placed inside a sealed container with an opening adjusted for

connection to the CO gas tank. The CO valve was opened to release gas into the container and the wells for 2-3 mins at 20-30 PSI. The plate was removed from the container, and the sealant protecting one of the wells was removed. To each well, 5 µL (0.5 M) of Sodium dithionate was added and mixed. The plate was analyzed with a spectrophotometer at 5 min intervals (5, 10, and 15 mins. Functional protein would bind to CO that would be identified in the spectrum at 450 nm peak, representing the heme group in the microsome. Microsome preparations containing CYP4G35-CPR were flash frozen and stored at -80 ºC for up to 1 month.

Substrate Specificity Assays

Each reaction contained 25 pmol of microsomal CYP, assay buffer (1.2 mM $MgCl_2$, 1.2 mM $CaCl_2$, 0.4 mM DTT), 25 µg substrate (octadecanol, and decanal), and 1.0 mM NADPH with a total reaction volume of 500 µL. The reactions were incubated at 30 °C overnight in a hybridization chamber and quenched with 200 µL 2 M HCl. Approximately 20 mg of NaCl was added to each reaction, and products were extracted with 500 µL hexane: ether (1:1). Extracted products were analyzed using a Shimadzu QP2020 gas chromatograph-mass spectrometer with a molecular weight scanning range of 50 - 550 atomic mass units (AMU). A trace chromatograph containing a 30m, 25µm film thickness DB-5 capillary column (Shimadzu) was programmed with the following parameters: initial temperature of 40 ºC for 10 carbon chain long substrates with no hold, programmed at 5 ºC per minute to 250ºC.

IV. Results

Molecular characterization of CYP4G35

Heterologous protein expression: A carbon monoxide (CO) difference spectrum was used to test the activity of cytochrome P450 in the recombinant CYP4G fusion enzymes. The spectrum had a short yet clear peak at 450 nm, indicating that CYP4G35 and CYP4G55 cytochromes were functionally folded and were active (Fig. 4.1).

The oxidation of NADPH through CPR is required to provide electron transport to the cytochrome P450. Therefore, the oxidation of NADPH to NADP+ in the presence of the fusion protein containing CPR was measured. The control consisted of the substrate (decanal), assay buffer, and NADPH. CYP4G35 and CYP4G55 microsomes were added separately to the assay buffer containing NADPH in the experiments. The reduction of NADPH to NADP+ is indicated by the decrease in absorbance at 340 nm; both CYP4G35 and CYP4G55 partner reductase showed this decrease in absorbances (Fig. 4.2). and indicated that both CYP4G35-CPR and CYP4G55-CPR fusion protein had CPR activity (Fig. 4.2).

Substrate Assay: Microsomes expressing recombinant CYP4G55-CPR and CYP4G35-CPR were tested against decanal and octadecanol. Neither CYP4G55 nor CYP4G35 produced the expected hydrocarbon product of n-nonane when incubated with the decanal substrate (Fig. 4.3. A). However, the substrate (decanal) and the n-octanol marker were identified in GC-MS peaks (Fig. 4.3. A), suggesting that the purification steps worked. Similarly, no product was identified (Fig. 4.3 B).

VII. Discussion

In the present work, the results indicated that we were able to generate an active fusion protein for CYP4G35-CPR and CYP4G55-CPR. However, our substrate assays did not work even for the positive control CYP4G55-CPR.

CYP4G55 and CYP4G11 both (CYP415-like) have been shown to catalyze the oxidative decarbonylation of aldehydes to tridecane (C13) and decanal to nonane (Calla et al., 2018; MacLean et al., 2018). Our approach to characterizing CYP4G35 was very similar to other studies (Balabanidou et al., 2016; Calla et al., 2018; MacLean et al., 2018). We used well-characterized CYP4G55 in our experiments alongside CYP4G35 because it reduces various substrates of different carbon-chain sizes (MacLean et al., 2018).

The selection of substrates for CYP4G35 assay, such as decanal, was based on our previous work on identifying compounds that illicit attraction behavior in mosquitoes. The complex blend of human and plant volatiles ranges from 8 to 18 carbon-chained aldehydes, ketones, and alcohols (McBride et al., 2014; Zhao et al., 2022). We hypothesized that CYP4G35 might process clearing short-chain aldehyde and alcohols from sensilla from the antennae.

Here, we attempted to characterize potential substrates of CYP4G35 to understand its function. Future experiments will use different methods to extract the products from the substrate assay and use different carbon-length substrates.

VIII. Figures

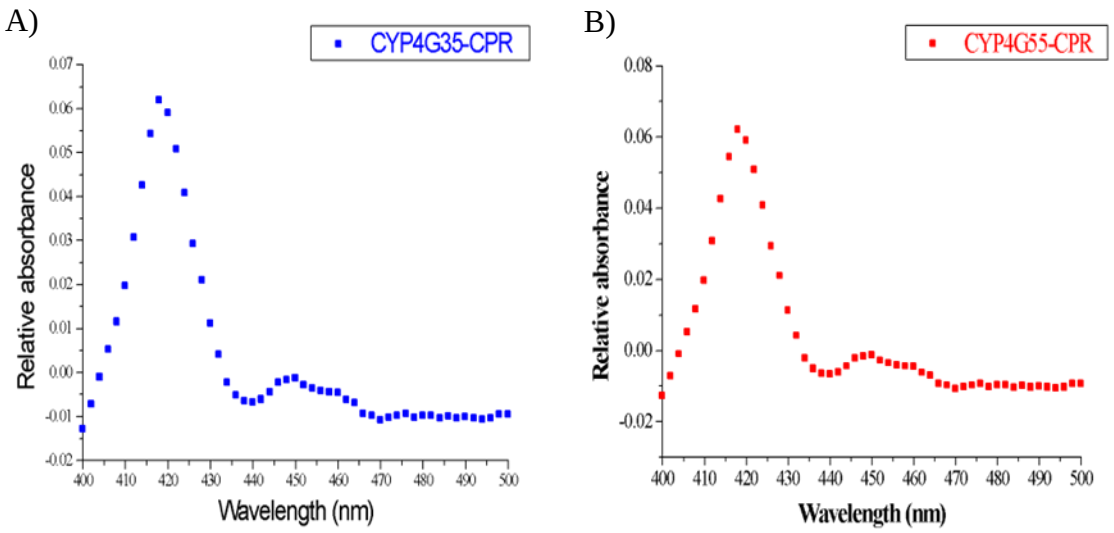

Figure 4.1. Validation of functional Cytochrome P450 using CO difference spectrum for CYP4G35 and CYP4G55. CO-difference spectra of microsomes prepared from Sf9 cells producing recombinant A) CYP4G35-CPR (blue) and B) CYP4G55-CPR (red). The fusion proteins produce the 450-nm peak characteristic of functional cytochromes P450.

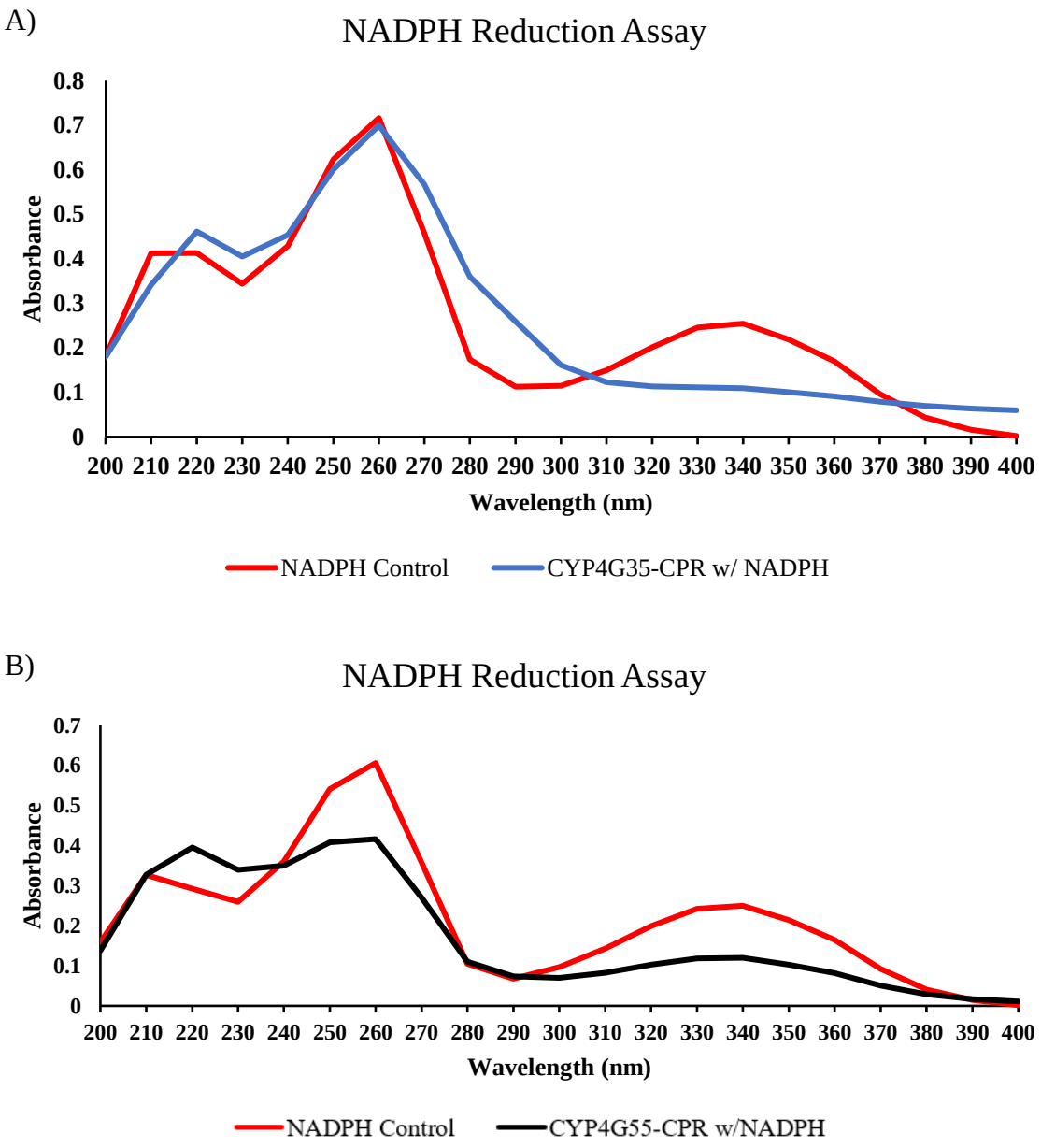

Figure 4.2. Cytochrome P450 partner reductase activity using NADPH reduction assay for CYP4G35-CPR and CYP4G55-CPR. CYP4Gx-CPR activity was measured using NADPH reduction to NADP+, indicated by a decrease in absorbance at 340 nm. A) CYP4G35-CPR activity was indicated through the reduction of NADPH to NADP+

compared to the now NADPH control assay. B) CYP4G55-CPR activity was indicated through the reduction of NADPH to NADP+ compared to the NADPH control assay.

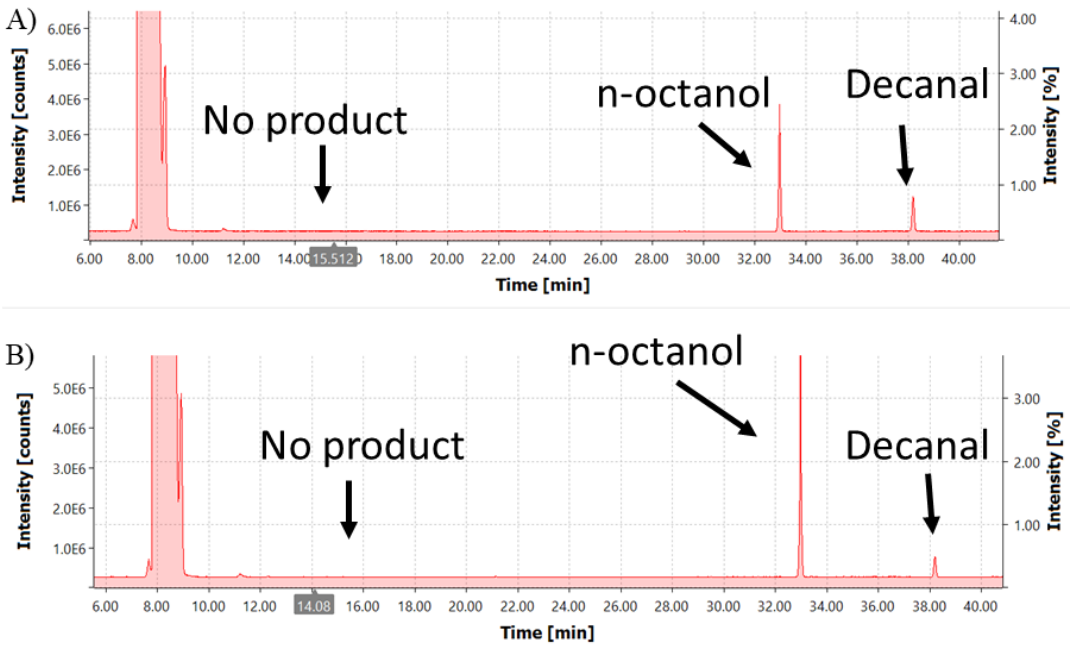

Figure 4.3. Products from incubations of CYP4G55-CPR and CYP4G35-CPR with decanal. GC/MS analysis of any products from the substrate assay with Octacdecanol in Sf9 microsomes expressing CYP4G55-CPR (a), CYP4G35-CPR (b). There was no hydrocarbon product substrate from the substrate assay from recombinant CYP4G55-CPR (a) and CYP4G35-CPR (b) fusion enzymes. The peak at 32.97 min is the n-octanol standard. The peak at 38.19 min is the decanal substrate. The mass spectrum of n-octanol and decanal matches the mass spectrum of authentic standards (not shown).

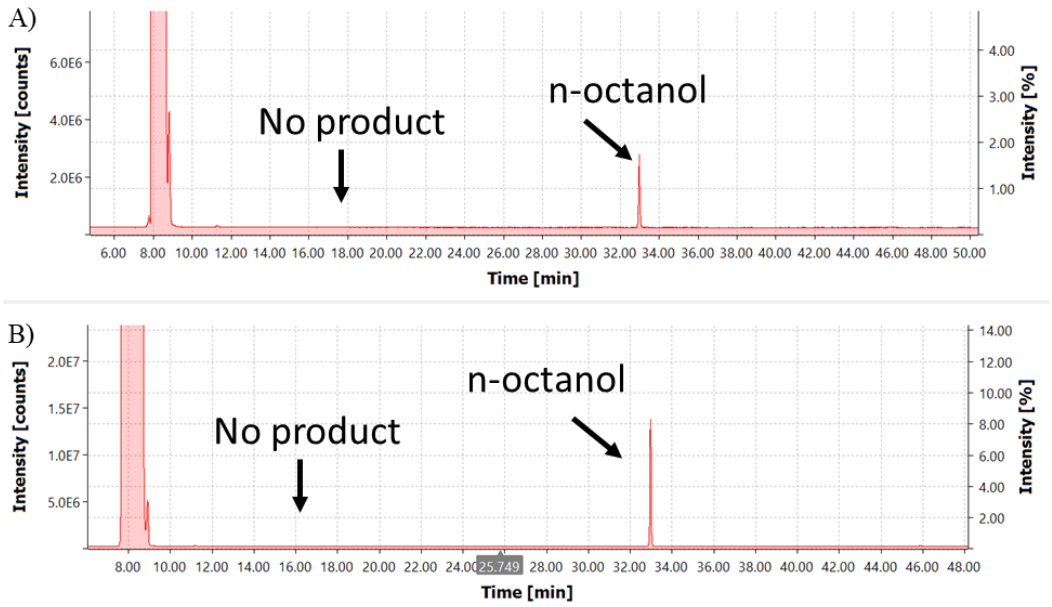

Figure 4.4. Products from incubations of CYP4G55-CPR and CYP4G35-CPR with octadecanol. GC/MS analysis of any products from the substrate assay with octacosanol in Sf9 microsomes expressing CYP4G55-CPR (a), CYP4G35-CPR (b). There was no octadecanol substrate from the substrate assay from recombinant CYP4G55-CPR (a) and CYP4G35-CPR (b) fusion enzymes. The peak at 32.97 min is the n-octanol standard. Neither the initial substrate nor product was detected in either a) or b). The mass spectrum of n-octanol matches the mass spectrum of the authentic standard (not shown).

VIII. References

Abuin, L., Bargeton, B., Ulbrich, M. H., Isacoff, E. Y., Kellenberger, S., & Benton, R. (2011). Functional Architecture of Olfactory Ionotropic Glutamate Receptors [Article]. *Neuron*, *69*(1), 44-60. https://doi.org/10.1016/j.neuron.2010.11.042

Adusumilli, R., & Mallick, P. (2017). Data Conversion with ProteoWizard msConvert. *Proteomics: Methods and Protocols*, *1550*, 339-368. https://doi.org/10.1007/978-1-4939-6747-6_23

Ahmad, I., & Ray, P. K. (1987). Factors conferring resistance to endosulfan in developmental biology of musca-domestica [Meeting Abstract]. *Journal of Cellular Biochemistry*, 24-24.

Alphey, L. (2014). Genetic Control of Mosquitoes. In M. R. Berenbaum (Ed.), *Annual Review of Entomology, Vol 59, 2014* (Vol. 59, pp. 205-224). Annual Reviews. https://doi.org/10.1146/annurev-ento-011613-162002

Alphey, L. S., Crisanti, A., Randazzo, F., & Akbari, O. S. (2020). Standardizing the definition of gene drive [Editorial Material]. *Proceedings of the National Academy of Sciences of the United States of America*, *117*(49), 30864-30867. https://doi.org/10.1073/pnas.2020417117

Andrews, K. A., Wesche, D., McCarthy, J., Mohrle, J. J., Tarning, J., Phillips, L., . . . Grasela, T. (2018). Model-Informed Drug Development for Malaria Therapeutics. In P. A. Insel (Ed.), *Annual Review of Pharmacology and Toxicology, Vol 58* (Vol. 58, pp. 567-582). Annual Reviews. https://doi.org/10.1146/annurev-pharmtox-010715-103429

Balabanidou, V., Kampouraki, A., MacLean, M., Blomquist, G. J., Tittiger, C., Juarez, M. P., . . . Vontas, J. (2016). Cytochrome P450 associated with insecticide resistance catalyzes cuticular hydrocarbon production in Anopheles gambiae [Article]. *Proceedings of the National Academy of Sciences of the United States of America*, *113*(33), 9268-9273. https://doi.org/10.1073/pnas.1608295113

Baldwin, S. R., Mohapatra, P., Nagalla, M., Sindvani, R., Amaya, D., Dickson, H. A., & Menuz, K. (2021). Identification and characterization of CYPs induced in the Drosophila antenna by exposure to a plant odorant [Article]. *Scientific Reports*, *11*(1), 14, Article 20530. https://doi.org/10.1038/s41598-021-99910-9

Benton, R., Vannice, K. S., Gomez-Diaz, C., & Vosshall, L. B. (2009). Variant Ionotropic Glutamate Receptors as Chemosensory Receptors in Drosophila. *Cell*, *136*(1), 149-162. https://doi.org/10.1016/j.cell.2008.12.001

Berman, J., & Radhakrishna, T. (2017). The Tropical Disease Priority Review Voucher: A Game-Changer for Tropical Disease Products [Review]. *American Journal of Tropical Medicine and Hygiene*, *96*(1), 11-13. https://doi.org/10.4269/ajtmh.16-0099

Briegel, H., & Horler, E. (1993). Multiple blood meals as a reproductive strategy in anopheles (Diptera, culcidae). *Journal of Medical Entomology*, *30*(6), 975-985. https://doi.org/10.1093/jmedent/30.6.975

Calla, B., MacLean, M., Liao, L. H., Dhanjal, I., Tittiger, C., Blomquist, G., & Berenbaum, M. (2018). Functional characterization of CYP4G11a highly

conserved enzyme in the western honey bee Apis mellifera [Article]. *Insect Molecular Biology*, *27*(5), 661-674. https://doi.org/10.1111/imb.12516

Cano-Ramirez, C., Lopez, M. F., Cesar-Ayala, A. K., Pineda-Martinez, V., Sullivan, B. T., & Zuniga, G. (2013). Isolation and expression of cytochrome P450 genes in the antennae and gut of pine beetle Dendroctonus rhizophagus (Curculionidae: Scolytinae) following exposure to host monoterpenes. *Gene*, *520*(1), 47-63. https://doi.org/10.1016/j.gene.2012.11.059

Chung, H., Sztal, T., Pasricha, S., Sridhar, M., Batterham, P., & Daborn, P. J. (2009). Characterization of Drosophila melanogaster cytochrome P450 genes. *Proceedings of the National Academy of Sciences of the United States of America*, *106*(14), 5731-5736. https://doi.org/10.1073/pnas.0812141106

Daborn, P., Boundy, S., Yen, J., Pittendrigh, B., & Ffrench-Constant, R. (2001). DDT resistance in Drosophila correlates with Cyp6g1 over-expression and confers cross-resistance to the neonicotinoid imidacloprid [Article]. *Molecular Genetics and Genomics*, *266*(4), 556-563. https://doi.org/10.1007/s004380100531

Daborn, P. J., Yen, J. L., Bogwitz, M. R., Le Goff, G., Feil, E., Jeffers, S., . . . ffrench-Constant, R. H. (2002). A single P450 allele associated with insecticide resistance in Drosophila [Article]. *Science*, *297*(5590), 2253-2256. https://doi.org/10.1126/science.1074170

Despres, L., David, J. P., & Gallet, C. (2007). The evolutionary ecology of insect resistance to plant chemicals [Review]. *Trends in Ecology & Evolution*, *22*(6), 298-307. https://doi.org/10.1016/j.tree.2007.02.010

Dickens, J. C., Billings, R. F., & Payne, T. L. (1992). Green leaf volatiles interrupts aggregation pheromone response in bark beetles infesting southern pines [Article]. *Experientia*, *48*(5), 523-524. https://doi.org/10.1007/bf01928180

Doerr, A. (2015). DIA mass spectrometry. *Nature Methods*, *12*(1), 35-35. https://doi.org/10.1038/nmeth.3234

Dunipace, L., Meister, S., McNealy, C., & Amrein, H. (2001). Spatially restricted expression of candidate taste receptors in the Drosophila gustatory system. *Current Biology*, *11*(11), 822-835. https://doi.org/10.1016/s0960-9822(01)00258-5

Durand, N., Carot-Sans, G., Bozzolan, F., Rosell, G., Siaussat, D., Debernard, S., . . . Maibeche-Coisne, M. (2011). Degradation of Pheromone and Plant Volatile Components by a Same Odorant-Degrading Enzyme in the Cotton Leafworm, Spodoptera littoralis [Article]. *Plos One*, *6*(12), 7, Article e29147. https://doi.org/10.1371/journal.pone.0029147

Durand, N., Carot-Sans, G., Chertemps, T., Montagne, N., Jacquin-Joly, E., Debernard, S., & Maibeche-Coisne, M. (2010). A diversity of putative carboxylesterases are expressed in the antennae of the noctuid moth Spodoptera littoralis [Article]. *Insect Molecular Biology*, *19*(1), 87-97. https://doi.org/10.1111/j.1365-2583.2009.00939.x

Feyereisen, R. (2012). *Insect CYP Genes and P450 Enzymes*. Elsevier Academic Press Inc. https://doi.org/10.1016/b978-0-12-384747-8.10008-x

Feyereisen, R. (2020). Origin and evolution of the CYP4G subfamily in insects, cytochrome P450 enzymes involved in cuticular hydrocarbon synthesis [Article].

Molecular Phylogenetics and Evolution, *143*, 15, Article 106695. https://doi.org/10.1016/j.ympev.2019.106695

Gantz, V. M., Jasinskiene, N., Tatarenkova, O., Fazekas, A., Macias, V. M., Bier, E., & James, A. A. (2015). Highly efficient Cas9-mediated gene drive for population modification of the malaria vector mosquito Anopheles stephensi [Article]. *Proceedings of the National Academy of Sciences of the United States of America*, *112*(49), E6736-E6743. https://doi.org/10.1073/pnas.1521077112

Geng, C. Q., Li, X. Y., Wu, X. J., Yu, H., Zhang, F., Zhou, Z. Y., & Ren, Z. Q. Liquid-liquid equilibrium and mechanism study on separation of short carbon chain hydrocarbon mixtures by Cyrene. *Canadian Journal of Chemical Engineering*. https://doi.org/10.1002/cjce.24797

Gessulat, S., Schmidt, T., Zolg, D. P., Samaras, P., Schnatbaum, K., Zerweck, J., . . . Wilhelm, M. (2019). Prosit: proteome-wide prediction of peptide tandem mass spectra by deep learning. *Nature Methods*, *16*(6), 509-+. https://doi.org/10.1038/s41592-019-0426-7

Gillet, L. C., Navarro, P., Tate, S., Rost, H., Selevsek, N., Reiter, L., . . . Aebersold, R. (2012). Targeted Data Extraction of the MS/MS Spectra Generated by Data-independent Acquisition: A New Concept for Consistent and Accurate Proteome Analysis. *Molecular & Cellular Proteomics*, *11*(6), Article O111.016717. https://doi.org/10.1074/mcp.O111.016717

Gillies, M. T. (1980). The role of carbon dioxide in host-finding by mosquitos (Diptera, Culicidae) - a review. *Bulletin of Entomological Research*, *70*(4), 525-532. https://doi.org/10.1017/s0007485300007811

Hammond, A., Galizi, R., Kyrou, K., Simoni, A., Siniscalchi, C., Katsanos, D., . . . Nolan, T. (2016). A CRISPR-Cas9 gene drive system-targeting female reproduction in the malaria mosquito vector Anopheles gambiae [Article]. *Nature Biotechnology*, *34*(1), 78-83. https://doi.org/10.1038/nbt.3439

Harrington, L. C., Edman, J. D., & Scott, T. W. (2001). Why do female Aedes aegypti (Diptera : Culicidae) feed preferentially and frequently on human blood? *Journal of Medical Entomology*, *38*(3), 411-422. https://doi.org/10.1603/0022-2585-38.3.411

He, P., Zhang, Y. F., Hong, D. Y., Wang, J., Wang, X. L., Zuo, L. H., . . . He, M. (2017). A reference gene set for sex pheromone biosynthesis and degradation genes from the diamondback moth, Plutella xylostella, based on genome and transcriptome digital gene expression analyses. *Bmc Genomics*, *18*, Article 219. https://doi.org/10.1186/s12864-017-3592-y

Hecht, D., & Fogel, G. B. (2012). Modeling the evolution of drug resistance in malaria [Article]. *Journal of Computer-Aided Molecular Design*, *26*(12), 1343-1353. https://doi.org/10.1007/s10822-012-9618-2

Heydel, J. M., Holsztynska, E. J., Legendre, A., Thiebaud, N., Artur, Y., & Le Bon, A. M. (2010). UDP-glucuronosyltransferases (UGTs) in neuro-olfactory tissues: expression, regulation, and function [Review]. *Drug Metabolism Reviews*, *42*(1), 74-97. https://doi.org/10.3109/03602530903208363

Jing, T. X., Yuan, C. Y., Meng, L. W., Hou, Q. L., Liu, X. Q., Dou, W, Wang, J. J. (2022). CYP4G100 contributes to desiccation resistance by mediating cuticular

hydrocarbon synthesis in Bactrocera dorsalis. *Insect Molecular Biology*, *31*(6), 772-781. https://doi.org/10.1111/imb.12803

Jones, W. D., Cayirlioglu, P., Kadow, I. G., & Vosshall, L. B. (2007). Two chemosensory receptors together mediate carbon dioxide detection in Drosophila. *Nature*, *445*(7123), 86-90. https://doi.org/10.1038/nature05466

Juhn, J., & James, A. A. (2012). Hybridization in situ of Salivary Glands, Ovaries, and Embryos of Vector Mosquitoes [Article]. *Jove-Journal of Visualized Experiments*(64), 18, Article e3709. https://doi.org/10.3791/3709

Kefi, M., Balabanidou, V., Douris, V., Lycett, G., Feyereisen, R., & Vontas, J. (2019). Two functionally distinct CYP4G genes of Anopheles gambiae contribute to cuticular hydrocarbon biosynthesis [Article]. *Insect Biochemistry and Molecular Biology*, *110*, 52-59. https://doi.org/10.1016/j.ibmb.2019.04.018

Krieger, J., Grosse-Wilde, E., Gohl, T., & Breer, H. (2005). Candidate pheromone receptors of the silkmoth Bombyx mori [Article]. *European Journal of Neuroscience*, *21*(8), 2167-2176. https://doi.org/10.1111/j.1460-9568.2005.04058.x

Kwon, J. Y., Dahanukar, A., Weiss, L. A., & Carlson, J. R. (2007). The molecular basis of CO2 reception in Drosophila. *Proceedings of the National Academy of Sciences of the United States of America*, *104*(9), 3574-3578. https://doi.org/10.1073/pnas.0700079104

Laughlin, J. D., Ha, T. S., Jones, D. N. M., & Smith, D. P. (2008). Activation of pheromone-sensitive neurons is mediated by conformational activation of pheromone-binding protein [Article]. *Cell*, *133*(7), 1255-1265. https://doi.org/10.1016/j.cell.2008.04.046

Leal, W. S. (2013). Odorant Reception in Insects: Roles of Receptors, Binding Proteins, and Degrading Enzymes. In M. R. Berenbaum (Ed.), *Annual Review of Entomology, Vol 58* (Vol. 58, pp. 373-391). Annual Reviews. https://doi.org/10.1146/annurev-ento-120811-153635

Li, W., Yang, B., Liu, N. Y., Zhu, J. Y., Li, Z. B., Ze, S. Z., Zhao, N. (2022). Identification and Characterization of the Detoxification Genes Based on the Transcriptome of Tomicus yunnanensis. *Diversity-Basel*, *14*(1), Article 23. https://doi.org/10.3390/d14010023

Li, W. H., Wang, X. Y., Jiang, P., Yang, M. W., Li, Z. M., Huang, C. Y., & He, Y. P. (2022). A full-length transcriptome and gene expression analysis of three detoxification gene families in a predatory stink bug, Picromerus lewisi. *Frontiers in Physiology*, *13*, Article 1016582. https://doi.org/10.3389/fphys.2022.1016582

Liu, S., Rao, X. J., Li, M. Y., Feng, M. F., He, M. Z., & Li, S. G. (2015). Glutathione s-transferase genes in the rice leaffolder, cnaphalocrocis medinalis (lepidoptera: pyralidae): identification and expression profiles [Article]. *Archives of Insect Biochemistry and Physiology*, *90*(1), 1-13.

Lu, D. Y., Manovic, V., Hughes, R., & Anthony, E. J. (2007). Study of CO2 capture using CO2 looping combustion technology. *Proceedings of the 6th International Symposium on Coal Combustion*, 997-1007.

Macedo, P. A., Schleier, J. J., Reed, M., Kelley, K., Goodman, G. W., Brown, D. A., & Peterson, R. K. D. (2010). Evaluation of efficacy and human health risk of aerial

ultra-low volume applications of pyrethrins and piperonyl butoxide for adult mosquito management in response to west nile virus activity in sacramento county, california [Article]. *Journal of the American Mosquito Control Association*, *26*(1), 57-66. https://doi.org/10.2987/09-5961.1

MacLean, M., Nadeau, J., Gurnea, T., Tittiger, C., & Blomquist, G. J. (2018). Mountain pine beetle (Dendroctonus ponderosae) CYP4Gs convert long and short chain alcohols and aldehydes to hydrocarbons. *Insect Biochemistry and Molecular Biology*, *102*, 11-20. https://doi.org/10.1016/j.ibmb.2018.09.005

MacWilliam, D., Kowalewski, J., Kumar, A., Pontrello, C., & Ray, A. (2018). The signaling mode of the broad-spectrum conserved co2 receptor is one of the important determinants of odor valence in drosophila. *Neuron*, *97*(5), 1153-+. https://doi.org/10.1016/j.neuron.2018.01.028

Maıbeche, T. C. a. M. (2021). Odor degrading enzymes and signal termination. In *Insect pheromone biochemistry and molecular biology* (2nd ed., pp. 619 - 644). Academic Press is an imprint of Elsevier.

Maibeche-Coisne, M., Monti-Dedieu, L., Aragon, S., & Dauphin-Villemant, C. (2000). A new cytochrome P450 from Drosophila melanogaster, CYP4G15, expressed in the nervous system [Article]. *Biochemical and Biophysical Research Communications*, *273*(3), 1132-1137. https://doi.org/10.1006/bbrc.2000.3058

Mao, W., Schuler, M. A., & Berenbaum, M. R. (2015). Task-related differential expression of four cytochrome P450 genes in honeybee appendages [Article]. *Insect Molecular Biology*, *24*(5), 582-588. https://doi.org/10.1111/imb.12183

McAfee, A., Chapman, A., Iovinella, I., Gallagher-Kurtzke, Y., Collins, T. F., Higo, H., . . . Foster, L. J. (2018). A death pheromone, oleic acid, triggers hygienic behavior in honey bees (Apis mellifera L.). *Scientific Reports*, *8*, Article 5719. https://doi.org/10.1038/s41598-018-24054-2

McMeniman, C. J., Corfas, R. A., Matthews, B. J., Ritchie, S. A., & Vosshall, L. B. (2014). Multimodal Integration of Carbon Dioxide and Other Sensory Cues Drives Mosquito Attraction to Humans. *Cell*, *156*(5), 1060-1071. https://doi.org/10.1016/j.cell.2013.12.044

Melo, A. C. A., Rutzler, M., Pitts, R. J., & Zwiebel, L. J. (2004). Identification of a chemosensory receptor from the yellow fever mosquito, Aedes aegypti, that is highly conserved and expressed in olfactory and gustatory organs [Article]. *Chemical Senses*, *29*(5), 403-410. https://doi.org/10.1093/chemse/bjh041

Nie, H. Y., Xu, S. P., Xie, C. Q., Geng, H. Y., Zhao, Y. Z., Li, J. H., Su, S. K. (2018). Comparative transcriptome analysis of Apis mellifera antennae of workers performing different tasks [Article]. *Molecular Genetics and Genomics*, *293*(1), 237-248. https://doi.org/10.1007/s00438-017-1382-5

Peterson, R. K. D., Macedo, P. A., & Davis, R. S. (2006). A human-health risk assessment for West Nile virus and insecticides used in mosquito management [Article]. *Environmental Health Perspectives*, *114*(3), 366-372. https://doi.org/10.1289/ehp.8667

Pongtavornpinyo, W., Yeung, S., Hastings, I. M., Dondorp, A. M., Day, N. P. J., & White, N. J. (2008). Spread of anti-malarial drug resistance: Mathematical model

with implications for ACT drug policies [Article]. *Malaria Journal*, *7*, 12, Article 229. https://doi.org/10.1186/1475-2875-7-229

Pottier, M. A., Bozzolan, F., Chertemps, T., Jacquin-Joly, E., Lalouette, L., Siaussat, D., & Maibeche-Coisne, M. (2012). Cytochrome P450s and cytochrome P450 reductase in the olfactory organ of the cotton leafworm Spodoptera littoralis [Article]. *Insect Molecular Biology*, *21*(6), 568-580. https://doi.org/10.1111/j.1365-2583.2012.01160.x

Qiu, Y., Tittiger, C., Wicker-Thomas, C., Le Goff, G., Young, S., Wajnberg, E., Feyereisen, R. (2012). An insect-specific P450 oxidative decarbonylase for cuticular hydrocarbon biosynthesis [Article]. *Proceedings of the National Academy of Sciences of the United States of America*, *109*(37), 14858-14863. https://doi.org/10.1073/pnas.1208650109

Ridley, D. B. (2017). Priorities for the Priority Review Voucher [Review]. *American Journal of Tropical Medicine and Hygiene*, *96*(1), 14-15. https://doi.org/10.4269/ajtmh.16-0600

Ridley, D. B., Ganapathy, P., & Kettler, H. E. (2021). US Tropical Disease Priority Review Vouchers: Lessons In Promoting Drug Development And Access [Review]. *Health Affairs*, *40*(8), 1243-1251. https://doi.org/10.1377/hlthaff.2020.02273

Robertson, H. M., & Kent, L. B. (2009). Evolution of the gene lineage encoding the carbon dioxide receptor in insects. *Journal of Insect Science*, *9*, Article 19.

Rodrigues, V., & Siddiqi, O. (1978). Genetic-analysis of chemosensory pathway. *Proceedings of the Indian Academy of Sciences Section B*, *87*(7), 147-+.

Scott, J. G., & Wen, Z. M. (2001). Cytochromes P450 of insects: the tip of the iceberg [Article; Proceedings Paper]. *Pest Management Science*, *57*(10), 958-967. https://doi.org/10.1002/ps.354

Scott, K., Brady, R., Cravchik, A., Morozov, P., Rzhetsky, A., Zuker, C., & Axel, R. (2001). A chemosensory gene family encoding candidate gustatory and olfactory receptors in Drosophila. *Cell*, *104*(5), 661-673. https://doi.org/10.1016/s0092-8674(01)00263-x

Searle, B. C., Pino, L. K., Egertson, J. D., Ting, Y. S., Lawrence, R. T., MacLean, B. X., . . . MacCoss, M. J. (2018). Chromatogram libraries improve peptide detection and quantification by data independent acquisition mass spectrometry. *Nature Communications*, *9*, Article 5128. https://doi.org/10.1038/s41467-018-07454-w

Searle, B. C., Swearingen, K. E., Barnes, C. A., Schmidt, T., Gessulat, S., Kuster, B., & Wilhelm, M. (2020). Generating high quality libraries for DIA MS with empirically corrected peptide predictions. *Nature Communications*, *11*(1), Article 1548. https://doi.org/10.1038/s41467-020-15346-1

Seliskar, M., & Rozman, D. (2007). Mammalian cytochromes P450 - Importance of tissue specificity. *Biochimica Et Biophysica Acta-General Subjects*, *1770*(3), 458-466. https://doi.org/10.1016/j.bbagen.2006.09.016

Soderlund, D. M. (2012). Molecular mechanisms of pyrethroid insecticide neurotoxicity: recent advances [Review]. *Archives of Toxicology*, *86*(2), 165-181. https://doi.org/10.1007/s00204-011-0726-x

Souza-Neto, J. A., Powell, J. R., & Bonizzoni, M. (2019). Aedes aegypti vector competence studies: A review [Review]. *Infection Genetics and Evolution*, *67*, 191-209. https://doi.org/10.1016/j.meegid.2018.11.009

Sparks, J. T., Botsko, G., Swale, D. R., Boland, L. M., Patel, S. S., & Dickens, J. C. (2018). Membrane Proteins Mediating Reception and Transduction in Chemosensory Neurons in Mosquitoes [Review]. *Frontiers in Physiology*, *9*, 14, Article 1309. https://doi.org/10.3389/fphys.2018.01309

Steinbrecht, R. A. (1997). Pore structures in insect olfactory sensilla: A review of data and concepts [Review]. *International Journal of Insect Morphology & Embryology*, *26*(3-4), 229-245. https://doi.org/10.1016/s0020-7322(97)00024-x

Strode, C., Wondji, C. S., David, J. P., Hawkes, N. J., Lumjuan, N., Nelson, D. R., Ranson, H. (2008). Genomic analysis of detoxification genes in the mosquito Aedes aegypti [Article]. *Insect Biochemistry and Molecular Biology*, *38*(1), 113-123. https://doi.org/10.1016/j.ibmb.2007.09.007

Suh, G. S. B., Wong, A. M., Hergarden, A. C., Wang, J. W., Simon, A. F., Benzer, S., . . . Anderson, D. J. (2004). A single population of olfactory sensory neurons mediates an innate avoidance behaviour in Drosophila. *Nature*, *431*(7010), 854-859. https://doi.org/10.1038/nature02980

Syed, Z., & Leal, W. S. (2007). Maxillary palps are broad-spectrum odorant detectors in Culex quinquefasciatus. *Chemical Senses*, *32*(8), 727-738. https://doi.org/10.1093/chemse/bjm040

Tang, W. X., Wang, D., Wang, J. Q., Wu, Z. W., Li, L. Y., Huang, M. L., Yan, D. Y. (2018). Pyrethroid pesticide residues in the global environment: An overview [Review]. *Chemosphere*, *191*, 990-1007. https://doi.org/10.1016/j.chemosphere.2017.10.115

Tauxe, G. M., MacWilliam, D., Boyle, S. M., Guda, T., & Ray, A. (2013). Targeting a Dual Detector of Skin and CO2 to Modify Mosquito Host Seeking. *Cell*, *155*(6), 1365-1379. https://doi.org/10.1016/j.cell.2013.11.013

Turner, S. L., Li, N., Guda, T., Githure, J., Carde, R. T., & Ray, A. (2011). Ultra-prolonged activation of CO2-sensing neurons disorients mosquitoes. *Nature*, *474*(7349), 87-U114. https://doi.org/10.1038/nature10081

Turner, S. L., & Ray, A. (2009). Modification of CO2 avoidance behaviour in Drosophila by inhibitory odorants. *Nature*, *461*(7261), 277-U159. https://doi.org/10.1038/nature08295

Vector-borne diseases. (2020). Vector-borne diseases (who.int)

Wang, S. P., He, G. L., Chen, R. R., Li, F., & Li, G. Q. (2012). The involvement of cytochrome p450 monooxygenases in methanol elimination in Drosophila melanogaster larvae [Article]. *Archives of Insect Biochemistry and Physiology*, *79*(4-5), 264-275. https://doi.org/10.1002/arch.21021

Wang, S. Y., Price, J. H., & Zhang, D. (2019). Hydrocarbons catalysed by TmCYP4G122 and TmCYP4G123 in Tenebrio molitor modulate the olfactory response of the parasitoid Scleroderma guani. *Insect Molecular Biology*, *28*(5), 637-648. https://doi.org/10.1111/imb.12581

Weaver, S. C., Charlier, C., Vasilakis, N., & Lecuit, M. (2018). Zika, Chikungunya, and Other Emerging Vector-Borne Viral Diseases. In C. T. Caskey (Ed.), *Annual*

Review of Medicine, Vol 69 (Vol. 69, pp. 395-408). Annual Reviews. https://doi.org/10.1146/annurev-med-050715-105122

Werck-Reichhart, D., Hehn, A., & Didierjean, L. (2000). Cytochromes P450 for engineering herbicide tolerance. *Trends in Plant Science*, *5*(3), 116-123. https://doi.org/10.1016/s1360-1385(00)01567-3

Wojtasek, H., & Leal, W. S. (1999). Degradation of an alkaloid pheromone from the pale-brown chafer, Phyllopertha diversa (Coleoptera : Scarabaeidae), by an insect olfactory cytochrome P450 [Article]. *Febs Letters*, *458*(3), 333-336. https://doi.org/10.1016/s0014-5793(99)01178-3

Wu, H. H., Liu, J. Y., Liu, Y. M., Abbas, M., Zhang, Y. C., Kong, W. A., Zhang, J. Z. (2022). CYP6FD5, an antenna-specific P450 gene, is potentially involved in the host plant recognition in Locusta migratoria [Article]. *Pesticide Biochemistry and Physiology*, *188*, 9, Article 105255. https://doi.org/10.1016/j.pestbp.2022.105255

Wu, L. X., Zhang, Z. F., Yua, Z. T., Yu, R. R., Ma, E. B., Fan, Y. L., Zhang, J. Z. (2020). Both LmCYP4G genes function in decreasing cuticular penetration of insecticides in Locusta migratoria. *Pest Management Science*, *76*(11), 3541-3550. https://doi.org/10.1002/ps.5914

Younus, F., Chertemps, T., Pearce, S. L., Pandey, G., Bozzolan, F., Coppin, C. W., Oakeshott, J. G. (2014). Identification of candidate odorant degrading gene/enzyme systems in the antennal transcriptome of Drosophila melanogaster [Article]. *Insect Biochemistry and Molecular Biology*, *53*, 30-43. https://doi.org/10.1016/j.ibmb.2014.07.003

Younus, F., Fraser, N. J., Coppin, C. W., Liu, J. W., Correy, G. J., Chertemps, T., Oakeshott, J. G. (2017). Molecular basis for the behavioral effects of the odorant degrading enzyme Esterase 6 in Drosophila [Article]. *Scientific Reports*, *7*, 12, Article 46188. https://doi.org/10.1038/srep46188

Zakhari, S. (2006). Overview: How is alcohol metabolized by the body? *Alcohol Research & Health*, *29*(4), 245-254.

Zhang, L. Y., Shen, Y. D., Jiang, X. C., & Liu, S. (2022). Transcriptomic Identification and Expression Profile Analysis of Odorant-Degrading Enzymes from the Asian Corn Borer Moth, Ostrinia furnacalis [Article]. *Insects*, *13*(11), 18, Article 1027. https://doi.org/10.3390/insects13111027

Chapter 5

Summary and Future Work

I. Summary and Discussion

In this thesis work, I investigated the potential of CYP4G35 as an odor-degrading enzyme (ODE). The preliminary data from the Gulia-Nuss lab showed very high expression of this gene in the olfactory tissues of *Ae. aegypti*. Further additional preliminary work in the lab showed that the knockdown of CYP4G35 by RNAi negatively impacts female mosquitoes' attraction to vertebrate hosts resulting in delayed or no blood feeding. Similar effects on the attraction of both sexes on plant volatile and of females towards human odor in a Y-shaped olfactometer assay were observed in CYP4G35 knockout mosquitoes generated using CRISPR-Cas9. These data strengthened our hypothesis that CYP4G35 is involved in odor perception and integration. We argued that for an enzyme to be an ODE, it needs to be present in the lumen of the sensillary hair of the olfactory tissues, where odor perception occurs through the binding of the odor molecules to the odorant receptor. We further argued that an ODE would use short to medium-chain volatile compounds, typically between 8 and 15 carbon (range for a volatile aldehyde, alcohol, or ketone), that would be important for mosquitoes.

We used whole-mount immune histochemistry (WM-IHC) and *in-situ* hybridization (ISH) to localize CYP4G35 protein and mRNA in the primary olfactory tissues: antennae, palps, and proboscis. We also used an antibody for CYP4G36, another member of the CYP4G subfamily, to confirm the specificity of CYP4G35

localization. Our data support our hypothesis and show localization of both CYP4G35 mRNA and protein in sensillary hair in antennae and proboscis but not in palps. Our data also show the specificity of the localization of CYP4G35 because CYP4G36 does not localize in either tissue.

To understand the mode-of-action of CYP4G35, we carried out proteomics analysis of the head and body between CYP4G35 mutants vs. WT females. Our proteomics data further indicates the function of CYP4G35 as a putative ODE. The highest upregulated proteins in CYP4G35 mutant heads were membrane transport proteins (kinesin), other cytochrome P40s, and esterases. The kinesin protein has been well documented in the literature and helps transport olfactory receptors and olfactory receptor coreceptors (ORCO) to the cilia of sensory hair. Higher expression of kinesin in our mutants suggests a compensatory mechanism of bringing more ORs to the surface when odor perception is altered due to the possible buildup of odor molecules. Additional CYPs and esterase upregulation in the head of the mosquito might also compensate for the lack of CYP4G35 for removing odor molecules.

Our efforts to identify the substrate for CYP4G35 failed so far. However, we have the CYP4G35 protein fused with its reductase partner (CYP4G-CPR fusion protein), and we confirmed that the individual cytochrome P450 component and the housefly reductase of the protein fusion protein are active. We will continue improving this assay and extraction method to improve the ability to identify products.

Future Work: In this work, we explored the general localization of CYP4G35. We plan to take this a step further and begin testing whether the CYP4G35 localizes in all types of sensilla (general ODE) or is it specific to one type (specific ODE). Using our

mutant lines, we can now test the lack of CYP4G35 staining in mutants as better control. Our proteomics data suggests increased expression of other CYPs and esterases. Using RNA probes or antibodies against these enzymes, we can validate our proteomics data which will help develop a model for CYP4G35 function. We also noted increased expression of kinesin motor domain proteins in the head of CYP4G35 mutants. Therefore, we plan to use IHC or ISH to test if ORCO expression is higher in our mutants.

We used decanal to investigate the possibility of CYP4G35 for breaking down short, unsaturated aldehydes and ketones. Our previous work with CYP4G35 RNAi and mutant lines showed that these mutants do not respond to decanal in an olfactometer assay, suggesting it might be a substrate for CYP4G35. Decanal is converted to nonane by a related CYP4G (CYP4G55), but our substrate assay determination experiments were unsuccessful. With GC-MS, we could only show the initial substrate from the assay along with the n-octanol from the extraction mixture. We are optimizing our assay to keep the volatile products from being lost as the decrease in hydrocarbon chain length decreases the boiling point and increases the volatility (Geng et al.). Substrate identification improves our understanding of CYP4G35's function as either a general detoxification or odor-specific enzyme. This provides further insights into the molecular mechanisms of host-seeking behavior, specifically odor clearance.

II. References

MacLean, M., Nadeau, J., Gurnea, T., Tittiger, C., & Blomquist, G. J. (2018). Mountain pine beetle (*Dendroctonus ponderosae*) CYP4Gs convert long and short chain alcohols and aldehydes to hydrocarbons. Insect Biochemistry and Molecular Biology, 102, 11-20. https://doi.org/10.1016/j.ibmb.2018.09.005

Zhang, L. Y., Shen, Y. D., Jiang, X. C., & Liu, S. (2022). Transcriptomic Identification and Expression Profile Analysis of Odorant-Degrading Enzymes from the Asian Corn Borer Moth, *Ostrinia furnacalis* [Article]. Insects, 13(11), 18, Article 1027. https://doi.org/10.3390/insects13111027